Evolution and the climatic niche: Using genomics and niche modeling to explore how climate impacts evolutionary processes

A DISSERTATION SUBMITTED TO THE FACULTY OF THE UNIVERSITY OF MINNESOTA BY

Samuel Bennett Weaver

IN PARTIAL FULFILLMENT OF THE REQUIREMENTS FOR THE DEGREE OF DOCTOR OF PHILOSOPHY

Suzanne E. McGaugh and Kenneth H. Kozak

February 2022

ACKNOWLEDGMENTS

First, I would like to thank my co-advisors, Dr. Suzanne McGaugh and Dr. Kenneth Kozak. Drs. McGaugh and Kozak took me under their collective wing while I was writing a GRFP proposal as an undergrad, and they have been an unending source of support, wisdom, and ideas ever since. They were always incredibly patient with me despite my growing pains as I stumbled through gaining the technical skills required for my research, and were always there to push me forward when I felt like I was stalling. Dr. McGaugh and Dr. Kozak have always celebrated, promoted, and defended my work, and they taught me practically everything I know about conducting, writing, and presenting research. They are two of the most brilliant, supportive, and kind people I know, and I will forever be grateful to have been a part of their labs.

I would also like to thank the other members of my preliminary and thesis committees, Dr. Keith Barker and Dr. Yaniv Brandvain. Their generosity with their time and wisdom was always a welcome surprise, and their impact on my work can not be overstated. In addition to my committee members, I am incredibly thankful for the support and friendship of the amazing postdocs and graduate students that I have worked with in the McGaugh and Kozak Labs. In the Kozak lab, Marta Lyons, Tom Radomski, and Emma Roback have always gone above and beyond to provide feedback on manuscript, methods, and talks. Adam Herman, Tom Kono, Rachel Moran, and many other McGaugh/Brandvain postdocs helped me with countless coding and software installation problems, and I am forever in their debt.

There are many members of the EEB community at the University of Minnesota and at other institutions who merit acknowledgement. Lisa Wiggins, Kate Barry, and Neal Jahren were saints for helping me navigate program requirements and registration snafus. Dr. Ruth Shaw, Dr. Seema Sheth, and Dr. Steve Freedberg mentored me as an undergraduate researcher and encouraged me to attend graduate school, and I would not have come this far without their initial guidance and support. At the root of it all, my uncle, Andy Weaver, instilled a love of nature and all things biology in me from a young age, and I am forever grateful to have grown up with such a wonderful teacher to inspire me.

Lastly, I need to thank my parents, my siblings, and most of all my wife, Nicole. Their love and encouragement for the last five and a half years have always been my best source of support, and without them who knows if I would have been able to stay sane through all of this. I love you all, and I will always be grateful to have such wonderful people in my life.

Funding for my work was provided by the Bell Museum of Natural History, the Minnesota Herpetological Society, the University of Minnesota, Highlands Biological station, the National Science Foundation, and the Texas Parks and Wildlife department.

ABSTRACT

Climate shapes the distributions of and interactions among species and thus influences many evolutionary processes related to the generation and maintenance of biodiversity. Oscillations in climatic regimes have played an important role in shaping the patterns of diversity by driving speciation events when previously connected populations become allopatrically isolated in different environments. Changing climates also are associated with extinction events when populations are unable to track their climatic niche or adapt to novel conditions. The rapid climate change caused by human activity emphasizes the need to understand the role climate plays in mediating species interactions and distributions. This work combines the use of climatic and genomic data across a variety of vertebrate systems to explore how climate has shaped the processes of speciation and evolution, and how climate may threaten the continued persistence of both recognized and unrecognized diversity.

The evolution of a species' climatic niche, or the climatic conditions under which a species occurs, plays a central role in generating diversity and adaptation to new environmental conditions. Faster rates of climatic niche evolution are associated with increased diversification rates, suggesting that the exploration of novel climate space can facilitate isolation and subsequent diversification. The evolution of traits that may increase or decrease rates of climate niche evolution, then, may play an important role in the colonization of novel environments and the formation of species. In my first chapter, I show that the evolution of a short aquatic larval stage in *Desmognathus* salamanders led to an increase in the rate of climatic niche evolution, which may have played a central role in the adaptive radiation of this group.

Changes in climate have the potential to bring long-isolated species into contact with one another. Oftentimes, these species can produce viable offspring with one another and form hybrid zones. These hybrid zones often form along ecological gradients, with hybrids occurring in habitats intermediate to the climatic conditions occupied by the pure parental populations. In the Southern Appalachian Mountains, *Plethodon shermani* and *Plethodon teyahalee* hybridize extensively along an elevational gradient. *P. shermani*

occurs on different mountaintop isolates, and *P. teyahalee* is distributed in between them at lower elevations. In my second chapter, I explore the genomic evidence for hybridization between these two species and whether climatic variation associated with elevation maintains species boundaries in this system. All surveyed parental *P. shermani* populations have experienced some degree of introgression from *P. teyahalee*, and multiple lines of evidence suggest that selection for *P. teyahalee* alleles drives asummetric introgression from *P. teyahalee* into *P. shermani*. We identify no intrinsic genetic barriers to gene flow, suggesting that these hybrid zones are regulated by ecological, rather than intrinsic factors. These findings suggest that all *P. shermani* populations are in danger of swamping by *P. teyahalee* as conditions in the Appalachians become warmer and drier.

Genomics and niche modeling are powerful tools for identifying cryptic lineages of conservation concern within widespread species. In addition to identifying lineages, these approaches can inform managing agencies about threats to population persistence such as climate change-induced habitat loss and inbreeding. In my final chapter, I assess patterns of genomic and environmental differentiation among populations of *Kinosternon hirtipes*. Within this group, we identified multiple evolutionarily distinct lineages, many of which correspond to described subspecies. Genetic and ecological differentiation among these lineages appears to be due to vicariance associated with the Trans-Mexican Volcanic Belt. Northern populations exhibit low genetic diversity, high levels of inbreeding, and may lose over 85% of climatically suitable habitat to climate change, raising concern over their long-term viability.

Table of Contents

LIST OF TABLES

LIST OF FIGURES

CHAPTER 1

The evolution of an aquatic larval stage is associated with variation in rates of climatic niche evolution in *Desmognathus* salamanders

Abstract

Rates of climatic niche evolution vary widely across the tree of life and are strongly associated with rates of diversification among clades. However, why the climatic niche evolves more rapidly in some clades than others remains unclear. Variation in life history traits often plays a key role in determining the environmental conditions under which species can survive, and therefore, could impact the rate at which lineages can expand in available climatic niche space. Here, we explore the relationships among life-history variation, climatic niche breadth, and rates of climatic niche evolution. We reconstruct a phylogeny for the genus Desmognathus, an adaptive radiation of salamanders distributed across eastern North America, based on nuclear and mitochondrial genes. Using this phylogeny, we estimate rates of climatic niche evolution for species with long, short, and no aquatic larval stage. Rates of climatic niche evolution are unrelated to the mean climatic niche breadth of species with different life histories. Instead, we find that the evolution of a short larval period promotes greater exploration of climatic space, leading to increased rates of climatic niche evolution across species having this trait. We propose that morphological and physiological differences associated with variation in larval stage length underlie the heterogeneous ability of lineages to explore climatic niche space. Rapid rates of climatic niche evolution among species with short larval periods were an important dimension of the clade's adaptive radiation and likely contributed to the rapid rate of lineage accumulation following the evolution of an aquatic life history in this clade. Our results show how variation in a key life-history trait can constrain or promote divergence of the climatic niche, leading to variation in rates of climatic niche evolution among species.

Introduction

Why rates of evolution are faster in some clades than others is a fundamental question at the intersection of evolutionary biology and ecology. Understanding why rates of evolution vary is central to understanding the disparity in phenotypic diversity among clades across the tree of life (Harmon et al. 2010). Variation in rates of phenotypic evolution may also explain why some clades diversify more rapidly than others, and thereby obtain greater species richness (Simpson 1944; Schluter 2000).

The climatic niche includes the temperature and precipitation conditions that are required for a species to persist in a given area (Grinnell 1917; Soberón 2007) and arises from physiological constraints that determine where populations can persist (Helmuth et al. 2005; Kearney and Porter 2009). The rate at which the climatic niche evolves may underlie the capacity of lineages to explore available geographic and ecological space, and in turn, may influence rates of diversification by decreasing rates of extinction and/or increasing rates of speciation. Recent studies have shown that the rate of climatic niche evolution is positively associated with the rate at which clades diversify, and also with the species richness of clades (Kozak and Wiens 2010, 2016; Gomez-Rodriguez et al. 2015; Title and Burns 2015; Castro-Insua et al. 2018).

Why, then, do rates of climatic niche evolution vary across the tree-of-life? One might expect rates of climatic niche evolution to be associated with climatic niche breadth. For example, clades containing species with broad climatic niches might be more prone to vicariant speciation (Sanmartín and Ronquist 2004; Weir and Schluter 2004) and also less susceptible to extinction given that they are more likely to be able to tolerate changing climatic conditions over time (Jansson and Dynesius 2002). Both of the latter processes should result in elevated rates of climatic niche evolution. Conversely, specialization for a narrow range of climatic conditions might constrain the ability of species to evolve (Futuyma and Moreno 1988), resulting in decreased rates of climatic niche evolution. Smith and Beaulieu (2009) found that flowering plant lineages with a woody growth form occupy smaller climatic spaces than herbaceous lineages, which seemingly slows rates of climatic niche evolution.

Nevertheless, the relationship between climatic niche breadth and rates of climatic niche evolution remains unclear (Fisher-Reid et al. 2012). If evolving a broad climatic

niche promotes higher dispersal rates, larger population sizes, and higher rates of intraspecific gene flow (Gaston and Blackburn 1996; Pyron 1999; Birand et al. 2012; Slatyer et al. 2013), then niche generalization could lead to slower rates of climatic niche evolution. In contrast, niche specialization might increase opportunities for speciation through local adaptation and divergent selection (Kozak and Wiens 2007; Birand et al. 2012), thereby promoting faster rates of climatic niche evolution (e.g., Kozak and Wiens 2010; Title and Burns 2015; but see Baselga et al. 2011).

Finally, the rate at which the climatic niche evolves may be more strongly associated with the variance in niche breadth among species within a clade than with how wide or narrow species' niches are (Fisher-Reid et al. 2012). Clades in which there is substantial variation in niche breadth among species may encompass more climatic space than those that generally contain species with wide (or narrow) niches, possibly leading to faster rates of niche evolution. For example, when the proliferation of species is linked to ecological opportunity (Yoder et al. 2010), the evolution of traits that promote (or limit) expansion of species in ecological space could influence rates of climatic niche evolution (Owens and Bennett 1995; Beaulieu and Smith 2009; Pöyry et al. 2009). In mammals and damselfish, trophic and dietary specialization constrains the exploration of environmental space, resulting in slower rates of climatic niche evolution in more specialized lineages (Cooper et al. 2011; Litsios et al. 2012).

Here, we examine the relationships among climatic niche breadth, life-history variation, and rates of climatic niche evolution in a salamander adaptive radiation. Plethodontid salamanders of the genus Desmognathus exhibit a wide range of variation in developmental life history, body-size, and microhabitat use that is exceptional among salamanders. The clade is unique among plethodontids in having species with direct development and aquatic larval periods (Hairston 1949). Body size-variation among Desmognathus species is also remarkable among vertebrate genera (Tilley and Bernardo 1993; Bruce 1996). Species in the clade partition niche space along a stream-to-forest floor microhabitat gradient, and larval development and body size covary with the position that species occupy across the gradient (Hairston 1949). Large-bodied species have multi-year aquatic larval periods and occupy the stream channel. Medium-sized

species have larval periods of 1 year or less and inhabit stream banks, seepages, and forest floor. The smallest species are fully terrestrial and exhibit direct development (lack of a free-living aquatic larval stage). Comparative phylogenetic analyses indicate the ancestral life history mode for Desmognathus is direct development and that the aquatic larval stage was re-evolved early in the evolution of Desmognathus (Titus and Larson 1996; Chippindale et al. 2004; Mueller et al. 2004), leading to a rapid accumulation of lineages and adaptive phenotypic disparity (Kozak et al. 2005).

Shifts in developmental life history may underlie variation in the rate of climatic niche evolution by promoting or restricting the exploration of climatic space. In order to reach reproductive maturity, Desmognathus species with long larval periods (2–4 years, Tilley and Bernardo 1993) require climates that maintain cool, fast-flowing streams with permanent flow regimes (Camp et al. 2000), conditions that are geographically localized in the southern Appalachian Highlands region within the clade's range. Similarly, although one might predict that direct developers would have fewer habitat constraints because they lack the requirement of aquatic microhabitats, their small size leaves them more susceptible to thermal and desiccation stress (Ray 1958; Tracy et al. 2010), which also restricts their geographic ranges to cooler, wetter climates. In contrast, given that species with short larval periods metamorphose rapidly (<1 year, Tilley and Bernardo 1993), they are more resistant to dehydration and thermal stress than small-bodied species, which may promote access to a greater range of climatic conditions.

In this study, we quantify the relationship between developmental life history (i.e., length of aquatic larval period), climatic niche breadth, and rates of climatic niche evolution in salamanders of the genus Desmognathus. We present phylogenetic hypotheses for the group based on 10 nuclear loci and one mitochondrial locus. Using this salamander clade as a case study, we illustrate how variation in a key life-history trait influences the rate of climatic niche evolution.

Methods

Phylogeny reconstruction

We obtained genomic DNA from 62 individual salamanders representing 24 taxa including: (1) 21 of the 22 currently recognized species of Desmognathus, missing only the newly described D. valentinei (Means et al. 2017), (2) two highly divergent mitochondrial lineages that may represent undescribed cryptic species (D. ocoee C and H, D. fuscus AB and C; Kozak et al. 2005), and (3) one Phaeognathus hubrichti, the sister taxon of Desmognathus (Titus and Larson 1996; Chippindale et al. 2004; Kozak et al. 2005, Kozak et al. 2009). We note that some recent studies suggest that D. auriculatus, D. conanti, D. fuscus, and D. ocoee may contain additional cryptic species that we have not included here (Beamer and Lamb 2008, 2020; Tilley et al. 2013; Pyron et al. 2020). All of these putative species belong to the life-history group with the fastest rate of climatic niche evolution (short larval period). Therefore, not including these putative cryptic species should not bias our findings given that incomplete taxon sampling is expected to underestimate evolutionary rates.

Many of our included samples were sequenced previously for the mitochondrial ND2 gene (Kozak et al. 2005). We sequenced the remaining individuals for ND2 following Kozak et al. (2005) and also obtained sequence data at 10 nuclear loci for all individuals. All loci were sequenced in both directions. Locus information, primer sequences, sources, and PCR conditions are provided in the online Dryad supplement (doi:10.5061/dryad.m0cfxpp0k). We visualized chromatograms, edited base calls, called heterozygous sites, trimmed flanking primer sequence, ensured an open reading frame in protein-coding sequence, and created contigs in Geneious (Kearse et al. 2012). We resolved length heterozygotes (due to polymorphic indels) with the aid of the program Indelligent (Dmitriev and Rakitov 2008a,b). We used MUSCLE (Edgar 2004) to generate alignments for each locus and visually inspected them for accuracy. For each nuclear locus, we used PHASE (Stephens et al. 2001) to phase alleles and then determined the best substitution model for each alignment using the Bayesian Information Criterion in jModelTest (Guindon and Gascuel 2003; Posada 2008).

We inferred a species tree with the 11-locus dataset using *BEAST in BEAST version 1.8.0 (Drummond et al. 2006; Heled and Drummond 2010). We partitioned sequence data by locus and further partitioned ND2 by codon position. We unlinked the

gene trees of each locus, gave each locus its own uncorrelated lognormal relaxed clock model (Drummond et al. 2006), and inferred a species tree under a birth-death speciation process. We conducted three independent searches of 500 million generations sampling every 10,000th. We viewed log files in Tracer version 1.6 (Rambaut et al. 2014) to ensure that tree -lnL values and parameter estimates had reached stationarity, independent runs converged on similar results, and Effective Sample Size (ESS) for all parameters was >200 when the three runs are combined (Drummond and Bouckaert 2015). We discarded 20% of initial species tree samples in each run as burn-in. We then used LogCombiner (Drummond and Rambaut 2007) to combine post-burn-in species trees from the three runs, resampling every fourth tree to yield 10,000 trees per run, 30,000 trees total. Finally, we used TreeAnnotator (Drummond and Rambaut 2007) to generate a maximum clade credibility species tree with mean node heights. Nodes were considered to have high support when the Bayesian posterior probability (PP) was ≥0.95. We acknowledge that the inferred species tree does not account for the possibility that gene flow between species may influence the reconstruction of phylogenetic relationships. However, recent work suggests that any reticulation events that occurred during the clades's evolutionary history are between species with short larval periods (Pyron et al. 2020). Therefore, we do not expect our evolutionary rate estimates to be confounded as a result of hybridization between species with different developmental life histories.

In addition to a species tree, we also ran a concatenated analysis using single exemplars of each of the 24 species. For the 10 nuclear loci, we used IUPAC ambiguity codes for heterozygous positions. We constructed a chronogram using BEAST version 1.8.0 (Drummond et al. 2006), which employs a Bayesian approach to simultaneously infer phylogenetic relationships and estimate divergence times. We partitioned sequence data by locus and further partitioned ND2 by codon position. We chose the most appropriate substitution model for each partition using jModelTest (Guindon and Gascuel 2003; Posada 2008). We gave each locus its own uncorrelated lognormal relaxed clock model (Drummond et al. 2006) and inferred a single tree from the 11-locus concatenated dataset under a birth-death speciation process. To calibrate the timescale of the tree, we used the age estimate for the most recent common ancestor (MRCA) of Desmognathus

and P. hubrichti from Kozak et al. (2009) to place a lognormally distributed prior (Mean = 37.0 million years, SD = 0.05) on the root age of the tree. Divergence times from Kozak et al. (2009) were based on a fossil-calibrated penalized-likelihood analysis of three mitochondrial genes (cytb, ND2, ND4) and three nuclear genes (BDNF, POMC, RAG1) for 184 plethodontid taxa. Although divergence time estimates for plethodontids vary among studies, ages from Kozak et al. (2009) are more similar to those of a recent study using 50 nuclear loci for a reduced set of plethodontid taxa (Shen et al. 2015). Our root age prior specified 95% of sampling to occur between 33.5 and 40.8 million years, allowing some uncertainty. Regardless, relative ages are more important than absolute ages for the questions being addressed here and thus, our choice of a root-age constraint should have little to no effect on results. We conducted two independent searches of 50 million generations sampling every 2000. We viewed log files in Tracer version 1.6 (Rambaut et al. 2014) to ensure that tree -lnL values and parameter estimates had reached stationarity, both independent runs converged on similar results, and Effective Sample Size (ESS) for all parameters was >200 (Drummond and Bouckaert 2015). We discarded 20% of initial tree samples as burn-in. We used LogCombiner and TreeAnnotator (Drummond and Rambaut 2007) to combine post-burn-in trees from the two runs and generate a maximum clade credibility tree with mean node heights. Nodes were considered to have high support when the Bayesian posterior probability (PP) was ≥0.95.

Ancestral state reconstruction

To reconstruct patterns of life-history evolution, we categorized species as having direct development (no free-living aquatic larval stage), long larval periods (>2 years), or short larval periods (<1 year). Life history and microhabitat associations of species are summarized in **Table 1.1**. We mapped ancestral life-history states along the species tree and the chronogram for the concatenated dataset using the continuous-time reversible Markov model in the make.simmap function in the R-package phytools version 0.6-60 (Revell 2012). We used a model assuming equal rates of transition between the three character states to perform 1000 stochastic-character mapping simulations. The resulting simmaps were used to test for differences in rates of climatic niche-evolution among

lineages with direct development, long larval periods, and short larval periods (see below).

Climate data, climatic niche breadth, and rates of climatic niche evolution

We mapped 2038 occurrence records obtained from published systematic studies and VertNet (vertnet.org). These records summarize the known distributions of the 24 species/lineages of Desmognathus and Phaeognathus included in the chronogram. The geographic distributions are well known for the species in this study, and the georeferenced samples span the geographic ranges of each species, ensuring that climatic variation is adequately represented. We plotted all points in ArcGIS version 9.3.1 to verify that georeferenced localities fit within the known geographic distribution of each species, and to ensure that points did not occur in the same 1 km2 grid cell, were reasonably spread across the extent of the known range, and were not clustered within particular areas. All occurrence records are available in the online Dryad supplement (doi:10.5061/dryad.m0cfxpp0k).

For each record, we extracted the values for five climatic variables from the WorldClim data set at 30 s (~1 km2) spatial resolution (Hijmans et al. 2005): Bio2, mean diurnal temperature range, Bio5 maximum temperature of the warmest month; Bio6, minimum temperature of the coldest month; Bio15, precipitation seasonality (calculated as the coefficient of variation in annual precipitation); and Bio17, precipitation of the driest quarter. Each of these variables represents one of a group of highly correlated variables ($r \geq 0.75$) that were identified from the Pearson-product correlation matrix of the 19 climatic variables in the WorldClim dataset. We then calculated the mean value for each of the five variables for each species. To characterize climatic variation across the geographic ranges of each species, we conducted a principal components analysis (PCA) on the correlation matrix of the five climatic variables.

Our analyses on the climatic niche assume that there is a relationship between climatic variation and the climatic tolerances of species and that the trait that actually evolves is the physiology that limits species' ranges (i.e., it is not the climatic variables that are evolving, but rather the association between climatic and physiological

variation). We also assume that a relationship exists between the realized climatic niche modeled by Maxent (Phillips and Dudík 2008) and the breadth of the fundamental climatic niche. Finally, we assume that our estimates of climatic niche breadth are not biased with respect to developmental life history. For example, if the climatic niche breadths of species with direct development and long larval periods are underestimated because factors other than climate limit their geographic ranges (e.g., competitors, predators), then rates of climatic niche evolution across species with short larval periods could also be underestimated, resulting in a spurious relationship between life history grouping and rates of climatic niche evolution. Recent work on plethodontids demonstrates strong correlations between estimates of climatic niche breadth calculated from climatic versus physiological data (Markle 2015). Moreover, mechanistic niche models based on physiology produce similar estimates of the contemporary geographic distributions of plethodontid species (e.g., Gifford and Kozak 2012; Lyons and Kozak 2020), Together, these findings suggest that violations of these assumptions should not bias our results.

To quantify the climatic niche breadth of each species, we first used MaxEnt version 3.4.1 (Phillips and Dudík 2008) to model the potential geographic distribution of each species based on its occurrence records and variation across the five climatic variables. Climate data layers were trimmed to an area that included the Ouachita Highlands and Eastern North America. Models were constructed using auto features and the default regularization multiplier. Model performance was evaluated by dividing species' occurrence records into training and test sets (75% vs 25%, respectively) and AUC (area under the curve). For all species, models strongly discriminated test localities from randomly selected background points (AUC $\geq$ 0.95). The models were then imported into ENMtools version 1.3 (Warren et al. 2010) to estimate the climatic niche breadth for each species. ENMTools treats suitability as proportional to utilization for the purposes of the breadth metrics, and calculates two niche breadth metrics, Levins' B1 and Levins' B2 (Levins 1968). Both metrics are based on the uniformity of each species' distribution in association with environmental variation, and higher values of each metric are associated with a broader climatic niche.

We used phylogenetic analyses of variance implemented in the R-package phytools version 0.6-60 (Revell 2012) to test whether species with direct development, long larval periods, and short larval periods differed in mean climatic niche breadth, with the life-history group membership of species as the factor and climatic niche breadth as the dependent variable.

We used two approaches that assumed a Brownian motion model of evolution to test whether lineages with direct development, long larval periods, and short larval periods have different rates of climatic niche evolution. First, we used the phytools brownie.lite function (Revell 2012), to test whether a model assuming different rates for the three life-history groups received greater support than one in which a single rate is assumed for all lineages. For this analysis, we estimated rates of evolution for the first two principal component axes, which explained 82% of the variation in climate.

Second, we used the compare.evol.rates function in the R-package geomorph (Adams and Otárola-Castillo 2013) to test whether multivariate rates of climatic niche evolution calculated using all five principal components differ among the three life-history groups. This method tests whether the observed rank-ordered ratio of the rates for different groups is significantly >1. Significance was evaluated by comparing the observed ratio to a distribution of possible ratios that is generated from phylogenetic simulations assuming the null hypothesis of no rate difference between groups (Adams 2014). We also performed the analyses on the species tree and the chronogram from the concatenated analysis with Phaeognathus hubrichti excluded to ensure that this outgroup was not driving any observed differences in rates of niche evolution between the three life-history groups.

Results

Phylogeny

The species tree inferred from 10 nuclear loci and one mitochondrial locus (6998 base-pairs) recovers some relationships in common with a previously published phylogeny of Desmognathus using only mtDNA (Mead et al. 2001; Rissler and Taylor 2003; Kozak et al. 2005; Beamer and Lamb 2008; Tilley et al. 2008), but also provides

some novel insight into the evolutionary history of the genus. As in prior studies, a clade containing the direct-developing D. wrighti + D. organi is resolved as the sister lineage to all remaining species of Desmognathus (**Fig. 1.1A**). Also, all taxa with an aquatic larval phase formed a clade with the direct-developing D. aeneus being the sister taxon to this clade (PP = 1.0). The D. quadramaculatus group (D. folkertsi + D. marmoratus + D. quadramaculatus) also formed a monophyletic group, although support was low (PP = 0.70). All other taxa with an aquatic larval phase formed a well-supported clade (PP = 1.0) sister to the D. quadramaculatus group. This clade includes D. imitator, which in previous studies was recovered as the sister taxon of the D. quadramaculatus group + all other biphasic taxa (Kozak et al. 2005). The remaining species are grouped into two well-supported clades that also parallel those recovered in previous studies, although most relationships within these clades have low support: (1) D. apalachicolae + D. conanti + D. monticola + two lineages of D. ocoee + D. santeetlah (PP = 1.0), (2) D. carolinensis + D. ochrophaeus + D. orestes + D. abditus + D. auriculatus + two lineages of D. fuscus + D. planiceps + D. welteri (PP = 0.92). Relationships among these two clades and D. brimleyorum, the lone species from the Interior Highlands, are unresolved. Direct development is inferred as the most likely ancestral life-history mode with an aquatic larval phase evolving a single time and long-larval periods evolving in parallel in the D. folkertsi + D. marmoratus + D. quadramaculatus clade, and in D. welteri.

Bayesian analysis of the concatenated nuclear and mitochondrial dataset (6998 base-pairs) resulted in a phylogeny in which most nodes were supported with posterior probabilities ≥ 0.95 (**Fig. 1.1B**). The two exceptions include the node grouping D. ocoee H + D. monticola (PP = 0.88) and the node grouping D. auriculatus and D. planiceps (PP = 0.94). As in the species tree, a clade containing D. wright + D. organi was resolved as the sister lineage to all remaining species of Desmognathus. However, the D. quadramaculatus group (D. folkertsi + D. marmoratus + D. quadramaculatus), which formed a clade in the species tree, is paraphyletic. Desmognathus imitator is resolved as the sister lineage to D. aeneus + a clade containing all remaining species that have free-living aquatic larvae. These remaining species are grouped into the same two clades as recovered in the species tree except that an undescribed lineage of "D. fuscus" (D.

fuscus C) from the South Carolina Piedmont (Kozak et al. 2005) is resolved as the sister species to clade 1 and D. brimleyorum is resolved as the sister species to clade 2. Notably, D. carolinensis is recovered as the sister taxon of a D. ochrophaeus + D. orestes clade in the concatenated tree. The concatenated analysis indicates that direct development was the likely ancestral life-history mode for Desmognathus, that an aquatic larval period evolved later in the evolutionary history of the clade, and that direct development and long aquatic larval periods evolved in parallel in D. aeneus and D. welteri, respectively

Climatic niche evolution

Principal components analysis separated species along axes reflecting variation in precipitation and seasonality of temperature (PC1), and average annual temperature and extremes of temperature (PC2). Together, the first two principal components accounted for 82% of the variation in climate among species (**Table 1.2**).

Climatic niche breadth varied widely among species (**Table 1.1**). Species with the widest niche breadths have short larval periods (**Table 1.1**), and overall the total climatic space occupied by species with short larval periods was greater than that for species with long larval periods or direct development (**Fig. 1.2**). However, species in the three life-history groups did not differ significantly in climatic niche breadth (phyANOVA: P = 0.492–0.672).

When rates of climatic niche evolution were calculated separately for PC1 and PC2 , brownie.lite supported models where the three different life-history groups had different rates for PC1, but not PC2 (PC1: P = 0.003 ; PC2: P = 0.125). On average, species with long larval periods had the slowest rate, direct developers were intermediate, and species with short larval periods had the fastest rate (**Table 1.3; Fig. 1.3)**. These results are for the species tree and were qualitatively unchanged for the concatenated data chronogram (**Table 1.4, Fig. 1.4**) and when P. hubrichti is excluded (results not shown).

Multivariate rates of climatic niche evolution also differed with respect to life history mode (**Tables 1.3 and 1.4**). Species with long larval periods have the slowest rate of climatic niche evolution ($\sigma 2$ = 0.999). Direct-developing species exhibit an

intermediate rate ($\sigma^2 = 2.024$), and species with short larval periods exhibit the highest rate of climatic niche evolution ($\sigma^2 = 12.733$). In pairwise comparisons of rate ratios, the short larval period group significantly differed from both other life-history groups in their rates of climatic niche evolution (σ^2short larval period/σ^2direct development = 6.291, $P < 0.001$; σ^2short larval period/σ^2long larval period = 12.746, $P < 0.001$). However, there was no significant difference in rates between the long larval and direct developing groups (σ^2direct development/σ^2long larval period = 2.022, $P = 0.273$). The rate ratios and P-values reported above are taken from the multivariate analysis of the species tree; the results were qualitatively unchanged for the analysis of the concatenated data chronogram, and when P. hubrichti is excluded.

Discussion

Rates of climatic niche evolution vary widely across the tree of life (Jezkova and Wiens 2016) and are strongly associated with the accumulation of species diversity among clades (Kozak and Wiens 2010, 2016; Title and Burns 2015). The rate at which the climatic niche evolves might also be important for buffering clades and species from extinction in a rapidly changing global climate (Quintero and Wiens 2013; Jezkova and Wiens 2016). However, few studies have addressed why the climatic niches of some species evolve more rapidly than others (e.g. Lawson and Weir 2014; Pie et al. 2017) Here, we showed that variation in life history (i.e. larval development time) is associated with differential rates of climatic niche evolution, likely by constraining (or promoting) the exploration of climatic niche space.

Many studies suggest that rates of climatic niche evolution should be associated with climatic niche breadth (Fisher-Reid et al. 2012). On average, climatic niche breadth does not differ among species in the different life-history groups. Indeed, Desmognathus species with direct-development, short, and long larval periods are concentrated in montane habitats in the southern Appalachian Highlands leading to this conserved pattern. Only species with short larval periods have been able to expand into the surrounding warmer, drier climates that are currently found at lower elevations. As a

result, species with short larval periods have evolved more rapidly in climatic niche space than those with long larval periods or direct development.

The strong linkage between developmental life history and rates of climatic niche evolution is likely explained by a combination of intrinsic and extrinsic factors that govern the distribution of species in climatic space. We hypothesize that ecological and physiological constraints underlie the slower rates of climatic niche evolution across species with direct development and long aquatic larval periods. Climatic conditions for species with direct development and long-aquatic larval conditions (i.e., cool, wet) are generally restricted to the southern Appalachian Highlands, limiting opportunities for expansion into adjacent, low-elevation regions in eastern North America where the climates are warmer and drier. Conversely, species with short larval periods metamorphose rapidly (<1 year) and are also larger in size than miniaturized direct-developing species (D. aeneus, D. organi, and D. wrighti) making them less susceptible to thermal and dehydration stress (Ray 1958; Tracy et al. 2010). Thus, species with short larval periods have been able to colonize a wide range of climates found across highland and lowland regions of eastern North America where streamside and seepage microhabitats dry intermittently, resulting in faster rates of climatic niche evolution. Intriguingly, extensive overlap (ecological interactions) among coexisting clades appears to constrain rates of climatic niche evolution in plethodontids (Kozak and Wiens 2010), suggesting that evolution of a short larval period may have increased rates of climatic-niche evolution by providing ecological access to new climatic niches beyond the southern Appalachians where few species of Desmognathus are sympatric. Phenotypes that promote access to a greater range of climatic conditions also seemingly underlie faster rates of climatic niche evolution in mammals (Cooper et al. 2011) and damselfish (Litsios et al. 2012), suggesting that similar processes may explain variation in rates of climatic niche evolution across a wide range of taxa.

Our results have important implications for understanding the accumulation of species over time, as they imply that increases in rates of climatic niche evolution may also underlie increases in diversification rates. Following the origin of a biphasic life history, the rate of diversification in Desmognathus increased rapidly as species diverged

in body size, larval-period length, and microhabitat use along an aquatic-terrestrial gradient (Kozak et al. 2005). This shift in life history seemingly promoted ecological access to an aquatic adaptive zone, resulting in rapid adaptive diversification as species radiated into stream, stream-edge, and seepage microhabitats (Chippindale et al. 2004; Kozak et al. 2005). Our results suggest that rapid rates of climatic niche evolution across species with short larval periods were also an important dimension of this clade's adaptive radiation and likely contribute to the rapid rate of diversification following the evolution of an aquatic life history in the clade.

Faster rates of climatic niche evolution are associated with increased rates of diversification across a range of taxa (Evans et al. 2009; Kozak and Wiens 2010, 2016; Title and Burns 2015; Castro-Insua et al. 2018). In plethodontid salamanders, sharper climatic zonation of tropical mountains seemingly increases opportunities for diversification, and explains variation in rates of climatic niche evolution among major clades (Kozak and Wiens 2007, 2010). However, there is also great variation in rates of climatic niche evolution among plethodontid clades that are restricted to tropical versus temperate regions (Kozak and Wiens 2010). Among temperate plethodontid clades, rates of diversification and climatic niche evolution are rapid in Desmognathus (Kozak and Wiens 2016). How might evolution of the climatic niche promote diversification in this adaptive radiation (and possibly others)?

Many studies have linked life-history variation with physiological diversity and diversification rates (Winemiller and Rose 1992; Ricklefs and Wikelski 2002; Goldberg et al. 2010). Among species of Desmognathus with short larval periods, there is substantial variation in thermal physiology (i.e., thermal tolerance breadth, thermal acclimation capacity, and metabolic rate) that is associated with how restricted or widespread species are (Bernardo et al. 2007; Kearney and Porter 2009; Markle 2015; Markle and Kozak 2018). In temperate regions like North America, where the climate has been unstable over space and time, the ability to tolerate and to exploit a wider diversity of climatic conditions may promote speciation and the long-term persistence of lineages (Jansson and Dynesius 2002). For example, if some species can expand their climatic niches to occupy areas in which other lineages cannot persist, this could increase

opportunities for isolation and speciation (Kozak and Wiens 2010; Sobel et al. 2010; Yoder et al. 2010). A capacity for rapid climatic niche evolution may also make species less susceptible to extinction during periods of climate change (Holt 1990; Carlson et al. 2014), resulting in higher diversification rates.

In summary, variation in rates of climatic niche evolution is associated with patterns of diversification and species richness across a wide variety of taxa. Yet, traits underlying divergence of the climatic niche have rarely been studied. Our results show how variation in a key life-history trait (larval development time) can constrain or promote divergence of the climatic niche. Overall, we find no support for a direct link between species' climatic niche breadths and rates of climatic niche evolution; species with different larval development times have similar climatic niche breadths. Instead, the evolution of a short larval period promotes greater variance in climatic niche breadth and rapid exploration of climatic space, leading to increased rates of climatic niche evolution across species having this trait. A deeper understanding of the mechanistic basis of this pattern will require further comparative phylogenetic study of the relationship between life history and key physiological traits that govern the distribution of lineages in climatic and geographic space

Figures and Tables

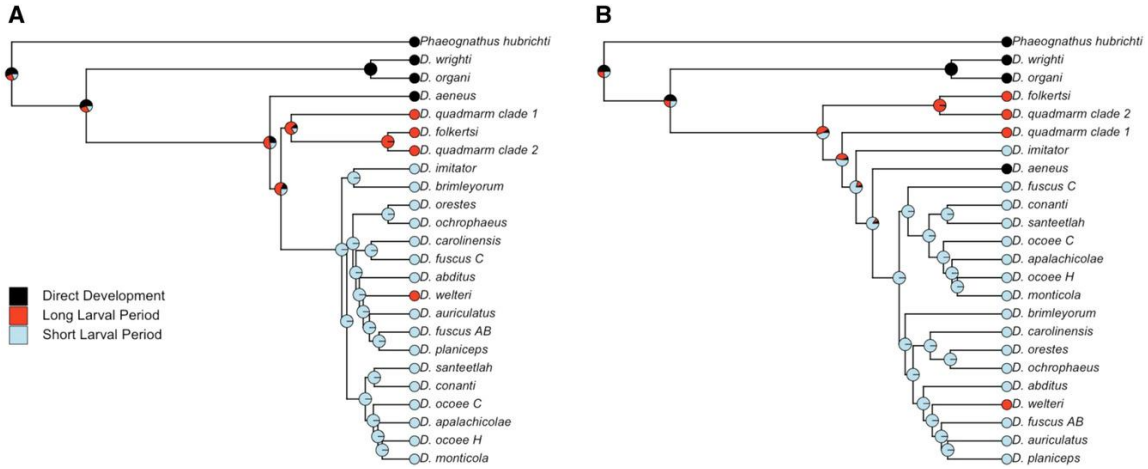

Figure 1.1: Ancestral state reconstruction. (A) Species tree of *Desmognathus* based on 11 loci with mapped ancestral-state likelihoods, support values for all species tree nodes can be found in the online Dryad supplement. (B) Chronogram of *Desmognathus* based on a concatenated alignment of 11 loci with mapped ancestral-state likelihoods. All nodes have a posterior probability ≥ 0.95, except for *D. ocoee* H + *D. monticola* (PP = 0.88), and *D. auriculatus* + *D. planiceps* (PP = 0.94).

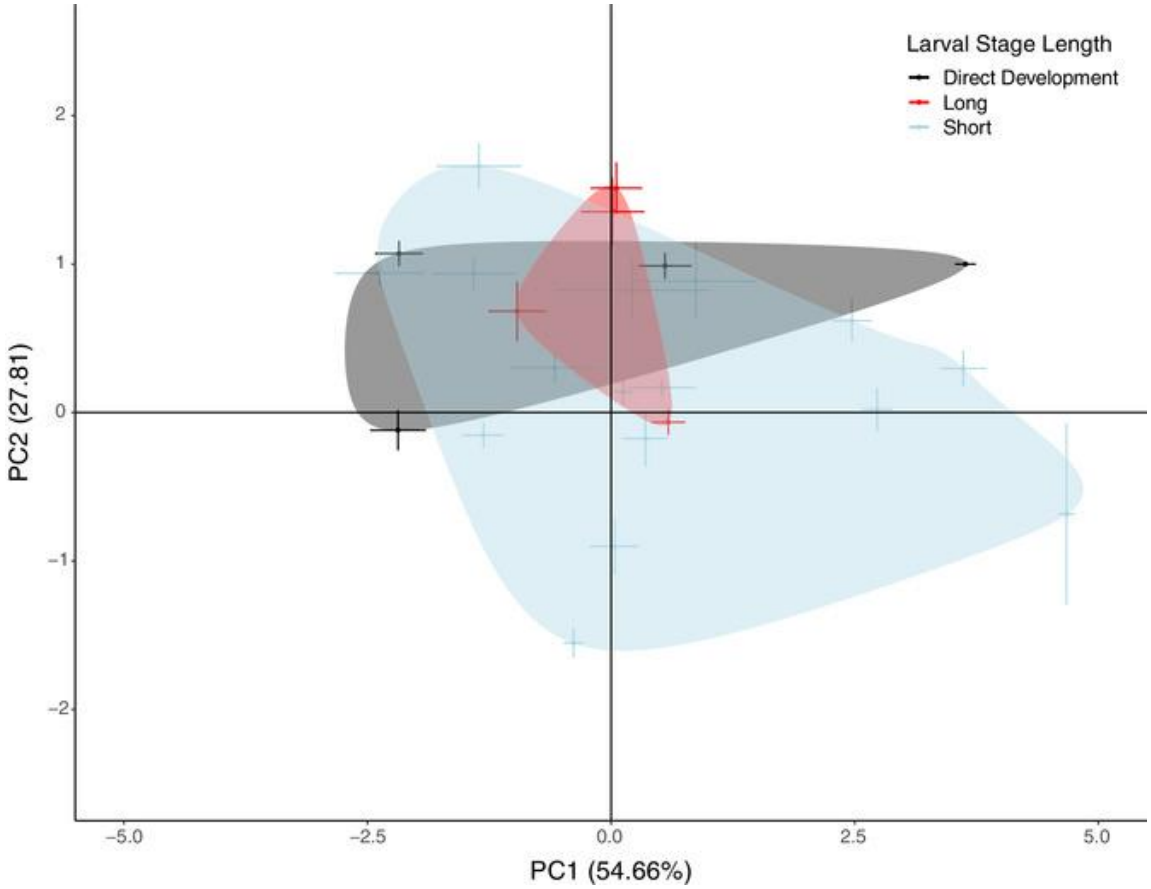

Figure 1.2: Species climatic niche position. Visualization of the climatic niche space occupied by the three life-history groups in this study.

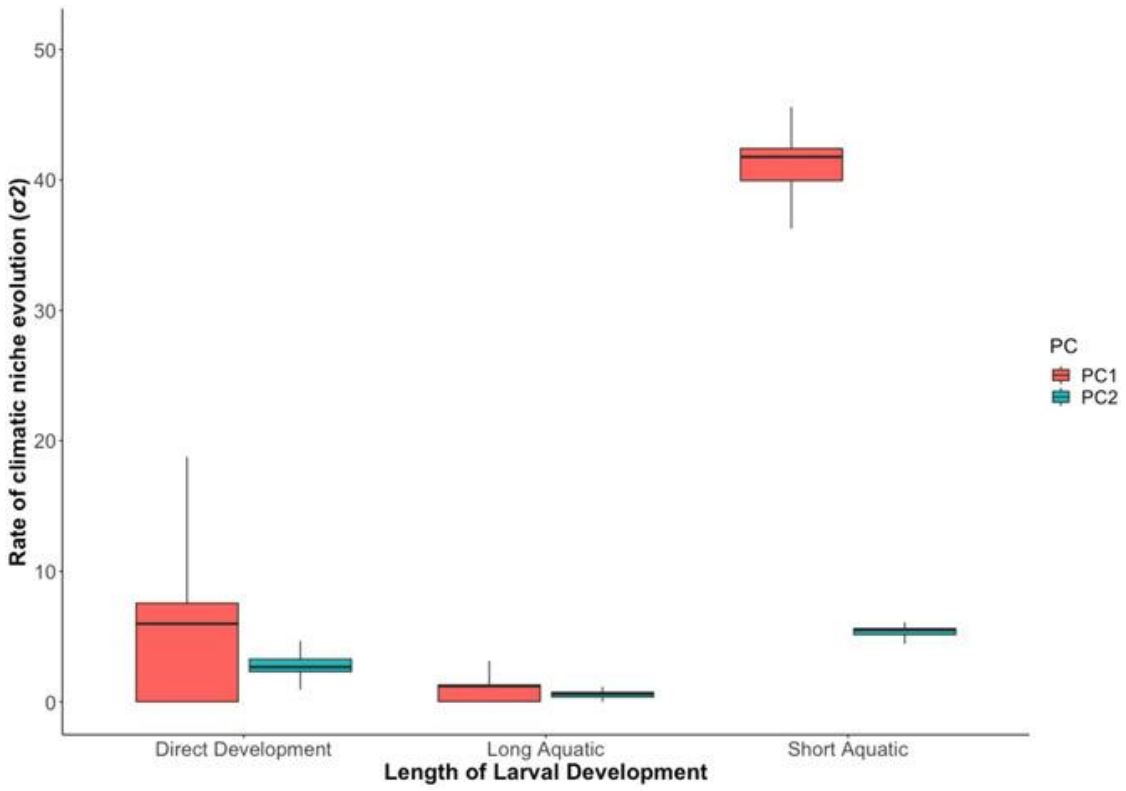

Figure 1.3: Climatic niche evolution rate estimates- species tree. Rates of climatic niche evolution for each life-history group along the first two principal component axes for the species tree

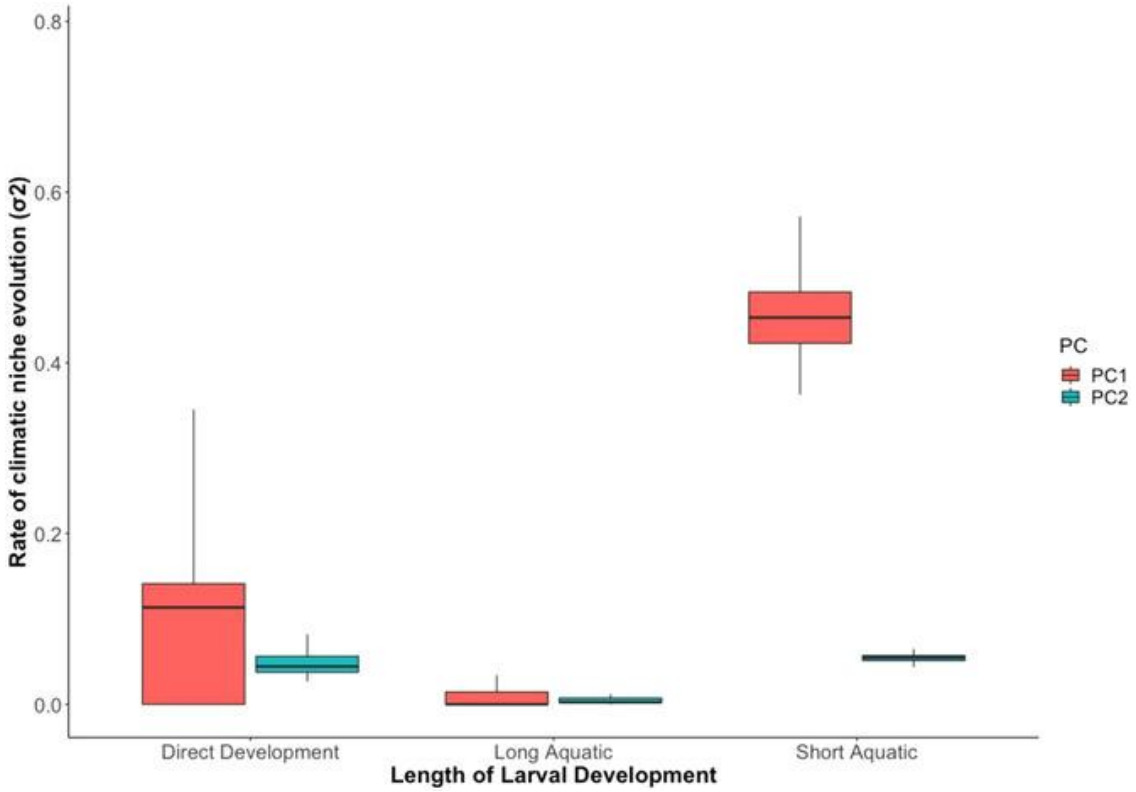

Figure 1.4: Climatic niche evolution rate estimates- concatenated alignment. Rates of climatic niche evolution for each life-history group along the first two principal component axes for the concatenated alignment.

Species	Microhabitat	Larval Period	Levins' B1	Levins' B2
D. abditus	seepage	short	0.016	0.769
D. aeneus	terrestrial	direct development	0.02	0.79
D. apalachicolae	seepage	short	0.04	0.823
D. auriculatus	stream edge	short	0.082	0.854
D. brimleyorum	stream edge	short	0.022	0.813
D. carolinensis	seepage	short	0.009	0.751
D. conanti	stream edge	short	0.192	0.906
D. folkertsi	stream edge	long	0.004	0.701
D. fuscus AB	stream edge	short	0.188	0.915
D. fuscus C	stream edge	short	0.072	0.866
D. imitator	seepage	short	0.002	0.672
D. monticola	stream edge	short	0.096	0.875
D. ochrophaeus	seepage	short	0.078	0.86
D. ocoee C	seepage	short	0.005	0.726
D. ocoee H	seepage	short	0.011	0.747
D. orestes	seepage	short	0.006	0.723
D. organi	terrestrial	direct development	0.003	0.689
D. planiceps	stream edge	short	0.011	0.743
D. quadramaculatus	stream	long	0.009	0.752
D. marmoratus	stream	long	0.015	0.782
D. santeetlah	stream edge	short	0.005	0.714
D. welteri	stream edge	long	0.029	0.803
D. wrighti	terrestrial	direct development	0.003	0.698
Phaeognathus hubrichti	terrestrial	direct development	0.002	0.643

Table 1.1: **Larval period designations and niche breadth metrics.** Microhabitat, larval group designation, and values for two niche breadth metrics (Levins 1968) for Desmognathus species included in this study. Microhabitat categories follow Kozak et al. (2005). Larval period data are from Tilley and Bernardo (1993) and Kozak et al. (2005).

Variable	PC1	PC2	PC3	PC4	PC5
BIO2	0.72	−0.36	−0.57	0.14	−0.07
BIO5	0.97	−0.08	0	−0.10	0.21
BIO6	0.69	−0.59	0.36	−0.17	−0.12
BIO15	0.76	0.47	0.33	0.3	−0.03
BIO17	−0.46	−0.83	0.18	0.24	0.08
Eigenvalue	2.73	1.39	0.59	0.21	0.07
% Variation	54.66	27.81	11.8	4.25	1.48

Table 1.2: Climatic PCA loadings. Factor loadings and eigenvalues from the principal-components analysis of the five environmental variables. PC1-PC2 explained 82% of the variation

Larval Stage	PC1 σ	PC2 σ	σ (multivariate)
Direct Development	6.528	2.935	2.024
Long	1.45	0.554	0.999
Short	40.897	5.348	12.733

Table 1.3: Species tree climatic niche evolution rates. Rates of climatic niche evolution for each life-history group along the first two principal component axes for the species tree.

Larval Stage	PC1 σ	PC2 σ	σ (multivariate)
Direct Development	0.012	0.047	0.035
Long	0.113	0.005	0.012
Short	0.459	0.055	0.148

Table 1.4: Concatenated alignment climatic niche evolution rates. Rates of climatic niche evolution for each life-history group along the first two principal component axes for the concatenated alignment.

CHAPTER 2
Warming temperatures influence the dynamics of a salamander hybrid in the Southern Appalachian Mountains.

Abstract

Climate change has facilitated shifts in the distributions of many species, oftentimes bringing previously isolated lineages into contact with one another. When these lineages meet, they may produce offspring if there are insufficient barriers to reproduction, leading to the formation of hybrid zones. If the two hybridizing species are adapted to different environments, these hybrid zones may form along environmental clines in latitude or elevation. The lungless salamander *Plethodon shermani* is distributed across multiple mountaintop isolates and frequently hybridizes with its congener, *Plethodon teyahalee,* at the lower edge of its elevational range. In this study, we use ddRAD sequencing to explore genome-wide patterns of introgression across four hybrid zones to assess whether ecological selection maintains species boundaries in this system, and how warming climatic conditions may impact the outcome of hybridization between these species. At all four hybrid zones, significant introgression was detected between *P. shermani* and *P. teyahalee* populations along the elevational gradient which spans the two parental populations. Introgression appears to be widespread and asymmetric from *P. teyahalee* into *P. shermani*, particularly in loci that may potentially be involved in local adaptation. The findings presented here, combined with past studies in this system, all point towards a hybrid zone strongly regulated by ecological factors, especially elevational variation in climate. As the Appalachians continue to warm, these findings suggest that all *P. shermani* isolates are in danger of genomic extinction due to genetic swamping by the introgression of *P. teyahalee* alleles as the hybrid zone continues to move upwards in elevation.

Introduction

Periods of climate change often facilitate the expansion or movement of species' ranges as they track the conditions to which they are adapted (Parmesan and Yohe 2003; Root et al. 2003; MacLean and Beissinger 2017). Global temperatures have steadily

climbed since the last glacial maxima ~20,000 years ago, and anthropogenic activities have more recently contributed to rapid changes in the Earth's climate (Prentice et al. 1991; Smith et al. 1999). This change in climate has facilitated shifts in many species distributions, leading to the formation of hybrid zones where previously isolated species come into secondary contact with one another. (Brennan et al. 2014; Chunco 2014; Grabenstein and Taylor 2018). Hybridization can result in a number of evolutionary outcomes. Speciation can occur when the novel genotypic combinations in hybrid offspring result in new traits that can contribute to isolation and diversification (Mallet 2007; Keller et al. 2013; Richards and Martin 2017). On the other hand, genetic swamping of one species by the other can lead to genomic extinction as one or both pure parental genotypes are lost to introgression (Rhymer and Simberloff 1996; Todesco et al. 2016). This is more likely if the two hybridizing species freely breed with one another without fitness consequences in admixed individuals (Coleman et al. 2014; Bog et al. 2017). A third result, however, occurs when backcrossing is limited and species boundaries remain intact, leading to the formation of a stable hybrid zone (Moore 1977; Barton 1979; Barton and Hewitt 1985).

Stable hybrid zones provide a useful system in which to investigate the effects of different environmental and intrinsic factors that contribute to reproductive isolation in different systems (Anderson 1948; Barton and Hewitt 1989), especially since many hybrid zones form along ecological gradients in latitude (Garroway et al. 2010; Taylor et al. 2014; Calfee et al. 2020) and elevation (Rasmussen et al. 2012; Abbott and Brennan 2014; DuBay and Witt 2014; Filatov et al. 2016). In these systems, hybrids form, but hybridization is limited to a narrow part of the geographic range of both parental species due to selection against hybrids and limited dispersal out of the hybrid zone (Barton and Hewitt 1985; Rand and Harrison 1989; Curry 2015). Different selective forces, both endogenous and exogenous, act within stable hybrid zones to limit introgression between parental species and maintain species boundaries. Endogenous selection is independent of the environment, and selects against hybrids due to genetic incompatibilities that form as a result of divergence between the parental species (Barton 1980; Turner et al. 2012; Blanckaert and Payseur 2021). Likewise, the breakdown of adaptive gene complexes in

hybrids often reduces fitness or fertility in advanced hybrids while not reducing fitness in F1 hybrids, limiting backcrossing and introgressionbetween species (Barton and Hewitt 1981; Muhlfeld et al. 2009; Gibson et al. 2013; Lafon-Placette and Köhler 2015; Stelkens et al. 2015).

Exogenous factors, such as environmental selection and competitive interactions, also play an important role in maintaining species boundaries, especially when the hybridizing species are adapted to different environments (Barton and Hewitt 1985; Jiggins and Mallet 2000; Swenson 2006). Adaptive differences between species should limit the free exchange of genes between them, since alleles which are better suited for opposing environmental conditions in one species may reduce fitness if they are introgressed into the other species (Barton and Hewitt 1985; Wolf et al. 2001). Hybrids also frequently suffer reduced fitness if they exhibit intermediate phenotypes which are unfit in the habitat of either of the parental species (Rice and Hostert 1993; Hatfield and Schluter 1999).

Hybrid zones limited by ecological selection have shifted upwards in elevation and latitude as species track their ecological niches (Taylor et al. 2014; Billerman et al. 2016; Ryan et al. 2018; Wielstra 2019). In montane systems, the rates of this upward shift have accelerated as warming rates have increased (Chen et al. 2009, 2011). As warming persists, montane endemic species find themselves on an "escalator to extinction," being pushed to higher and higher elevations until they run out of suitable habitat in which to shift (Freeman et al. 2018; Urban 2018). As lower elevation species are increasingly able to persist in the habitat of the high elevation specialist, the hybrid zone will shift upward in elevation as the fitness differential that limited introgression between the species becomes negligible. This may lead to increased introgression of DNA from the low elevation species into the high elevation species, resulting in genetic swamping and genomic extinction of the high elevation specialist (Gómez et al. 2015; Bog et al. 2017).

The lungless salamander *Plethodon shermani* is native to the southern Appalachian Mountains and occurs across multiple mountaintop isolates (Stejneger 1906). *P. shermani* is known to frequently hybridize with other congeneric species at the lower edge of its elevational range, particularly *Plethodon teyahalee* (Highton and

Peabody 2000). *Plethodon shermani* is characterized by bright red legs and uniform, black dorsal coloration. *Plethodon teyahalee* lacks red legs but exhibits extensive white spotting on its back and sides (**Fig. 2.1**). Phenotypic data suggests that the number of individuals exhibiting more *P. teyahalee*-like traits has increased at intermediate and higher elevations, suggesting an upward shift in elevation of this hybrid zone as climate change makes the Appalachian mountains warmer (Walls 2009). Global Circulation Models predict that climate change will lead to higher temperatures across the Appalachians (Flato and Boer 2001, Johns et al. 2003). This may facilitate increased introgression of *P. teyahalee* alleles at higher elevations resulting in swamping of high-elevation *P. shermani* populations as seen in other montane hybrid zones impacted by climate change (Muhlfeld et al. 2014). This may have already occurred at some hybrid zones between *P. shermani* and *P. teyahalee*, as two mountaintop populations of *P. shermani* individuals exhibit mitochondrial haplotypes of *P. teyahalee*, whereas almost no *P. teyahalee* individuals possess *P. shermani* mitochondrial haplotypes. This suggests a directional exchange of genetic material from female *P. teyahalee* to *P. shermani* (Weisrock et al. 2005).

Here, we use genomic data to explore the evolutionary dynamics of four hybrid zones between *P. shermani* and *P. teyahalee* in the southern Appalachian mountains. We characterize the genetic structure of these hybrid zones by assessing genetic differentiation within and between species. To determine whether any pure *P. shermani* populations remain, we assess the extent of admixture between *P. shermani* and *P. teyahalee* across each hybrid zone and conduct tests for introgression. To determine the relative contributions of intrinsic and extrinsic factors in maintaining the boundaries between these two species, we use genomic clines to identify loci that may resist introgression. We also test for asymmetric gene flow that may facilitate lineage merging and swamping to determine if warming conditions have favored increased introgression of *P. teyahalee* alleles. Finally, we assess whether variation in color morphology, used in previous studies in this system, is a good predictor of genetic composition of hybrid and parental genotypes. These analyses inform our understanding of whether *P. shermani* and *P. teyahalee* can remain distinct species across their range in the face of climate change.

Methods

Sample Collection

Tissue samples used in this study were taken from tail tips collected from 2010 to 2011 along four contact zones between *Plethodon shermani* and *P. teyahalee* in the Southern Appalachian mountains (**Fig. 2.1**). At each hybrid zone, individuals were captured along an elevational transect consisting of six sites, with the lowest sites intended to capture the "pure" *P. teyahalee* genotype in each hybrid zone and the highest sites intended to represent pure *P. shermani* genotpes. The Snowbird Mountain hybrid zone is located in the Unicoi subrange of the Appalachians, and has the lowest maximum elevation of all four hybrid zones sampled. This hybrid zone, notably, lacks any individuals with completely red legs even at the highest elevation site. The Fire's Creek contact zone is in the Tusquitee mountains, but we were unable to sequence any individuals from intermediate populations at this transect. Wayah Bald and Coweeta, the final two hybrid zones, are both located in the Nantahala mountains and have the highest maximum elevations of all four hybrid zones. At Coweeta, four additional sites were sampled in 2019 for a total of ten sites.

At Snowbird, we sequenced 12 samples from the lowest site, 30 samples from intermediate sites, and 13 samples from the highest site (55 total). At Fire's Creek, we sequenced 5 samples from the lowest and highest sites (10 total). At Wayah, we sequenced 10 individuals from the lowest site, 26 individuals from intermediate sites, and 6 individuals from the highest site (42 total). At Coweeta, we obtained 15 samples from the lowest elevation site, 16 samples from two high elevation sites, and 38 samples from sites at intermediate elevations (69 total).

For a subset of individuals (n = 106), color scores were calculated using the morphological scoring system of Hairston et al. (1992). When selecting samples for genomic sequencing, we chose to maximize the diversity of phenotypic scores at each site in order to assess the relationships between color score and genomic composition.

Outgroup samples (*P. metcalfi* and *P. cinereus*) were captured in 2009, and were obtained from the Genetic Resources collection from the Bell Museum of Natural History.

DNA extraction and sequencing

The University of Minnesota Genomics Center (UMGC) used Qiagen's DNeasy Blood & Tissue kit to extract DNA from tail tips. The UMGC performed genotyping-by-sequencing (GBS) with a double-digest Restriction site-Associated DNA (ddRAD) protocol. Briefly, 100 ng of DNA was digested with 10 units each of *TaqI* and *SbfI* restriction enzymes and incubated at 37°C for 2 hours. Enzymes were heat inactivated at 80°C for 20 minutes. Samples were then ligated with 200 units of T4 ligase (NEB) and phased adaptors with GATC and TGCA overhangs at 22°C for 1 hour. Ligase was then heat killed, and the ligated samples were purified with SPRI beads and then amplified for 18 cycles with 2X NEB Taq Master Mix to add barcodes. Libraries were purified, quantified, pooled and size selected for the 238-370bp library region, and diluted to 2 nM for sequencing on the Illumina NextSeq 550 using single-end 1X100 reads in three separate batches.

Variant calls

Raw reads were cleaned using a custom script and processed with Stacks v. 2.5 (Catchen et al. 2011; Rochette et al. 2019). Since there is no reference genome available for any *Plethodon* species, all loci were constructed using the de novo Stacks pipeline. In UStacks, each haplotype had to be covered by at least three reads, and up to three mismatches between reads were allowed to be in the same haplotype. For CStacks, we allowed three mismatches between haplotypes from the same sample for building the consensus sequence in the catalog file. In populations, we required that each locus be present in at least one sample per population and that the locus be present in at least 10% of all samples. We also excluded singletons, sites missing in more than 30% of individuals, and sites with a read depth lower than 10, as well as sites with a read depth higher than 40. We removed any non-outgroup individuals with more than 30% missing data. This resulted in a VCF containing 400,764 sites and 183 individuals. We further

filtered the VCF to thin sites for linkage disequilibrium by keeping only one site per RAD locus. This dataset consisted of 68,123 sites. ADMIXTURE can only run on datasets with fewer than 45,000 loci, so we further filtered the LD-thinned dataset to exclude sites missing in more than 20% of samples to meet that requirement (43,985 SNPs).

Population Structure

We implemented both ordination and model-based approaches to investigate patterns of population structure among and within hybrid zones for *Plethodon shermani* and *P. teyahalee* samples. We performed a genomic principal components analysis (PCA) using the SNPRelate v1.24 package (Zheng et al. 2012) in R. We also used the model-based genetic assignment method implemented by ADMIXTURE v1.3 (Alexander et al. 2009) to identify genetic populations. ADMIXTURE was run in two different ways. First, we ran the program including every sample from all four hybrid zones. We also ran ADMIXTURE separately for each of the three hybrid zones for which we had samples from intermediate elevational sites (Coweeta, Wayah Bald, and Snowbird Mountain). For all ADMIXTURE runs, we implemented the block optimization method with a convergence criterion of $\epsilon = 10{-}4$, and used 5-fold cross-validation to assess model performance. We used the results of ADMIXTURE to designate individuals as parental *P. shermani* or *P. teyahalee* within each transect. Individuals were assigned to parental populations if they had a score of 0.9999 for either *P. teyahalee* or *P. shermani* ancestry. We designated these individuals as parental *P. shermani* or parental *P. teyahalee* for the calculation of divergence metrics among and within all hybrid zones.

To better understand the degree of differentiation and divergence among and within the *P. shermani* and *P. teyahalee* isolates from the sampled transects, we estimated pairwise measures of absolute divergence (D_{XY}) and relative differentiation (Weir and Cockerham's F_{ST}) among parental populations across all four transects. D_{XY} was calculated as the average number of pairwise differences between populations using a custom python script, and Weir and Cockerham's F_{ST} was calculated at each locus and at the population level using vcftools v0.1.17 (Danecek et al. 2011).

Association between color score and genomic hybrid index

To determine whether color scores are a good indicator of the genetic composition of individuals collected across hybrid zones, we collected color morphology data for individuals sampled at intermediate sites and two parental populations at Coweeta. Color scores were calculated using the morphological scoring system of Hairston et al. (1992), with white dorsal spotting associated with *P. teyahalee* ancestry and red legs associated with *P. shermani* ancestry. These scores range from 0 to 3. To calculate a composite score, we subtracted the spot score from the leg score. A score of 0 for red legs indicates no red pigmentation on any of the four legs, while a score of 3 indicates abundant red pigmentation on all four legs. A score of 0 for white spots corresponds to no dorsal spotting, while a score of 3 indicates abundant spotting on the back and sides. We constructed a mixed linear model with transect included as a random effect to determine whether this composite color score, which has been used in other studies as a proxy for hybrid index (Hairston Sr. et al. 1992; Walls 2009; Lowe 2016), is associated with genomic composition (hybrid index derived from K=2 admixture proportion within each transect).

Tests for introgression

To assess the levels of introgression among *P. teyahalee* and *P. shermani* at different transects, we used the used the program Dsuite (Malinsky et al. 2021) to calculate D statistics (ABBA/BABA) and f4 ratios between parental isolates of each species as defined in Patterson et al. 2012. For all ABBA/BABA comparisons and calculations of f4 ratios, *P. metcalfi* samples were used as an outgroup and three *P. shermani / P. teyahalee* isolates were compared for tree-like relationships among them (**Fig. 2.2)**. To calculate standard errors and assess the significance of D statistics, we used a jackknife approach separating SNPs into blocks of 500 sites.

Genomic clines

To identify loci that may resist introgression between *P. shermani* and *P. teyahalee* and assess whether there is asymmetric gene flow from *P. teyahalee* into *P. shermani*, we used the Bayesian genomic cline approach implemented in the program bgc (Gompert and Buerkle 2011, 2012). Given the high degree of genetic differentiation among *P. shermani* isolates, we conducted genomic cline analyses separately for each hybrid zone. Bgc requires that population assignment (P1, P2, or admixed) is done before running the program. Parental and admixed population designations for each individual were assigned based on hybrid index values obtained from the K=2 runs of ADMIXTURE when run separately for each hybrid zone. If an individual had a score of 0.9999 for either *P. teyahalee* or *P. shermani*, they were assigned to the parental populations. All other samples were designated as hybrids. For our bgc runs, we used the LD-thinned genomic dataset (68,123 loci). We ran two iterations of bgc for each of the three hybrid zones that were sampled, and used these runs to assess convergence of the MCMC chains. For each chain, we incorporated a genotype uncertainty error of 0.0001. Each run consisted of 50,000 MCMC steps with the first 5,000 steps discarded as a burn-in, and we retained every 25th value. Parameter convergence was assessed visually.

After running bgc, we used the R package ClineHelpR (https://github.com/btmartin721/ClineHelpR) to visualize clines and identify outlier loci. We were primarily interested in two parameters generated by bgc; α and ß. The α parameter estimates the center of the genomic cline, which represents the probability of ancestry from one species or another at a locus given the genome-wide admixture proportion. α outliers represent loci that have more ancestry than expected from one parental species given the genetic background of the individual, and can be interpreted as alleles introgressing from the species that the center is biased towards into the other species. The ß parameter represents the steepness of the genomic cline, or the rate of transition in the probability of ancestry from one species to the other. ß outliers represent alleles that either resist introgression (positive outliers) or introgress at a higher rate than the genomic background (negative outliers). Loci were designated as outliers under one of two scenarios. First, if the credibility interval of the posterior probability distribution

of α or ß excluded zero, the locus was designated as an outlier. Second, if the posterior estimate of α or ß for an allele was not contained in the interval bounded by the 0.025 and 0.975 quantiles of all estimates for that parameter, the locus was identified as an outlier.

Fst outliers

We were interested in identifying loci that exhibit high levels of differentiation between species, since such loci are more likely to have been influenced by divergent selection than nonoutlier loci (Beaumont and Nichols 1996; Nosil et al. 2009b; Gompert and Buerkle 2011b) We generated pairwise levels of differentiation between parental isolates by calculating Weir and Cockerham's F_{ST} among all pairs of parental populations using vcftools. We also calculated locus-specific Weir and Cockerham's F_{ST} between each pair of parental populations within each hybrid zone to identify loci that exhibit the highest levels of differentiation between *P. shermani* isolates and *P. teyahalee*. We identified outlier F_{ST} loci as loci that were in the 95th percentile or higher of Fst values across all sites. Since these loci are more likely to have been influenced by divergent selection than nonoutlier loci (Beaumont and Nichols 1996; Nosil et al. 2009b; Gompert and Buerkle 2011b), we chose to investigate whether these loci introgress more frequently from one species than the other to see if selection might favor introgression of alleles from either species. We summarized the average α values (from the genomic cline analysis) of all F_{ST} outlier alleles to see whether the ancestry of these F_{ST} outliers were consistently biased towards one species or another.

Results

Variant Calling and Filtering

We generated two genomic datasets from the sequence data; one consisting of biallelic SNPs and one containing both variant and invariant sites. The variant + invariant dataset was used to calculate absolute measures of diversity (π) and divergence (D_{XY}). The SNP-based dataset was used to calculate F_{ST} and perform all other genomic analyses. The Stacks workflow to call SNPs and filter individuals with high levels of missing data

identified 400,764 Single Nucleotide Polymorphisms (SNPs) across 183 individuals. After applying the filtering parameters to create an LD-thinned set of loci (see Methods, above), we retained 68,123 variant sites. This dataset contained 3 *P. cinereus* individuals, 5 *P. metcalfi* individuals, and all other individuals represented *P. shermani, P. teyahalee,* and their hybrids. For all comparisons including invariant sites, pairwise comparisons among *P. teyahalee* and *P. shermani* ranged from 1,086,306 to 2,481,535 base pairs (median 1,823,097). Comparisons between these two species and the outgroup species ranged from 34,197 sites to 602,493 for *P. cinereus* comparisons and 133,780 to 1,852,505 sites for *P. metcalfi* comparisons.

Population genetics

Measures of absolute divergence and diversity were obtained from the variant + invariant genomic dataset (**Fig. S2.1 / S2.2, Table 2.1)**. We estimated the average nucleotide diversity (π) of each individual identified as "pure" *P. shermani* and "pure" *P. teyahalee* at each hybrid zone. The average nucleotide diversity in *Plethodon shermani* isolates ranged from 0.0190 to 0.0239 (mean 0.0218). Nucleotide diversity was lower across *P. teyahalee* populations, ranging from 0.0129 to 0.0155 (mean 0.0140). No consistent trends were observed among transects, although the Snowbird mountain isolates exhibited the lowest π among *P. shermani* and the highest π among *P. teyahalee* populations which may suggest a hybrid swarm.

We also calculated the average number of pairwise differences among individuals across all isolates (D_{XY}). Estimates of D_{XY} among *P. shermani* populations ranged from 0.0265 to 0.0301 (mean 0.0285). These levels of divergence are much higher than divergence among *P. teyahalee* populations, which ranged from 0.0149 to 0.0168 (mean = 0.0160). D_{XY} values were consistently lowest when comparing Wayah populations of both species to their corresponding conspecific populations at Coweeta. D_{XY} estimates between *P. shermani* and *P. teyahalee* isolates were 0.0205 - 0.0292 (mean .0277). Interspecific D_{XY} was always lowest when comparing *P. shermani* from the Snowbird transect to any *P. teyahalee* isolate, further suggesting extensive swamping of the *P. shermani* at Snowbird by alleles from *P. teyahalee*.

Population structure

The best-fitting ADMIXTURE model supported three distinct populations when run on a dataset combining all hybrid zones together (**Fig. S2.3)**. The first population corresponded to *Plethodon teyahalee* across all transects. The second population primarily included *P. shermani* from the Nantahala mountains (Wayah Bald and Coweeta). *P. shermani* from the Unicoi and Tusquitee mountains (Snowbird and Fire's Creek, respectively) comprised the third population. At both Snowbird and Fire's Creek, our ADMIXTURE analysis suggested that no "pure" *P. shermani* were sampled. We also ran ADMIXTURE separately for each hybrid zone, where K=2 was the most strongly supported model in every hybrid zone. We observed a large degree of admixture within each isolate, with ancestry progressively shifting from *P. teyahalee* at lower elevations to *P. shermani* at higher elevations (**Fig. 2.2B)**. Across all three hybrid zones, we observed a lack of backcrossed *P. teyahalee*-like individuals relative to the number of *P. shermani*-like individuals.

Our genomic PCA revealed several population clusters that strongly corresponded with the populations identified by the K=3 ADMIXTURE model (**Fig. 2.2A)**. "Pure" *P. teyahalee* individuals clustered together, with *P. teyahalee* from each transect distinguished by minor separation in PC space. *P. shermani* isolates showed a much clearer pattern of differentiation consistent with divergence among disparate mountaintops with the exception of the Wayah Bald and Coweeta isolates (both located in the Nantahala Mountains), which were nearly indistinguishable from one another in PC space. Each of the three *P. shermani* clusters was clearly defined along both PC axis 1 (5.5% of variance explained) and PC2 (2.9% variance explained). The Snowbird isolate samples clustered much closer to *P. teyahalee* than any other *P. shermani* isolates, but could still be distinguished from other *P. teyahalee* and *P. shermani* populations. Admixed individuals occupied intermediate areas of PC space between parental populations, with most hybrids clustering closer to the transect's *P. shermani* samples.

Estimates of Weir & Cockerham's F_{ST} further support the patterns of population structure observed above **(Table 2.2)**. Intraspecific differentiation was much stronger

among *P. shermani* populations than among *P. teyahalee* populations. Levels of differentiation between Wayah Bald and Coweeta were consistently lower than intraspecific comparisons within *P. shermani* and *P. teyahalee* across all other hybrid zones. It is worth noting that these populations did not exhibit levels of nucleotide diversity (π) that were higher than other populations in both species, so variation in π does not explain these patterns in Fst. Interspecific differentiation was lowest when comparing Snowbird *P. shermani* to any *P. teyahalee* populations, mirroring the findings from our D_{XY} comparisons and ADMIXTURE analyses that suggest Snowbird *P. shermani* has experienced extensive introgression of alleles from *P. teyahalee*. There were relatively few loci that exhibited fixed differences between parental populations at each transect (1 at Snowbird, 164 at Wayah Bald, and 40 at Coweeta).

Association between coloration and genomic hybrid index

We found a fairly strong, positive correlation between each species' associated color score and genomic hybrid index at the Wayah Bald and Coweeta hybrid zones. We observed a strong, positive relationship between *P. shermani* ancestry and the amount of red pigmentation on an animal's leg ($r^2 = 0.708$, $p < 0.005$) We also observed a significant, negative relationship between *P. shermani* ancestry and the amount of lateral/dorsal spotting ($r^2 = 0.557$, $p < 0.005$). This relationship was not observed at Snowbird Mountain, where genomic swamping of *P. shermani* by *P. teyahalee* has resulted in a nearly complete loss of the red legs associated with *P. shermani* ancestry in that hybrid zone (**Fig. 2.4)**. While these color scores do generally appear to characterize genome-wide ancestry at Coweeta and Wayah, they are inaccurate when used to describe individuals as "pure" *P. teyahalee* or *P. shermani*. Many individuals exhibiting the pure *P. shermani* phenotype displayed a high degree of admixture in their genome. Many individuals with the pure *P. teyahalee* phenotype also exhibited evidence of admixture despite showing no phenotypic evidence of introgression.

Genomic clines / Outlier loci

Genomic clines were estimated separately for the Snowbird, Coweeta, and Wayah Bald hybrid zones. Out of the 68,123 alleles that were surveyed, we detected no ß outliers across the three hybrid zones, suggesting that all of the loci sampled introgress at a relatively uniform rate, with no sites resisting introgression or introgressing at a rate faster than the genomic background. We did detect a large number of α outliers, or loci with a cline center biased towards one species or the other given their genome-wide ancestry. We classified loci as either positive outliers (biased towards *P. shermani* ancestry), negative outliers (biased towards *P. teyahalee* ancestry), or non-outliers. Generally, we found far more outliers that were biased towards *P. teyahalee* ancestry than *P. shermani*, consistent with introgression being biased from low to high elevation. At Coweeta, we identified 1,505 positive α outliers and 6,004 negative α outliers. At Wayah Bald, we identified 755 positive α outliers and 3,335 negative α outliers. At Snowbird, we identified 712 positive α outliers and 2,764 negative α outliers. We found that α outliers biased towards *P. teyahalee* were frequently outliers at two or more of the three hybrid zones, suggesting consistent retention of a subset of *P. teyahalee* alleles in hybrids **(Fig. 2.5)**. In contrast, we found very few outliers towards *P. shermani* ancestry that were shared across two or more transects.

We identified 3,528 F_{ST} outliers at Coweeta, 3,336 F_{ST} outliers at Wayah Bald, and 3,186 outliers at Snowbird. At Coweeta, 64 loci were identified as both F_{ST} and bgc α outliers, and the average α values for the F_{ST} outliers was -0.668, while average α for background sites was .016. At Wayah Bald, 12 sites were identified as both F_{ST} and bgc α outliers, and the average α values for the F_{ST} outliers was -0.493, while average α for background sites was .011. At Snowbird, 34 of the Fst outliers were also α outliers, and the average α values for the F_{ST} outliers was -0.668, while average α for background sites was 0.016. The difference in mean α values between F_{ST} outliers and background sites was highest at Coweeta, intermediate at Wayah, and lowest at Snowbird. All sites identified as both F_{ST} and α outliers had cline centers biased towards *P. teyahalee* ancestry.

Tests for introgression

D statistics supported non-treelike relationships among 49 out of the possible 56 trios of species when setting *P. metcalfi* as an outgroup. To focus on patterns of introgression within each hybrid zone, we focus our reporting of D statistics and f-4 ratios on comparisons between *P. shermani* and *P. teyahalee* pairs across all four hybrid zones. There was significant evidence for gene flow at Coweeta, where *P. shermani* shared excess ancestry with Coweeta *P. teyahalee* relative to *P. teyahalee* isolates at Snowbird and Fire's Creek ($p \sim 0$). The f-4 ratios for these comparisons were 0.216 and 0.177, respectively. The only non-signficant signature of introgression was when determining whether Coweeta *P. shermani* shared excess ancestry with Coweeta vs. Wayah *P. teyahalee* ($p = 0.786$, f-ratio = 0.00453285). Results at Wayah Bald strongly mirrored the results from Coweeta comparisons. There was significant evidence for introgression between Wayah *P. shermani* and Wayah *P. teyahalee* vs. *P. teyahalee* from Snowbird and Fire's Creek. The lack of genetic differentiation between the Coweeta and Wayah *P. teyahalee* isolates is likely driving the insignificant D statistics at Wayah and Coweeta, not a lack of introgression between local *P. shermani* and *P. teyahalee* isolates. At Fire's Creek, we also observed significant patterns of introgression between *P. shermani* and *P. teyahalee* ($p < 0.01$ for all comparisons). At Snowbird, we observed significant shared ancestry between local *P. shermani* and *P. teyahalee* in all comparisons, and f-4 ratios ranged between 0.422 and 0.446, which were much higher than ratios at any other transect. This, along with all other results, suggests that the Snowbird *P. shermani* population is the most admixed of any surveyed population.

Discussion

The genetic structure of this hybrid zone is complex; *P. teyahalee* populations exhibit much lower levels of intraspecific differentiation than *P. shermani*, implying greater connectivity among *P. teyahalee* populations than in *P. shermani*. On the other hand, there are distinct genetic clusters of *P. shermani* with clear differentiation between *P. shermani* from the Nantahala mountains (Wayah and Coweeta) and *P. shermani* in the Tusquitee and Unicoi mountains (Fire's Creek and Snowbird). In fact, there is greater divergence between these two *P. shermani* lineages than between some *P. shermani*

populations and *P. teyahalee.* There are multiple evolutionary forces that could contribute to these patterns of differentiation. Allopatric isolation and subsequent drift within *P. shermani* populations on separate mountaintops could facilitate genetic differentiation as seen in other montane species (Osborne et al. 2019; Pato et al. 2019; Arriaga-Jiménez et al. 2020). Additionally, ancient introgression from another species into *P. shermani* from Fire's Creek and Snowbird could facilitate high observed levels of differentiation (Mao et al. 2013; Zhang et al. 2019). There is some evidence from mitochondrial DNA that these two isolates share ancestry with *Plethodon aureolus* and *Plethodon glutinosus*, supporting ancient introgression from other, unsampled taxa as another potential driver of differentiation among *P. shermani* isolates (Weisrock et al. 2005). Nucleotide diversity (π) was, on average, much higher in *P. shermani* (0.0227) relative to *P. teyahalee* (0.0140), which seems counterintuitive given the wider, connected range of *P. teyahalee* relative to *P. shermani.* This difference may be explained by asymmetric gene flow from *P. teyahalee* into *P. shermani*, which has driven similar differences in π between species in other hybrid zones (Zalapa et al. 2010; Brunet et al. 2013; Alex Sotola et al. 2019) due to an increase in nucleotide diversity in the species that receives an influx of alleles from the other. It is also worth noting that diversity estimates in each species are within the range of estimates obtained in other salamander species (Liang et al. 2019; Sunny et al. 2019; Nice et al. 2021).

High differentiation among *P. shermani* populations is likely not due to hybridization with sympatric *P. teyahalee* populations for multiple reasons. Primarily, differentiation among *P. teyahalee* populations is clearly lower than differentiation among *P. shermani* isolates, so introgression of *P. teyahalee* alleles alone could not explain the observed levels of differentiation in *P. shermani*. Additionally, alleles that are highly differentiated among *P. shermani* isolates show high levels of differentiation between *P. shermani* and *P. teyahalee* within hybrid zones which suggests that gene flow from *P. teyahalee* has not provided the alleles underlying differentiation among *P. shermani* isolates.

Our results imply that there are no "pure" *P. shermani* isolates remaining at any of the four hybrid zones sampled. Genomic evidence suggests that all *P. shermani*

populations have experienced some degree of introgression from *P. teyahalee*, meaning that whatever the "pure" *P. shermani* genotype was historically, it has almost certainly been lost due to introgression of *P. teyahalee* alleles. We detected a strong signature of introgression among all sympatric *P. shermani* and *P. teyahalee* isolates within each hybrid zone, consistent with observations based on phenotypes, allozymes, and mitochondrial DNA (Highton and Peabody 2000; Weisrock et al. 2005). The degree of introgression also varied across hybrid zones, with the Snowbird *P. shermani* population exhibiting the highest degree of introgression among the four *P. shermani* populations, consistently exhibiting lower levels of differentiation and divergence from *P. teyahalee*. Weisrock et al. (2005) found that the mitochondrial haplotype of the Snowbird *P. shermani* isolate has been completely swamped by the *P. teyahalee* mitochondrial haplotype, and all our genomic analyses support near total genetic swamping of *P. shermani* by *P. teyahalee* at this site. The Snowbird hybrid zone has by far the lowest maximum elevation, and the swamping of *P. shermani* at this site may be due to an inability of *P. shermani* to competitively exclude *P. teyahalee* even at the highest elevation conditions at this hybrid zone. *P. shermani* populations at Wayah and Coweeta exhibited similar amounts of admixture with *P. teyahalee* to one another, with a lower degree of mixture relative to the Snowbird isolate.

We found very little evidence for intrinsic incompatibilities that may contribute to reproductive isolation between *P. shermani* and *P. teyahalee*. Oftentimes, despite widespread introgression across the genome, there are some loci that resist introgression which are associated with reproductive isolation between the hybridizing species (Carneiro et al. 2010; Coughlan and Matute 2020; Dufresnes et al. 2021). Such loci should exhibit steep genomic clines, and should exhibit steeper clines than the genomic background (Gompert et al. 2012b). We found no slope (ß) outliers at any of the hybrid zones sampled, which is consistent with weak isolation between species or diffuse isolation spread across a wide variety of loci. A lack of loci that resist introgression suggests that gene flow will likely continue uninhibited unless constrained by exogenous factors.

We found strong evidence for asymmetric introgression from *P. teyahalee* into *P. shermani* despite general uniformity in cline slopes. We identified thousands of α outlier loci that exhibit cline centers which are predominantly biased towards *P. teyahalee* ancestry. This pattern is consistent with asymmetric gene flow from *P. teyahalee* into *P. shermani* (Gompert and Buerkle 2011). Asymmetric gene flow from *P. teyahalee* into *P. shermani* is also consistent with our earlier observations of elevated π in *P. shermani* relative to *P. teyahalee*. Widespread, moderate α outliers biased towards ancestry from one species is consistent with divergent selection affecting many traits (Gompert and Buerkle 2011). A large proportion (22.2-59.6%) of outliers are shared among hybrid zones, consistent with selection for the retention of the same loci across hybrid zones. Locus-specific F_{ST} outliers also suggest that alleles potentially involved in local adaptation appear to consistently be biased towards *P. teyahalee* ancestry across all hybrid zones, which has been shown in other systems where selection favors the alleles of one species over the other (Gompert et al. 2012a; Taylor et al. 2014; Baiz et al. 2019; Ebersbach et al. 2020). There are other potential explanations for directional selection in favor of elevated *P. teyahalee* ancestry. If hybrids or *P. shermani* individuals disproportionately prefer to mate with *P. teyahalee*-like individuals that could also drive asymmetric introgression, causing clines to shift towards *P. teyahalee* ancestry. This is unlikely since courtship trials show that, with the exception of the Fire's Creek Hybrid Zone, *P. shermani* males do not mate with *P. teyahalee* females at a higher rate than they mate with hybrid or *P. shermani* females (Lowe 2016).

Asymmetric introgression of *P. teyahalee* alleles may reflect warming temperatures in the region, which should select for alleles from *P. teyahalee*, which is better adapted to the warmer, drier conditions associated with low elevations. This may explain why the Snowbird *P. shermani* isolate has been swamped while other isolates remain well differentiated from *P. teyahalee*, as Snowbird Mountain exhibits by far the lowest maximum elevation (1,036m) of any transect (Fire's Creek = 1,323m, Coweeta = 1,412m, Wayah = 1,564m). Physiological modeling suggests *P. teyahalee* can survive at high altitudes but are currently excluded from those environments by *P. shermani* (and other members of the *P. jordani* complex) due to aggression by *P. shermani* towards other

Plethodon species (Drummond 2014). Warming temperatures may impede the ability of *P. shermani* to exclude *P. teyahalee* at high elevations, which may cause the hybrid zone to shift further upwards in elevation. This scenario is consistent with observed increases in *P. teyahalee*-like phenotypes at higher elevations as climate warms (Hairston Sr. et al. 1992; Walls 2009). Given that the color scores used for these observations are a fairly good representation of increased *P. teyahalee* ancestry, we can reasonably infer that selection for *P. teyahalee* alleles is driving an upward shift in the hybrid zone as climate change progresses. If *P. shermani* are eventually unable to exclude *P. teyahalee* or hybrids through competition at high elevations, it could lead to the genetic swamping of all *P. shermani* populations by *P. teyahalee* alleles.

The color scores used in previous studies in this system generally appear to be a good indicator of genomic hybrid index outside of the Snowbird hybrid zone, where no individuals retain red legs even at the highest elevations. An increase in white spotting is associated with increased *P. teyahalee* ancestry, while an increase in red leg coloration is associated with an increase in *P. shermani* ancestry. The only potential issue in using these color scores would be assuming white spots and a lack of red legs indicate un-admixed *P. teyahalee* while a lack of white spots and abundant red leg pigmentation indicates pure *P. shermani*. Many individuals exhibiting these "pure" phenotypes exhibited genomic evidence of admixture, and even "pure" *P. shermani* genotypes possess introgressed alleles from *P. teyahalee*. Color-based monitoring of each hybrid zone's position through time should be a valuable way of tracking hybrid zone movement as climate change progresses.

Whether or not *P. shermani* and *P. teyahalee* should still be considered species given these results is an important question to consider. Hybridization is common among *Plethodon* species, yet genetic distances are similar between sympatric *Plethodon* species that do not hybridize compared to species pairs that do engage in hybridization (Highton and Peabody 2000), suggesting that even deeply diverged lineages within this family are capable of hybridization. Additionally, salamanders have been shown to hybridize at similar levels of genetic divergence to other tetrapods (Melander and Mueller 2020), and the genome-wide levels of differentiation and divergence between *P. shermani* and *P.*

teyahalee (mean F_{ST} = 0.336, mean D_{XY} = 0.277) are still greater than or equal to the divergence between hybridizing species in frogs, reptiles, and birds (Streicher et al. 2014; Manthey et al. 2021; Yang et al. 2021). These high levels of divergence would be consistent with species status in other systems, and support maintaining these groups as unique species. Additionally, estimates of the width of this hybrid zone from past studies indicate that the zone is narrower than expected given the timing of secondary contact and the dispersal abilities of both species (Lowe 2016). However, despite high genome-wide differentiation and evidence for a constrained hybrid zone, there are very few sites that exhibit fixed differences between parental *P. teyahalee* and *P. shermani* populations within each hybrid zone (164, 40, and 1 at Wayah, Coweeta, and Snowbird, respectively). Additionally, a lack of sites that exhibit steep genomic clines implies very few intrinsic genetic incompatibilities between these species, which is often required for the maintenance of species boundaries in the presence of gene flow (Behm et al. 2010; Lindtke and Buerkle 2015; Coughlan and Matute 2020). Monitoring parental populations of *P. shermani* and *P. teyahalee* to determine whether this differentiation can be maintained in the future would be a useful way to assess the long-term viability of these species and whether or not *P. shermani* can resist genetic swamping by *P. teyahalee*.

Conclusions

The findings presented here, combined with past studies in this system, all point towards a hybrid zone strongly regulated by ecological factors, especially elevational variation in climate. At all four hybrid zones, significant introgression was detected between *P. shermani* and *P. teyahalee* populations along the elevational gradient which spans the two parental populations. There were no loci that exhibited patterns consistent with resisting introgression, suggesting a lack of intrinsic genetic incompatibilities between these species. Furthermore, introgression appears to be widespread and asymmetric from *P. teyahalee* into *P. shermani*, consistent with selection for *P. teyahalee* alleles. Loci that may potentially be involved in local adaptation also show strong evidence for asymmetric introgression from *P. teyahalee* into *P. shermani*. Asymmetric gene flow from *P. teyahalee* into *P. shermani* may be the product of selection for *P.*

teyahalee alleles that are associated with warmer climatic conditions. This has important implications for the future of *P. shermani* as the climate in the Southern Appalachians continues to grow warmer.

Acknowledgements

We would like to thank Dr. John Maerz, Dr. Todd Pierson, and Cyndi Carter for their willingness to share tissues and their corresponding data from the Coweeta hybrid zone for genetic sequencing. Dr. Ben Lowe collected many *P. shermani* and *P. teyahalee* samples, and generously provided phenotypic and ecological data associated with these tissues. We thank Dr. Alex Buerkle for his correspondence and debugging support related to the use of bgc. We also thank Dr. Bradley Schaffer for his assistance with generating bgc input files. This work was supported by a National Science Foundation grant (DEB-094950) to Kenneth H. Kozak.

Figures and Tables

Figure 2.1: Species photographs and sampling site locations. Photographs of individuals exhibiting color morphologies of **A)** *Plethodon shermani* **B)** *Plethodon teyahalee* **C)** *P. shermani* x *P. teyahalee hybrid* **D)** Sampling locations across four hybrid zones between *P. shermani* and *P. teyahalee*. Red circles indicate sites designated as pure *P. shermani* isolates, while black circles indicate sites designated as pure *P. teyahalee* isolates. Gray sites represent sites that were composed of either entirely or partially of admixed individuals. No intermediate sites were included for the Fire's Creek hybrid zone.

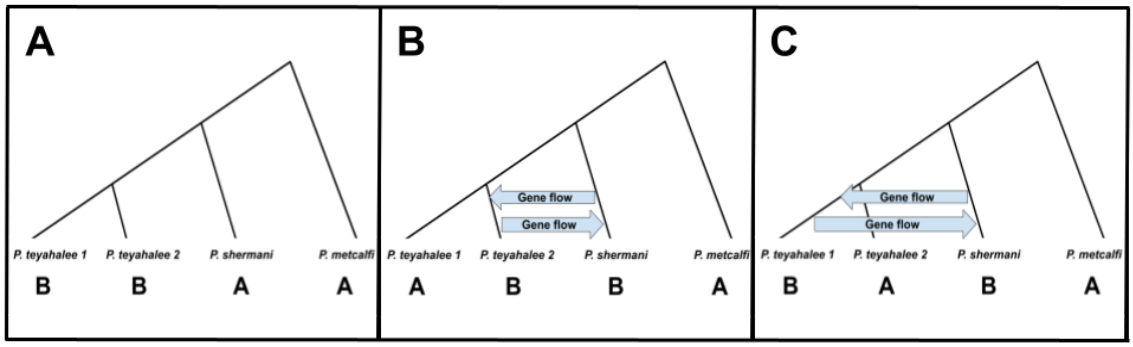

Figure 2.2: Four taxon topologies for introgression tests. Expected gene tree topologies under divergence histories with no gene flow (**A)** and gene flow between *P. shermani* and one of two potential *P. teyahalee* isolates (**B and C).** Under incomplete lineage sorting without gene flow, the number of alleles which exhibit ABBA topologies (**B**) should be equal to the number of alleles exhibiting BABA topologies (**C**).

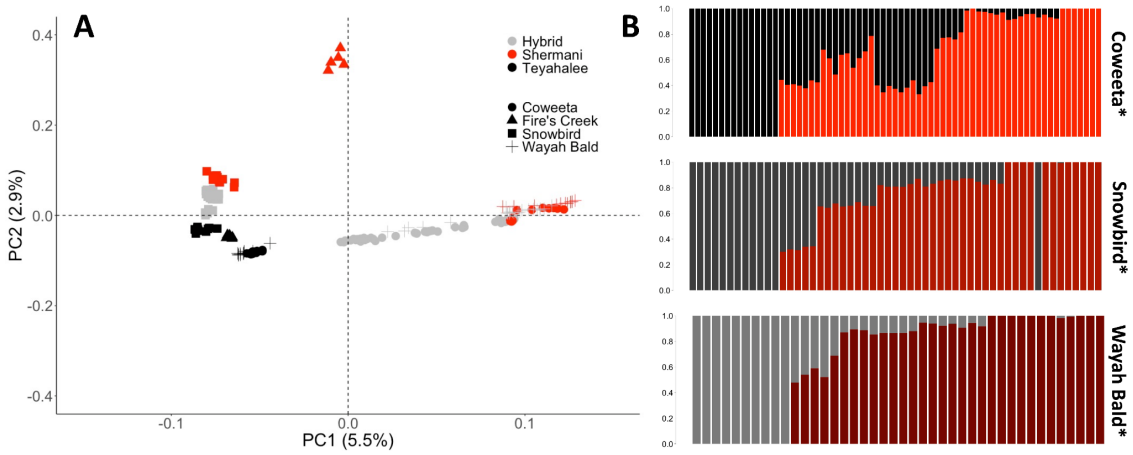

Figure 2.3: Population structure across hybrid zones. A) Genomic PCA of all samples in the study. Shapes indicate which hybrid zone the samples were taken from, and color indicates whether individuals were designated as *P. shermani* or *P. teyahalee* based on ancestry proportions in ADMIXTURE. **B)** Asterisks indicate that ADMIXTURE was run separately for each of the three hybrid zones. Each bar represents one individual, and the colors represent the percentage of all sites corresponding to ancestry from either *P. shermani* (red shades) or *P. teyahalee* (black and gray). Individuals are sorted within transects by elevation.

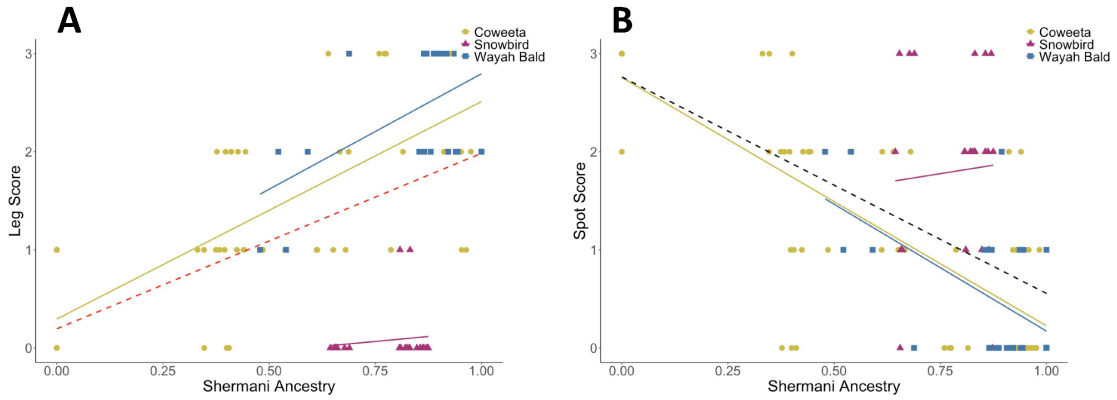

Figure 2.4: Associations between phenotype-based and genomic hybrid indexes. A) Association between Leg Score (amount of red coloration on the legs) and genomic hybrid index as determined by ADMIXTURE. **B)** Association between Spot Score (amount of lateral and dorsal spotting white spotting) and genomic hybrid index as determined by ADMIXTURE. Colors and shapes are associated with the three different hybrid zones where samples from intermediate elevation sites were collected.

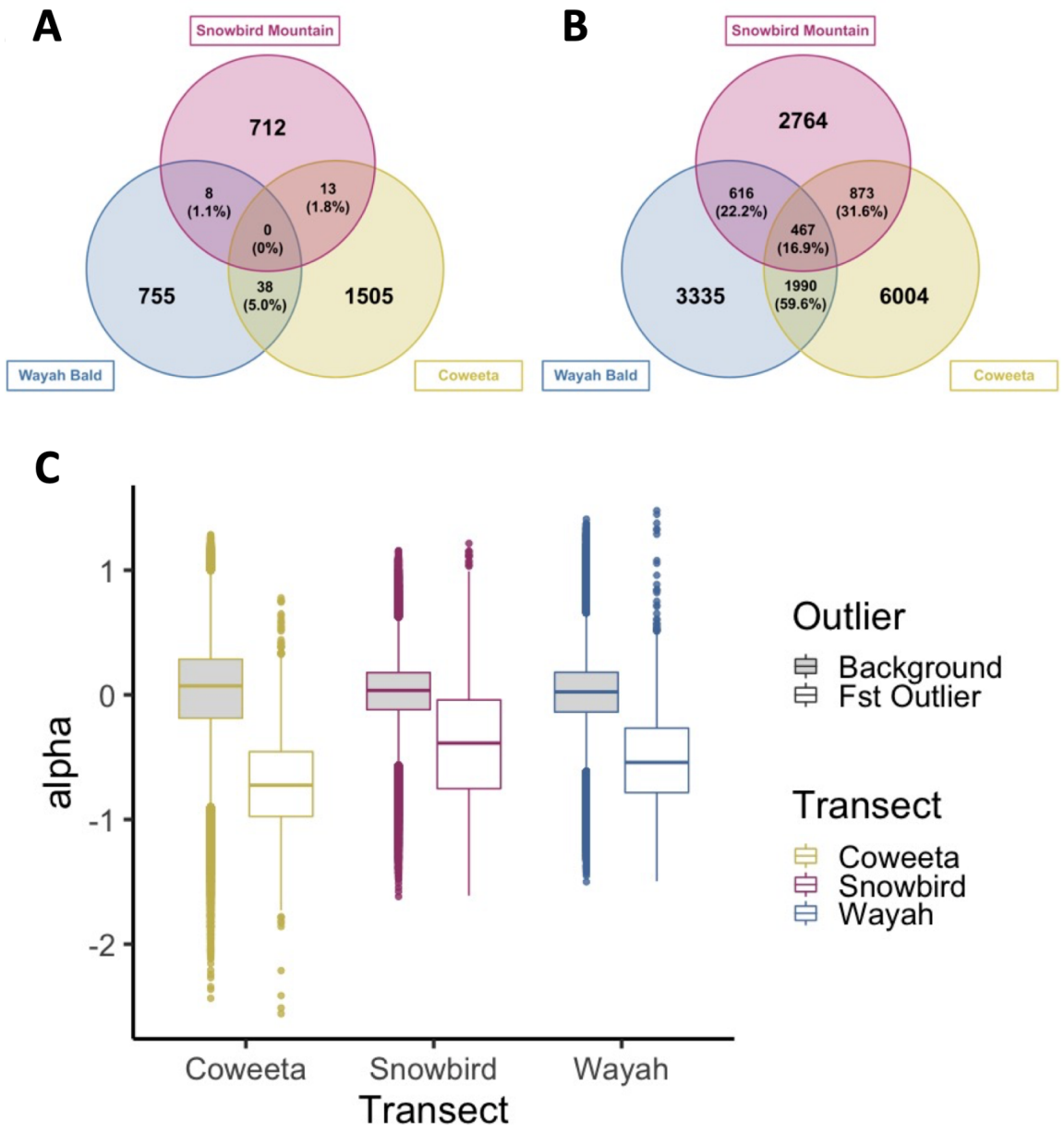

Figure 2.5: Cline center and F_{ST} outliers. A) Number of *P. shermani* biased (A) and *P. teyahalee* biased (B) α outliers identified by bgc. Numbers in the overlap between circles indicate loci designated as outliers at both transects. **B)** α values for F_{ST} outlier alleles that exhibited high differentiation between *P. shermani* and *P. teyahalee* populations at each transect. Negative values of α indicate a cline center biased towards *P. teyahalee,* while a positive α value indicates a cline center biased towards *P. shermani*.

Table 2.1: Absolute divergence and diversity metrics. Measures of the average number of pairwise difference between individuals within (π) and among (D_{XY})populations. Comparisons shaded in gray represent within population comparisons, whereas all other values represent comparisons between populations.

	Coweeta *P. sherman i*	Wayah *P. sherm ani*	Fire's Creek *P. shermani*	Snowbird *P. shermani*	Coweeta *P. teyahalee*	Wayah *P. teyahalee*	Fire's Creek *P. teyahalee*	Snowbird *P. teyahalee*
Coweeta *P. shermani*	0.024	0.026	0.030	0.029	0.027	0.028	0.028	0.028
Wayah *P. shermani*		0.023	0.030	0.029	0.028	0.028	0.028	0.029
Fire's Creek *P. shermani*			0.022	0.027	0.027	0.027	0.027	0.027
Snowbird *P. shermani*				0.019	0.021	0.021	0.021	0.020
Coweeta *P. teyahalee*					0.014	0.015	0.016	0.017
Wayah *P. teyahalee*						0.013	0.016	0.016
Fire's Creek *P. teyahalee*							0.013	0.017
Snowbird *P. teyahalee*								0.015

Table 2.2: Relative genetic differentiation. Estimates of Weir and Cockerham's F_{ST} between all parental populations sampled in this study. Comparisons shaded in gray represent comparisons of different intraspecific parental populations, whereas all other values represent comparisons between species.

	Coweeta *P. teyahalee*	Wayah *P. teyahalee*	Fire's Creek *P. teyahalee*	Snowbird *P. teyahalee*	Coweeta *P. shermani*	Wayah P. *shermani*	Fire's Creek *P. shermani*	Snowbird *P. shermani*
Coweeta *P. teyahalee*	0.000	0.028	0.052	0.067	0.319	0.366	0.336	0.217
Wayah *P. teyahalee*		0.000	0.070	0.080	0.336	0.381	0.360	0.233
Fire's Creek *P. teyahalee*			0.000	0.045	0.289	0.336	0.292	0.183
Snowbird *P. teyahalee*				0.000	0.332	0.375	0.306	0.173
Coweeta *P. shermani*					0.000	0.051	0.150	0.236
Wayah P. *shermani*						0.000	0.174	0.274
Fire's Creek *P. shermani*							0.000	0.190
Snowbird *P. shermani*								0.000

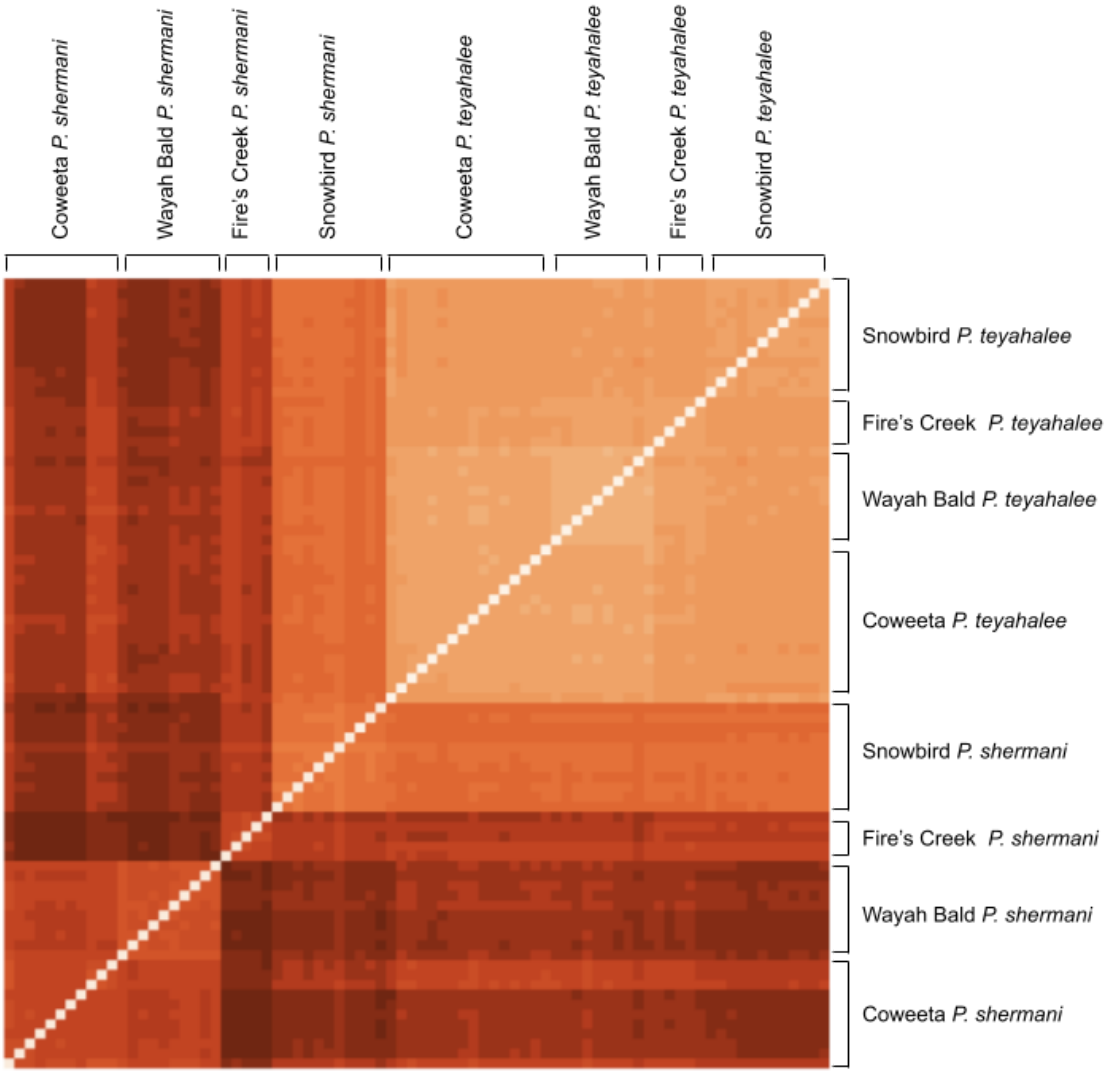

Figure S2.1: Parental population divergence patterns. Average pairwise differences among all *P. shermani* and *P. teyahalee samples.* Darker shades of orange indicate more differences, and lighter shades indicate fewer differences.

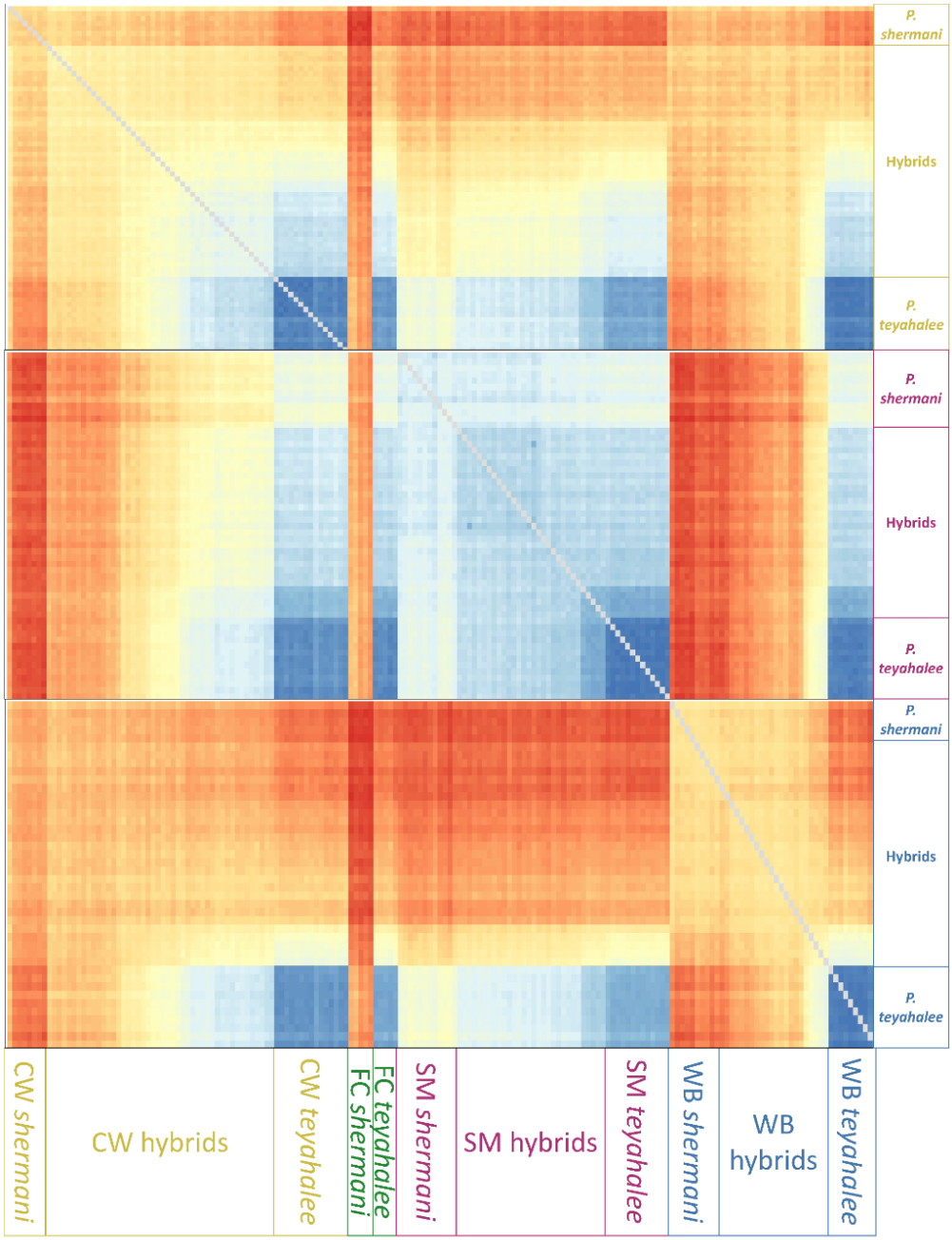

Figure S2.2: Divergence patterns among all samples. Average pairwise differences among all samples, including hybrids. Individuals are sorted by hybrid index within transects on the y-axis, and colors on the Y axis indicate which hybrid zone samples came from. Dark red shades indicate more differences between individuals, and blue shades indicate fewer differences.

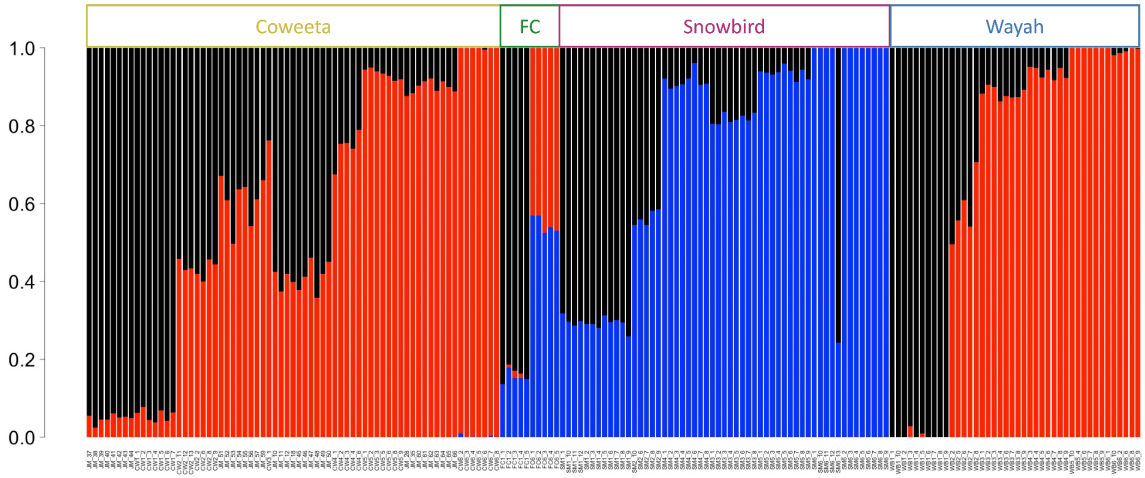

Figure S2.3: K=3 ADMIXTURE run. Admixture proportions for individuals when K=3 when run on all populations together. Each bar represents one individual, and the colors represent the percentage of all sites corresponding to ancestry from one of three potential populations. Individuals are sorted within transects by elevation.

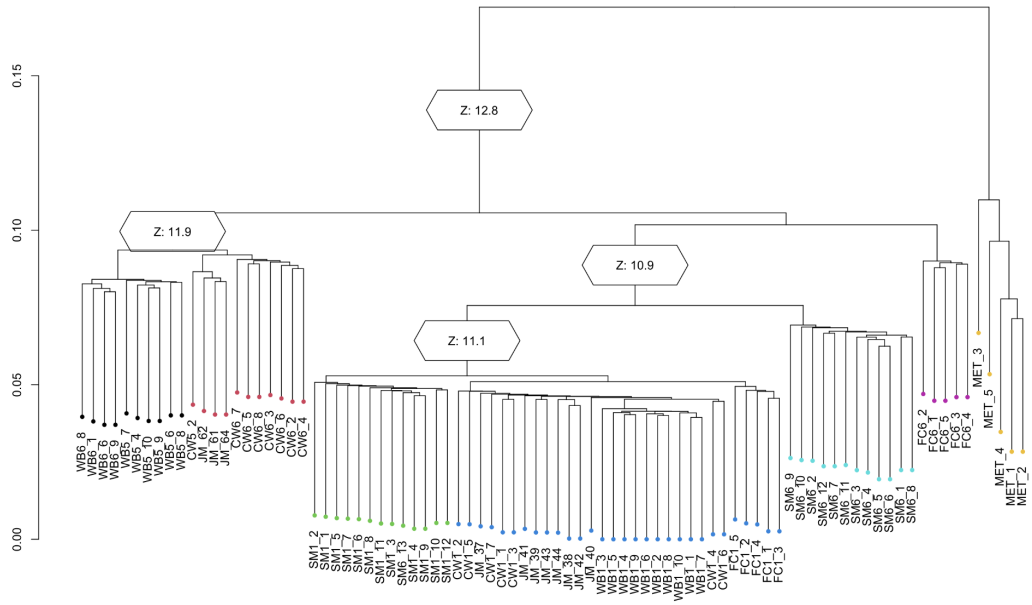

Figure S2.4: Neighbor-joining Dendrogram. Neighbor-joining dendrogram displaying relationships among individuals from parental populations. Coweeta and Wayah *P. shermani* samples are closely related to one another. Fire's Creek *P. shermani* form a second group while Snowbird Mountain *P. shermani* form a third. The final group consists of all the *P. teyahalee* populations.

CHAPTER 3
Assessing genomic and ecological differentiation among subspecies of the Rough-footed Mud Turtle, *Kinosternon hirtipes*

Abstract

Combining genetic and ecological measures of differentiation can provide compelling evidence for ecological and genetic divergence among lineages. The Rough-footed Mud Turtle, *Kinosternon hirtipes*, is distributed from the Trans-Pecos region of Texas to the highlands of Central Mexico and contains six described subspecies, five of which are extant. We use ddRAD sequencing and species distribution models to assess levels of ecological and genetic differentiation among these subspecies. We also predict changes in climatically suitable habitat under different climate change scenarios and assess levels of genetic diversity and inbreeding within each lineage. Our results show that there is strong genetic and ecological differentiation among multiple lineages within *K. hirtipes*, and that this differentiation appears to be the result of vicariance associated with the Trans-Mexican Volcanic Belt. We propose changes to subspecies designations to more accurately reflect the evolutionary relationships among populations, and assess threats to each subspecies.

Introduction

The identification and conservation of evolutionarily distinct lineages is vital for the preservation of functional and phylogenetic diversity as well as the protection of evolutionary potential in natural populations (Rosauer et al. 2017; Kling et al. 2019; Hanson et al. 2020). Such evolutionarily distinct lineages are often designated as subspecies (Wilson and Brown Jr 1953) to acknowledge their unique evolutionary trajectories and underscore the need for their conservation (Thakur et al. 2018; Humeau et al. 2020). Subspecies designations have traditionally been based on differences in habitat, distribution, and phenotype be

tween populations. Defining subspecies based on phenotype alone can be problematic since phenotypic differences between populations may be due to phenotypic plasticity in different habitats (Gruber et al. 2013; Ennen et al. 2014; Barrientos-Villalobos et al. 2018) or represent opposite ends of clinal variation instead of evolutionarily distinct lineages (Frost and Hillis 1990; Zink 2004; Phillimore and Owens 2006; Hillis 2019). To address these issues, most modern approaches to define subspecies or taxonomic units for conservation incorporate genetic data to identify lineages (Huang and Knowles 2016; Archer et al. 2017; Taylor et al. 2017; Hillis 2020). The use of genetic data has proven to be valuable in delimiting taxa that would not have been recognized based on morphology alone (Spinks and Shaffer 2005; Wenner et al. 2012; McElroy et al. 2018; Rodríguez et al. 2020).

Ecological differentiation is an important step in lineage diversification, as it may decrease gene flow between populations (Mayr 1947; Coyne and Orr 2004; Funk et al. 2006; Cortés et al. 2018). Notably, climatic niche differentiation has been associated with the diversification of many clades (Kozak and Wiens 2010; Title and Burns 2015; Seeholzer et al. 2017; Reis et al. 2018), and niche diversification is often associated with diversification in physiological and life-history traits (Ackerly et al. 2006; Lawson and Weir 2014; Weaver et al. 2020). Calls to incorporate ecological niche data into the identification of lineages (Raxworthy et al. 2007; Rissler and Apodaca 2007) have led to the increased use of ecological niche modeling to identify unrecognized phylogenetic diversity within species (Zheng et al. 2017; Alvarado-Sizzo et al. 2018; Wang et al. 2019), although some are hesitant to use ecological differentiation as support for lineage delimitation (e.g. Meik et al. 2015).

Mud turtles (genus *Kinosternon*) are distributed across the Americas, from southern Canada to northern Argentina. The Rough-footed Mud Turtle, *Kinosternon hirtipes* (Wagler 1830), is one of the most widespread species in the genus, ranging from Presidio County, Texas to the Trans-Mexican Volcanic Belt (TMVB) in central-southern Mexico (Iverson 1981). *Kinosternon hirtipes* contains six described subspecies; the nominotypical subspecies *K. h. hirtipes*, restricted to the Valle de México (Mexico City Valley); *K. h. murrayi* (Glass and Hartweg 1951), ranging from Presidio County, Texas to

the highlands of central Michoacán; *K. h. chapalaense,* endemic to lakes Chapala and Zapotlán in eastern Jalisco; *K. h. magdalense,* restricted to the Magdalena Valley in western Michoacán; *K. h. tarascense,* restricted to the Pátzcuaro basin in Michoacán; and the recently-extinct, microendemic *K. h. megacephalum*, known only from an isolated cienega in Viesca, Coahuila (Serb et al. 2001; Reyes-Velasco et al. 2013).

The description of these subspecies was primarily based on morphology and geography (Iverson 1981), and the evolutionary relationships among these subspecies are unclear. Previous studies have investigated the relationships among kinosternid species based on molecular data (Iverson et al. 2013; Spinks et al. 2014), but did not include samples of multiple *K. hirtpes* subspecies in their analyses, leaving the relationships among subspecies of *K. hirtipes* unresolved. Phylogenetic studies of other mud and musk turtles demonstrated that some widespread species are composed of multiple evolutionarily distinct lineages of conservation concern (Serb et al. 2001; Scott et al. 2018; Loc-Barragán et al. 2020), highlighting a need for genetic analyses to test for cryptic lineages and resolve relationships among *K. hirtipes* subspecies.

Although widely distributed, *Kinosternon hirtipes* faces many conservation threats from several anthropogenic factors including habitat loss and degradation, increased habitat fragmentation, and reduced connectivity among populations (Reyes-Velasco et al 2013; Smith 2016; Macip-Rios et al. 2021). Furthermore, the persistence of this species across much of its range is threatened by climate change, and it is expected to suffer a 39-66% reduction in suitable habitat by 2070 (Butler et al. 2016; Berriozabal-Islas et al. 2020), particularly in the Northern part of its range. Climate change may also render some populations of *K. hirtipes* inviable by skewing population sex ratios, which are thermally determined in this species (Ewert et al. 2004; Aparicio et al. 2018). Additionally, most of the currently recognized subspecies are represented by a few small populations or are restricted to a single small basin (as is the case with *K. h. tarascense* and *K. h. magdalense*). One subspecies, *K. h. megacephalum*, went extinct in the past half century due to the loss of habitat at its only known localities (Reyes-Velasco et al. 2013). *K. h. hirtipes* was also thought to be extinct due to habitat loss and the impacts of introduced species in the Valle de México. However, three *K. h. hirtipes*

individuals were captured in 2021 (Macip-Ríos, pers. com.), indicating the persistence of at least one population of this subspecies. Given the ongoing and projected loss of habitat, a rigorous, rangewide assessment of intraspecific diversity among populations of *K. hirtipes* is timely and may have significant implications with respect to its conservation status and management.

Here, we assess the status of *Kinosternon hirtipes* subspecies by conducting a range-wide population genetics analysis using reduced representation RADseq data. The goal of this project was to summarize genetic diversity and ecological divergence among subspecies and populations across the range of *K. hirtipes* to inform conservation efforts and help discern whether currently recognized subspecies are supported by genomic and ecological data.

Methods

Sample Collection

We sampled multiple populations (18 specific localities) intended to represent all extant *Kinosternon hirtipes* subspecies (*K. h. chapalaense, K. h. hirtipes*, *K. h. magdalense, K. h. murrayi*, and *K. h. tarascense)*, as well as four outgroup taxa; *K. chimalhuaca, K. integrum, K. oaxacae, K. sonoriense)*. Locations for *K. hirtipes* samples in the context of the species' full range are represented in **Fig. S3.1**. Identification keys from Iverson (1981) and Glass and Hartweg (1951) were used to morphologically assign individuals to *Kinosternon hirtipes* subspecies. Field sampling included populations of *K. hirtipes* in Texas and northern Mexico, with a focus on populations considered to be of conservation concern by the Texas Parks and Wildlife Department. Forty-one tissue samples were collected in Presidio County, Texas by catching turtles using double throat wire mesh traps (1 m long x 30 cm diameter) baited with sardines in oil. Each turtle was given a unique identifier by creating a 2 mm deep triangular notch on the marginal scutes. Scute shavings were collected and preserved in 98% ethanol. The right first claw was also clipped and preserved in ethanol. All animals were released at the point of capture following tissue collection.

Thirty-five samples were collected from the TMVB in 2016-2019. Either interdigital web skin was clipped and preserved in 98% ethanol or blood was sampled from the dorsal coccygeal vein in the tail and stored in Queen's lysis buffer (Seutin et al. 1991). We also took blood samples from thirty turtles that were trapped from a population in Galeana, Chihuahua using hoop traps baited with sardines, and each turtle was given a scute notch for identification. These samples were preserved in buffer (0.01 m Tris, 10 mm EDTA, 0.01 m NaCl, and 1% SDS) and frozen until use.

Outgroup samples included *K. chimalhuaca* (3), *K. integrum* (5), *K. oaxacae* (2), *K. sonoriense longifemorale* (2), and *K. s. sonoriense* (8). These samples were collected for previous studies by the authors with the exception of the samples of *K. sonoriens*e, which were donated by Phil Rosen and Paul Stone. We successfully extracted and sequenced DNA from 141 individuals representing five kinosternid species. Subspecies designation and basin of collection were used to assign population priors to all samples of *K. hirtipes* that were included in population genetics analysis (**Table S3.1**).

DNA Extraction and sequencing

The University of Minnesota Genomics Center (UMGC) used Qiagen's DNeasy Blood & Tissue kit to extract DNA from skin and muscle tissue and a modified version of the DNeasy Blood & Tissue kit (see Supplementary materials) to extract DNA from <100mg of bone, nail, carapace, and claw samples. DNA extraction protocols for all tissue types can be found in the Supplementary Materials. The UMGC performed a double-digest Restriction Site-Associated DNA (ddRAD) protocol. Briefly, 100 ng of DNA were digested with 10 units each of *BamHI*-HF and *NsiI*-HF (New England Biolabs; NEB) restriction enzymes and incubated at 37°C for 2 hours. Enzymes were heat inactivated at 80°C for 20 minutes. Samples were then ligated with 200 units of T4 ligase (NEB) and phased adaptors with GATC and TGCA overhangs at 22°C for 1 hour. The ligase was then heat killed, and the ligated samples were purified with SPRI beads and then amplified for 18 cycles with 2X NEB Taq Master Mix to add barcodes. Libraries were purified, quantified, pooled, and size selected for the 300-744 bp library region, and diluted to 2 nM for sequencing on the Illumina NextSeq 550 using single-end 1X150

reads in three separate batches. All raw reads can be found on NCBI's Sequence Read Archives under the SRA BioProject ID PRJNA679588.

Variant Calls

Single-read RADseq data were collected for a total of 141 individuals. Reads were cleaned with Trimmomatic 0.33 (Bolger et al. 2014) and processed with Stacks v. 2.5 (Catchen et al. 2011; Rochette et al. 2019). In UStacks, each haplotype had to be covered by at least three reads, and up to three mismatches between reads were allowed to be in the same haplotype. For CStacks, we allowed three mismatches between haplotypes from the same sample for building the consensus sequence in the catalog file. In the populations program, we required that each locus be present in at least one sample per population and that the locus be present in at least 10% of all samples. The parameters for the stacks pipeline were set to be particularly lenient to encourage the retention of more loci for downstream filtering. Under these settings, we produced a VCF (variant call file) that contained 147,507 single-nucleotide polymorphisms (SNPs) across 34,017 loci. We also exported the invariant sites for all samples at all loci, allowing us to calculate absolute average pairwise differences within and between populations (i.e. π and D_{XY}). Calculations of pairwise nucleotide differences including variant and invariant sites were based on this dataset, and the number of base pairs compared between individuals ranged between 524,798 bp and 4,668,039 bp**.**

From the VCF generated by Stacks, we calculated per-individual missing call rate, per-SNP missing call rate, per-site heterozygosity, and per-SNP minor allele frequency. We generated two genetic datasets for analyses; 1) a phylogenetic dataset that prioritized the inclusion of outgroup samples from other Kinosternid species and 2) a population genetics dataset that prioritized keeping only individuals and sites with low missingness for population genetics analyses. For the phylogenetic dataset, we filtered the VCF generated by Stacks to exclude all samples that had missing genotypes at >60% of loci. Then, we filtered out singletons (alleles only present in one individual), genotypes supported by fewer than 10 reads, and sites present in fewer than 90% of the remaining individuals. In total, this data set contained 21,576 biallelic SNPs and 101 individuals.

After filtering this dataset to retain one marker per locus, we retained 5,779 biallelic SNPs across 101 individuals.

For the population genetics dataset, we filtered the VCF generated by Stacks to produce a high-quality, high-density marker dataset. We excluded singletons, genotypes supported by fewer than 10 reads, SNPs missing in more than 30% of individuals, and individuals with more than 55% missing data. In total, this data set contained 55,310 biallelic SNPs and 90 individuals. Alleles in linkage disequilibrium (LD) with one another can violate the assumptions of some analyses, particularly those of population structure. For this reason, we filtered the population genetics dataset to randomly keep one site per RAD locus (a genomic location from which RAD tags are derived). This resulted in a set of 11,637 SNPs from 90 individuals that was used to explore patterns of isolation by distance and population structure (see below).

Phylogeny Construction

We used the maximum-likelihood approach for topology reconstruction implemented in RAxML-NG v1.0.1 (Kozlov et al. 2019) to explore the evolutionary relationships among the samples in our study. First, we generated a concatenated multi-sequence alignment of all the polymorphic sites from the filtered VCF containing the four outgroup species (*K. chimalhuaca, K. integrum, K. oaxaca, K. sonoriense*) and *K. hirtipes* samples using a custom Python script. Tree topologies estimated using only SNPs are most similar to full-sequence trees when no ascertainment bias correction is used, although not correcting for ascertainment biases can severely impact estimations of branch lengths (Leaché et al. 2015). Since we were primarily interested in the topology of the sampled taxa, we used no ascertainment bias correction and implemented a GTR + G model of nucleotide substitution to perform 600 bootstrap replicates and conduct an ML search from 300 parsimonious trees and 300 random trees. Samples from *K. chimalhuaca, K. integrum, K. oaxaca,* and *K. sonoriense* were used as an outgroup to root the phylogeny. The most likely topology with bootstrap support values was drawn using the phytools (Revell 2012) package in R v3.6.2 (R Core Team 2019).

We also utilized the quartet inference algorithm of SVDquartets implemented in PAUP* (Swofford 2003; Chifman and Kubatko 2014) to assess the topology of the phylogeny. SVDquartets infers tree topology by subsetting data into quartets, assessing the likelihood of each quartet under a coalescent model, and then combining quartets into a full tree (Chifman & Kubatko, 2014). Using the same SNP dataset as the Maximum Likelihood analysis, we estimated the topology of the most likely tree and generated 10,000 bootstrap replicates. Bipartitions observed in over 95% of replicate trees were considered to have strong support.

Population Genetic Analyses

The population genetic analyses summarized pairwise diversity among all samples and assessed the degree of population stratification in the samples. We calculated the number of differences per base pair for all pairwise comparisons both within taxa (π) and between taxa (D_{XY}). Average pairwise diversity for all invariant and variant sites was calculated with a custom Python script, and missing calls were handled on a pair-by-pair basis. We also calculated three relative measures of differentiation among all *Kinosternon* species and lineages in our dataset to explore how levels of differentiation among *K. hirtipes* lineages compared to levels of differentiation among species. These metrics were Weir & Cockerham's F_{ST} (Weir and Cockerham 1984), Nei's F_{ST} (Nei 1987), and Cavalli-Sforza and Edwards chord distance (Cavalli-Sforza and Edwards 1967).

The population stratification analyses used both principal components analysis of the polymorphic sites and model-based genetic assignment with ADMIXTURE v1.3 (Alexander et al. 2009). Principal components analysis was performed with the SNPRelate v1.24.0 package (Zheng et al. 2012) in R. ADMIXTURE was run on the LD-thinned dataset (11,637 SNPs) with K values (number of genetic clusters) ranging from 1 to 12. Each ADMIXTURE run was performed with the block optimization method, a convergence criterion of $\epsilon = 10{-}4$, and 5-fold cross validation.

To assess patterns of inbreeding within *K. hirtipes*, we assigned individuals to genetic populations based on the results of the phylogenetic and ADMIXTURE analyses. We estimated levels of inbreeding at two scales. First, we calculated inbreeding

coefficients (F) for each individual when all samples of *K. hirtipes* were considered as one panmictic population. Second, we generated inbreeding coefficients for each individual within their genetic subpopulation (F_{IS}). All inbreeding coefficients were calculated using vcftools v0.1.16 (Danecek et al. 2011).

To explore the extent of historic gene flow between taxa, we used Treemix v1.13 (Pickrell and Pritchard 2012) to model the number of migration events between taxa. Using the LD-thinned dataset, we ran Treemix allowing for 0-10 migration events (M) between taxa. For each value of M, we ran 5 separate iterations of the model. To assess which number of migration events best explained the evolutionary history of these taxa, we generated the maximum-likelihood tree (M=0) and added migration events until the proportion of variance explained by the models plateaued (Pickrell and Pritchard 2012).

Isolation by Distance

To understand how genetic diversity is structured across sampling locations, we tested for isolation-by-distance among populations of *Kinosternon hirtipes*. Under a scenario of limited dispersal driving genetic structure, we would expect to see a strong linear relationship between pairwise genetic and geographic distance across all samples. For the LD-thinned VCF, 103 samples of *K. hirtipes* had geographic data, and there were 18 unique geographic populations sampled. We constructed a matrix of allele counts for the minor allele for all individuals in each population, and another matrix with the same dimensions that included the counts of each allele at each locus in all populations. To construct the geographic distance matrix, we took the geographic coordinates for each population and calculated Euclidean distance between all pairwise points. We then implemented a Mantel test in the R package adegenet v2.1.4 (Jombart 2008; Jombart and Ahmed 2011) to test whether the observed patterns of genetic differentiation among populations of *K. hirtipes* could be explained mainly by isolation by distance.

Climatic Niche Construction and Analysis

We used the package ENMeval (Muscarella et al. 2014) in R (R Core Team 2019) in conjunction with Maxent (Phillips et al. 2006) to model the distribution of the clades of

Kinosternon hirtipes identified in our phylogeny. For the niche construction, we treated *K. h. tarascense* as a part of TMVB *K. h. murrayi* due to lack of genetic differentiation. Occurrence records for each subspecies included samples from this study, as well as occurrences obtained from the National Information System of Biodiversity database (CONABIO, 2019), Vertnet (http://vertnet.org), iNaturalist (https://www.inaturalist.org/home), Jennifer Smith, and John Iverson's personal collections. For this analysis, we designated all individuals north of the TMVB as *Kinosternon hirtipes murrayi*, and designated all other populations within the TMVB not assigned to *K. h. chapalaense* or *K. h. magdalense* as TMVB *K. h. murrayi*. All occurrence records were filtered to exclude duplicate localities within each clade. We only identified two unique *K. h. magdalense* occurrences, and constructing distribution models with so few occurrences is impossible, so that taxon was excluded from distribution modeling.

To assess the distributions and habitat suitability of each *K. hirtipes* clade, we extracted values for elevation and 19 bioclimatic (BIOCLIM) variables from Worldclim (Fick and Hijmans 2017). For each clade, we generated models with six Regularization Multipliers (RM) ranging from 0.5 to 3. Higher RMs penalize model complexity, such that higher values discourage the inclusion of additional parameters, making them more generalized. We explored a wide range of feature classes to allow for interactions between environmental variables, as well as simple linear and quadratic response curves. To sample background points for each clade, we drew a 10-km buffer around each known occurrence, and trimmed the environmental variables to match the buffer's extent. The 10-km distance was selected to reflect observed (albeit rare) dispersal of *Kinosternon sonoriense* individuals of over 7 km (Hall and Steidl 2007). We then drew 10,000 random points from within the buffer to serve as background points. We generated an initial set of Species Distribution Models (SDMs) using Maxent and the set of 19 BIOCLIM variables + elevation as predictors. After this initial round of modeling, we selected a reduced set of BIOCLIM variables (**Table S3.2**) by removing variables that had little to no influence on determining the distribution of the occurrences across all three clades based on the variable's permutation importance. We also excluded variables that exhibited high levels

of multicollinearity ($r > 0.8$, (Jones et al. 2010))**.** When deciding between two autocorrelated variables, we kept the variable that had a higher permutation importance across all three lineages.

After selecting our set of environmental predictors, we generated a second series of SDMs for each clade using the reduced variables. For each species, we constructed a set of 20 models that included different regularization multipliers and allowed for different interactions among variables. For Northern *K. h. murrayi* and TMVB *K. h. murrayi,* we used a block partitioning method to train and test models, where occurrences were divided into 4 spatial blocks with equal numbers of occurrences. In line with recommendations for species that have fewer than thirty occurrences (Shcheglovitova and Anderson 2013), we used a k-1 jackknife method to train and test the niche models for *K. h. chapalaense.* To choose the model that best described the present distribution of each clade, we selected one of the three models with the lowest AICc (Akaike's Information Criterion) that had the highest test AUC (area under the curve) for each species. This model was used for downstream analyses of niche overlap and projection onto future climates.

To determine whether there was significant overlap in the niches of the three taxa modeled, we implemented a symmetric background test as defined by Warren et al. 2008 in ENMTools (Warren et al. 2010). Background points were sampled in 10-km buffers around occurrences for each clade. First, we took the niche models constructed from the known occurrence records for each clade and calculated the pairwise overlap between each model to obtain empirical estimates of Schoener's D (Schoener and Gorman 1968) and the I statistic described in Warren et al. (2008). Each overlap metric ranges between 0 to 1 where 0 indicates no overlap in niche space and 1 means the models are identical. Second, we calculated overlap between the best-supported niche model of one species and a set of 100 niche models constructed from subsets of the background points of the other species. This results in a distribution of overlap values for comparisons between the niche model of clade A and the background of clade B (background comparison values). If the observed overlap between clade A and clade B is lower than 95% of the background comparison values, we can conclude that the climatic niches of the two

clades are more divergent than expected given the habitat available to clade B. If the value is significantly higher than the background comparison values, then they are more similar than expected given the habitat available to them.

To assess the future habitat suitability for each lineage, we obtained future climate data for 2050 and 2070 using the CNRM-CM5 climate projections (Voldoire et al. 2013) from Worldclim. We projected the best-fitting model for each clade onto the future climatic data at a resolution of 25 km^2. We investigated two climate change scenarios; SSP5-8.5 (represents the upper end of projected CO_2 emissions and warming) and SSP1-2.6 (represents the lowest emissions and is the best-case scenario for reduced future emissions (Gidden et al. 2019). For both climate change scenarios, we also explored three different GCMs (general circulation models) and projected habitat suitability across each GCM.

We assessed the amount of suitable habitat for each clade under the described climate scenarios. In order to determine a threshold of what suitability score should qualify an area as "suitable" for each clade, we took the mean suitability score for each occurrence record, as recommended by Liu et al. (2005). In each future climate scenario, we focused on suitable habitat near the current distribution of each clade where other populations could conceivably be found, or where turtles from existing populations could migrate. For this reason, we calculated the area of suitable habitat across their present range, which was defined by generating a convex hull with a 10-km buffer around all known occurrence records. We designated cells within the present range as suitable habitat if the suitability score was equal to or greater than the average suitability score for all occurrence records across the present range. The conservation status of *K. hirtipes* taxa was assessed using the NatureServe Conservation Rank Calculator (V3.2) (NatureServe 2015).

Results

Variant Calling and Filtering

The Stacks workflow resulted in a total of 147,507 variants across 34,017 loci. After applying the filtering parameters for the phylogenetic dataset (see Methods, above),

we retained 101 of the 141 originally sampled individuals and 21,576 biallelic SNPs. Following the removal of alleles that were on the same locus or in high linkage disequilibrium (LD) with one another, we retained 5,779 SNPs in the phylogenetic dataset. The filtering parameters for the population genetics dataset resulted in the retention of 90 individuals and 55,310 biallelic SNPs. After further filtering this dataset to remove alleles in LD with one another, we obtained a dataset of 11,637 biallelic SNPs. Sample sizes for each species or lineage, as well as the coverage for each, are presented in **Table S3.1.**

Phylogenetics

Using maximum-likelihood and coalescent methods, we reconstructed a phylogeny that supports several well-resolved clades within *Kinosternon hirtipes* (**Fig. 3.1**). We inferred two main clades that are deeply diverged and well-supported using both methodologies. Samples from populations north of the TMVB, which all represent *K. h. murrayi*, form the first of these two clades which ranges from Durango (MX) to the Trans-Pecos region of Texas (USA). Within this clade, there is a strongly supported divide between samples from north and south of the Rio Grande. The second major clade is composed of populations within the TMVB. Within the TMVB clade, there are three well-supported subclades which are consistent in their topology across both phylogenetic approaches. Two subclades represent described subspecies- *K. h. magdalense* and *K. h. chapalaense. K. h. chapalaense* is an outgroup to a clade containing *K. h. magdalense* and all other populations from the TMVB. The third subclade, as indicated above, is composed of all other *K. hirtipes* populations in the TMVB. Under the current taxonomy, the majority of these populations are considered to be *K. h. murrayi* and *K. h. tarascense,* with the exception of one sample from the Valle de Mexico, which geographically should represent *K. h. hirtipes*. This sample, however, was phenotypically identified as *K. h. murrayi* despite its geographic location, and may have been transplanted as a result of pet trade activity. Given that the TMVB *K. h. murrayi* populations are more closely related to all other populations within the TMVB than to *K. h. murrayi* populations north of the TMVB, we will hereafter refer to these populations as a separate lineage called TMVB *K.*

h. murrayi. Samples of *K. h. tarascense* are nested within this TMVB *K. h. murrayi* clade and do not form a well-supported clade, suggesting they are not an evolutionarily distinct lineage.

Population Genetics

Average nucleotide diversity varied greatly among lineages (**Table 3.1**), with Northern *K. h. murrayi* exhibiting the lowest levels of nucleotide diversity (0.004) and TMVB *K. h. murrayi* (as described above) exhibiting the highest (0.010). Pairwise D_{XY} estimates among all taxa, including kinosternid species and *K. hirtipes* lineages, ranged from 0.013 (TMVB *K. h. murrayi* vs *K. h. magdalense*) to 0.023 (*K. oaxacae* vs *K. sonoriense*) **(Fig. 3.2)**. D_{XY} estimates among the lineages within *K. hirtipes* ranged between 0.013 and 0.015, and W&C's F_{ST} estimates ranged between 0.252 and 0.680**. (Table S3.3).** When all lineages within *K. hirtipes* were considered as one panmictic population, mean inbreeding coefficients (F) were highest in Northern *K. h. murrayi* (0.817)*,* and lower in the TMVB lineages (0.523, 0.460, and 0.418 in *K. h. chapalaense, K. h. magdalense, and* TMVB *K. h. murrayi,* respectively). The northernmost populations of *K. h. murrayi* showed particularly strong evidence of inbreeding **(Fig. S3.2).** When considered within subpopulations (F_{IS}), patterns of inbreeding varied slightly. Northern *K. h. murrayi* still exhibited the highest levels of inbreeding (0.426), while *K. h. magdalense* and *K. h. chapalaense* showed low levels of inbreeding (0.073 and 0.037, respectively). TMVB *K. h. murrayi* was in between these estimates, with a mean F_{IS} value of 0.137 (**Table S4**).

Our Treemix analysis included models that ranged from zero migration events to ten. The amount of variance explained by the models increased from 78.5% to 82.8% when moving from zero migration to a single migration event between *K. h. magdalense* and *K. h. chapalaense*, but showed no increase when adding subsequent migration events (**Table S5)**. The low amount of variance explained by adding migration events suggests little historic gene flow among the lineages identified in this study.

Population Structure

We used the model-based approach implemented in ADMIXTURE to identify major clusters of genetic variation within *Kinosternon hirtipes*. Values of K (number of undefined populations to which individuals are assigned) with the lowest cross-validation error were 2 and 5 (**Fig. 3.3a, Table S3.6),** closely followed by K=3. At K=2, populations north of the TMVB were separated from those within the TMVB. At K=3, *K. h. chapalaense* and *K. h. magdalense* samples appear as a third population. At K=5, the populations almost perfectly correspond to the clades identified in the phylogenies. The results suggest minimal gene flow among the genetic groups in these samples, with most individuals displaying little to no evidence of admixture. The genomic PCA of all *Kinosternon hirtipes* samples also revealed multiple genetic clusters within the widespread species (**Fig. 3.3b)**. Northern *K. h. murrayi* was on one extreme of PC1 (18.2% variation explained), and the TMVB lineages clustered separately on PC1, similar to the results of the ML and coalescent-based phylogenetic trees. There was less differentiation among lineages along PC2 (6.0% variation), where *K. h. magdalense* and *K. h. chapalaense* cluster together and are more distant from the two *K. h. murrayi* lineages, which showed little differentiation on this axis. Samples of *K. h. tarascense* were nested in the center of TMVB *K. h. murrayi* along both PC axes, further supporting their lack of differentiation.

Given the high levels of structure and divergence across the range of *Kinosternon hirtipes,* we investigated the impact of isolation by distance on patterns of genetic differentiation among *K. hirtipes* populations to determine whether observed levels of differentiation can be explained by the distance between populations. The correlation between observed genetic and geographic distance matrices is not significantly greater than the correlation between the matrices obtained from 10,000 random permutations ($p = 0.376$, **Fig. S3.3**). This suggests that distance alone cannot explain the patterns of differentiation among the sampled populations of *K. hirtipes* in this study.

Niche Modeling

Species Distribution Models were successfully constructed for three lineages; Northern *Kinosternon hirtipes murrayi,* TMVB *K. h. murrayi,* and *K. h. chapalaense*

(**Fig. 3.4**). The most important variables for predicting climatic suitability of Northern *K. h. murrayi* were annual mean temperature, elevation, and precipitation during the warmest quarter. (**Table S3.7**). The most important variables for predicting habitat suitability of TMVB *K. h. murrayi* were annual precipitation, precipitation during the wettest quarter, and temperature seasonality (**Table S3.7**). The most important variables for predicting habitat suitability of *K. h. chapalaense* were annual mean temperature, precipitation during the warmest quarter, and temperature seasonality (**Table S3.7)**. We found evidence for niche differentiation among the three taxa for which we were able to construct models. Background tests showed that comparisons of niche overlap between lineages are significantly lower than expected given the overlap in their environmental backgrounds when comparing Northern *K. h. murrayi* to *K. h. chapalaense* or TMVB *K. h. murrayi* for both overlap metrics (**Table S3.8).** *K. h. chapalaense* and TMVB *K. h. murrayi* also exhibited strong patterns of ecological differentiation, although this differentiation was only marginally significant for both overlap metrics (p=.059) given their climatic backgrounds.

The average estimated suitability score of each occurrence record for Northern *K. h. murrayi,* TMVB *K. h. murrayi,* and *K. h. chapalaense* were 0.65, 0.48, and 0.74, respectively. While suitability scores themselves have no implicit biological meaning, the mean score of each occurrence record gives a threshold that represents the set of biological conditions that allow for population persistence. We used this value as a threshold for each lineage to determine the amount of suitable habitat available across their current range for each species in 2020 (present), 2050, and 2070 under both the best and worst-case climate change scenarios. Projected changes in the amount of habitat suitability vary across all three lineages **(Table 3.2).** Even under the best-case emissions scenarios, Northern *K. h. murrayi* is projected to lose more than 80% of suitable habitat by 2050, and even more by 2070. The TMVB lineages, on the other hand, may actually see an increase in climatically suitable habitat under different emissions scenarios. TMVB *K. h. murrayi* is projected to retain between 97 and 114% of its climatically suitable habitat by 2070. *K. h. chapalaense* is also projected to avoid a reduction in

climatically suitable habitat, ranging between 83.72 and 128.84% of its suitable habitat by 2070.

Conservation status

Conservation status assessments for all *Kinosternon hirtipes* lineages were based on the results provided by NatureServe Conservation Rank Calculator (V3.2) (NatureServe 2015). An intraspecific rank of T1 was calculated for *K. h. chapalaense,* TMVB *K. h. murrayi,* and *K. h. magdalense*. We calculated a rank of G1 (globally imperiled) for Northern *K. h. murrayi.* This taxon was previously assigned a global rank of G5/T5 (secure) with National (N) and Subnational ranks of N1/S1 (Critically Imperiled) for Texas populations. Critically imperiled taxa are "at very high risk of extirpation in the jurisdiction due to very restricted range, very few populations or occurrences, very steep declines, severe threats, or other factors." Assessment of conservation status revealed that all lineages within *Kinosternon hirtipes* are insecure (global, national, and subnational ranks < 3).

Discussion

The current taxonomy of *Kinosternon hirtipes* (Iverson 1981) recognizes six subspecies (five extant and one extinct) based on morphology and geographic distribution. Relationships among the subspecies of *K. hirtipes* were previously unclear due to limited sampling and reliance on morphological characters among members of a group that is famously conservative in terms of morphological variation (Cherepanov 2016). Given the broad geographic distribution of *Kinosternon hirtipes*, we investigated patterns of genetic population structure and analyzed the potential for lineages to find suitable climatic habitat over the next several decades. We observed strong patterns of differentiation among the sampled population, with the strongest differentiation separating populations north of the TMVB from populations within the TMVB in both model-based (Admixture) and ordination-based (PCA) approaches.

The two most divergent clades in our phylogeny separated populations within the TMVB from those north of the TMVB. The clade north of the TMVB generally

corresponds with previous descriptions of *K. h. murrayi*, and these populations have been described as morphologically divergent from other *K. hirtipes* populations, likely due to isolation resulting from geographic and climatic barriers (Iverson 1981). Within this Northern *K. h. murrayi* clade, there is a high degree of genetic differentiation between populations separated by the Rio Grande. This division has high support in the ML and coalescent-based trees and was also strongly supported by our Admixture analyses (**Fig. 3.3a**). Additional sampling at more intermediate sites, such as Durango, Zacatecas, and the Lerma-Santiago basin north of the TMVB, may further resolve relationships within this clade. It is worth noting that the Texas and Chihuahua populations of this Northern *K. h. murrayi* clade exhibited the highest measures of inbreeding across all *K. hirtipes* populations (**Fig. S3.2).** In addition to high levels of inbreeding, these populations also exhibited the lowest levels of heterozygosity. This lack of diversity could reflect post-glacial range expansion from lower latitudes, with populations on the leading (northern) edge of range expansion exhibiting less diversity than those in the ancestral range (Russell et al. 2014; Herman et al. 2018; Csapó et al. 2020).

The second clade within *K. hirtipes* contains samples from four subspecies from the TMVB; *K. h. chapalaense, K. h. magdalense, K. h. murrayi*, and *K. h. tarascense* (due to the phenotypic identification of the individual from the Valle de Mexico as *K. h. murrayi*, we do not explicitly consider this sample to represent *K. h. hirtipes*). This clade includes monophyletic groups that correspond to previously named subspecies. Samples of *K. h. chapalaense* and *K. h. magdalense* form well-supported monophyletic sister lineages to a clade which contains all other populations within the TMVB. These remaining populations represent a clade composed of samples representing multiple subspecies within the TMVB. Under the current taxonomy, populations of *K. hirtipes* outside the Valle de Mexico within the TMVB are designated as *K. h. murrayi.* Our results indicate that these populations are deeply diverged from Northern *K. h. murrayi* populations, and should not be considered part of the same lineage. A potential solution to this discordance could be to merge *K. h. murrayi* populations from the TMVB with *K. h. tarascense*, since *K. h. tarascense* populations are nested in this clade and the two sets of populations would form an evolutionarily distinct lineage if merged. *K. h. tarascense*

alone likely does not merit taxonomic recognition. At the very least, a thorough re-assessment of the status of *K. h. murrayi* as a single taxonomic unit should be considered. We recommend retaining the subspecies *K. h. magdalense* and *K. h. chapalaense,* as they form well-supported monophyletic lineages.

The TMVB serves as an important phylogeographic barrier for a wide variety of taxa such as fishes, snakes, salamanders, and hummingbirds (Ornelas-García et al. 2008; Bryson et al. 2011; Parra-Olea et al. 2012; Rodríguez-Gómez and Ornelas 2015; Everson et al. 2021), and it appears to play an important role in the evolutionary history of these lineages as well. Absolute genetic divergence (D_{XY}) between the two most deeply diverged clades within *K. hirtipes* (TMVB versus non-TMVB) was 0.015, which, while lower than comparisons among recognized kinosternid species included in our sampling, greatly exceeds those between recognized species in plants (Ferris et al. 2014; Papadopulos et al. 2019), insects (Talla et al. 2019), and birds (Chase et al. 2021). Furthermore, the genetic differentiation among populations identified is not an artifact of uneven sampling along a continuous cline in variation, as isolation by distance cannot explain the patterns of differentiation among samples. While these estimates of ecological and genetic divergence suggest a deep split between these lineages and unique evolutionary trajectories, a lack of sampling in the contact zone between these taxa near Zacatecas, Mexico, makes it difficult to determine whether these lineages should be recognized as anything more than subspecies.

In addition to the genetic evidence, we also identified strong patterns of ecological differentiation among lineages. We determined that each lineage occupies different habitats when accounting for their environmental background, indicating ecological divergence in the realized niche of each lineage. The observed ecological differentiation could contribute to the accumulation of genetic differences associated with their environments, which often drives lineage diversification in conjunction with drift experienced in allopatry (Schluter 2000; Rissler and Apodaca 2007; Lavinia et al. 2019; Antunes et al. 2021). Additionally, should these lineages come into secondary contact in the future, this ecological divergence may reduce the potential for gene flow in sympatry (Torre et al. 2014; Shaner et al. 2015; Sun et al. 2016). Future physiological studies could

provide more information on the degree of differentiation in the fundamental ecological niches among lineages to supplement the findings from our correlative methods. Notably, if geographic range limits in this species are not constrained by the abiotic variables that we investigated, but by biotic interactions or variables not included in this analysis, these results could be misleading.

Conservation Threats and Recommendations

High levels of inbreeding and low genetic diversity among populations of Northern *K. h. murrayi* may pose a serious threat to their future. The average nucleotide diversity in Northern *K. h. murrayi* (0.004) is greater than that in classic examples of inbreeding such as the Isle Royale wolves and Florida panther (Hedrick et al. 2019; Saremi et al. 2019), as well as some critically endangered turtle species (Vargas-Ramírez et al. 2012; Gallego-García et al. 2021). Nucleotide diversity was, however, lower than observed levels in red-listed populations of sharks, wolverines, and snow leopards (Phillips et al. 2006; Garcia et al. 2015; Ekblom et al. 2018; Janjua et al. 2020). Many Northern *K. h. murrayi* populations are undergoing steep declines, and some populations appear to be composed of only adults or only adult males (Smith 2016). Levels of standing genetic diversity among populations is vital to their potential to respond and adapt to environmental change (Pauls et al. 2013; Wernberg et al. 2018; Razgour et al. 2019), retain immunity to potential diseases (Spielman et al. 2004; Andersen et al. 2018; Kosch et al. 2019), and avoid the accumulation of deleterious genetic variation (Lynch et al. 1995; Allendorf et al. 2010; Kyriazis et al. 2021).

Captive breeding across inbred populations has been successful in other systems, increasing both reproductive rates and survival in outbred individuals (Hogg et al. 2006; Weeks et al. 2017; Heinrichs et al. 2019). Captive breeding of *Kinosternon hirtipes* could be challenging, due to limited information concerning their reproductive ecology and breeding, as well as unknown patterns of seasonal embryonic diapause (Rafferty and Reina 2012). With proper risk assessment and estimates of how much genetic variation could be gained from this strategy, augmenting the genetic variation in this way may prove valuable for their long-term persistence even in the face of other threats, such as

habitat loss due to human activity (Love Stowell et al. 2017; Bell et al. 2019). Conservation status assessments are critically important for the populations of *K. h. murrayi* known from north of the Rio Grande (Smith 2016). The estimated population size at the largest and most intact habitat complex is approximately 134 individual turtles (Smith 2016) and several sites have populations estimated to be in the single digits. Both acute and chronic anthropogenic declines in surface and groundwater availability as well as accelerating loss of aquatic and riparian habitat are widespread in the northernmost range of *K. hirtipes*. In consequence, human intervention and management of dwindling habitat and water resources on which *K. h. murrayi* depends may be critical to the persistence of this species in Texas.

Predictions regarding the future availability of climatically suitable habitat for each lineage are concerning only for populations north of the TMVB. Northern *K. h. murrayi,* are projected to lose over 80% of their suitable climatic habitat by 2050 and 2070 under all emissions scenarios. Conversely, *K. h. chapalaense* and TMVB *K. h. murrayi* may actually see an increase in the amount of climatically suitable habitat across their ranges. The projected loss of habitat is in line with predictions made in previous studies (Butler et al. 2016; Berriozabal-Islas et al. 2020). Narrowly distributed species are particularly prone to extinction since they are more sensitive to disturbances to habitat integrity across their small range of suitable habitat (Kruckeberg and Rabinowitz 1985; Lozada et al. 2008; Cordier et al. 2020; Laspiur et al. 2021), and the projections for the microendemic *K. h. chapalaense* provide a promising outlook for this subspecies. We could not assess the climatic niche of *K. h. magdalense,* which has an even smaller range and is also restricted to an isolated basin, due to only two verified geographic occurrences of this subspecies. However, given the projections for other geographically proximate TMVB lineages, climate change should not drastically reduce habitat suitability for *K. h. magdalense*, either.

We calculated NatureServe conservation ranks for the four lineages defined by our phylogenies. Vulnerable taxa are “at moderate risk of extirpation in the jurisdiction due to a fairly restricted range, relatively few populations or occurrences, recent and widespread declines, threats, or other factors” (NatureServe, 2012). Northern *K. h.*

murrayi was designated as imperiled (G1/N1) while the three TMVB lineages (*K. h. chapalaense,* TMVB *K. h. murrayi,* and *K. h. magdalense*) were all designated as critically imperiled (G1T1). These designations are dramatically different from the rank of G5 (globally secure) calculated for *K. hirtipes* as one taxonomic entity, highlighting the need to conserve the deeply diverged lineages within this species.

Conclusions

We identified strong genetic and ecological differentiation among multiple lineages within *Kinosternon hirtipes*. Patterns of differentiation appear to be driven, in part, by isolation among populations in the TMVB and are generally concordant with described subspecies. *K. h. murrayi* is the subspecies that most likely requires revision, and we recommend that *K. h. murrayi* be revised to reflect the deep split between *K. h. murrayi* populations found north of the TMVB and *K. h. murrayi* populations within the TMVB. We also suggest that *K. h. tarascense* should not be treated as a distinct taxonomic unit given its lack of genetic distinction from other lineages, particularly TMVB *K. h. murrayi*.

Northern *K. h. murrayi populations* are threatened by low levels of genetic diversity and high inbreeding. Furthermore, this lineage is projected to suffer the largest reduction in climatically suitable habitat. Lineages in the TMVB face little to no threat of habitat reduction due to climate change, and exhibit higher levels of genetic diversity. Anthropogenic activities are the primary threat to TMVB lineages, particularly the microendemics, *K. h. chapalaense* and *K. h. magdalense.* The dire conservation status of all lineages within *K. hirtipes* was previously obscured by their treatment as a single, wide-ranging lineage. It is our hope that the unique evolutionary trajectories of these lineages, and the revised conservation assessments based on them, will contribute to informed and focused management of these turtles.

Acknowledgements

We thank the University of Minnesota Genomics Center for their guidance and performing the DNA extractions, RADseq library preparations, and sequencing. The

Minnesota Supercomputing Institute (MSI) at the University of Minnesota provided resources that contributed to the research results reported within this paper. We thank Curtis Eckerman and students from New Mexico State University in Alamogordo for fieldwork and collections as well as private landowners for access and their continued partnership. We also thank Tom Radomski for providing advice on methods for niche modeling and overlap tests. John Iverson, Phil Rosen, and Paul Stone graciously provided tissue samples. The McGaugh-Brandvain labs and two anonymous reviewers provided constructive feedback on earlier drafts. John Iverson provided invaluable insights and comments that greatly improved the manuscript. Dr. Anders Rhodin generously provided data pertaining to the ranges of all extant *K. hirtipes* subspecies.

Figures and Tables

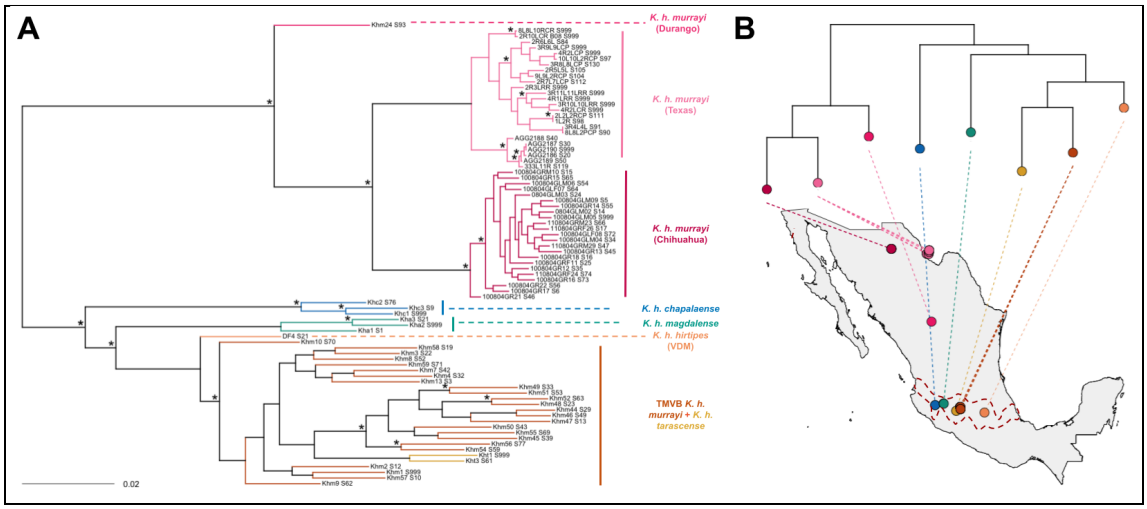

Figure 3.1) Relationships among *K. hirtipes* populations. A) Best-scoring maximum likelihood phylogeny generated in RAxML. Nodes with bootstrap support values over 95 are indicated with asterisks. *Kinosternon hirtipes* subspecies are color-coded, with different shades representing important geographic and genetic clusters within each subspecies. The geographic locations of samples from each of those clusters are mapped in **B**. The dashed red outline on the map shows the extent of the TMVB.

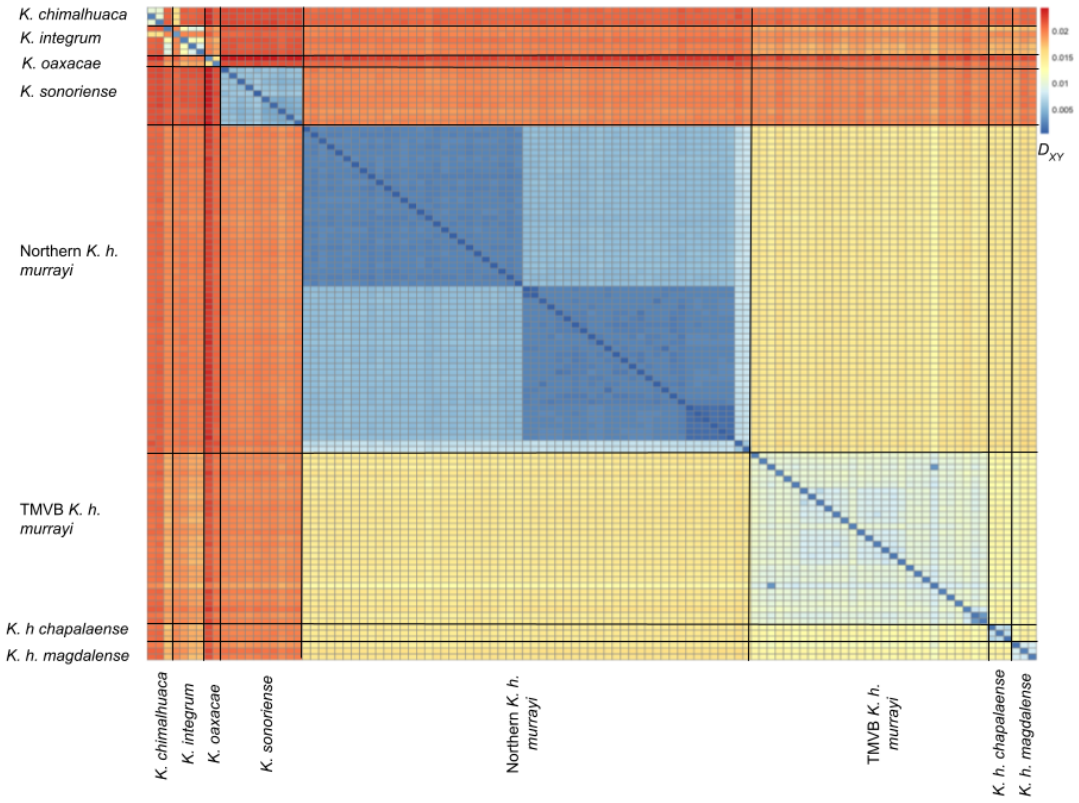

Figure 3.2) Pairwise difference matrix. Heatmap showing the average number of pairwise differences per site when comparing individuals to one another. Values in red indicate more differences between individuals, while blue values indicate fewer differences. Taxa are grouped together and denoted on the x and y axes.

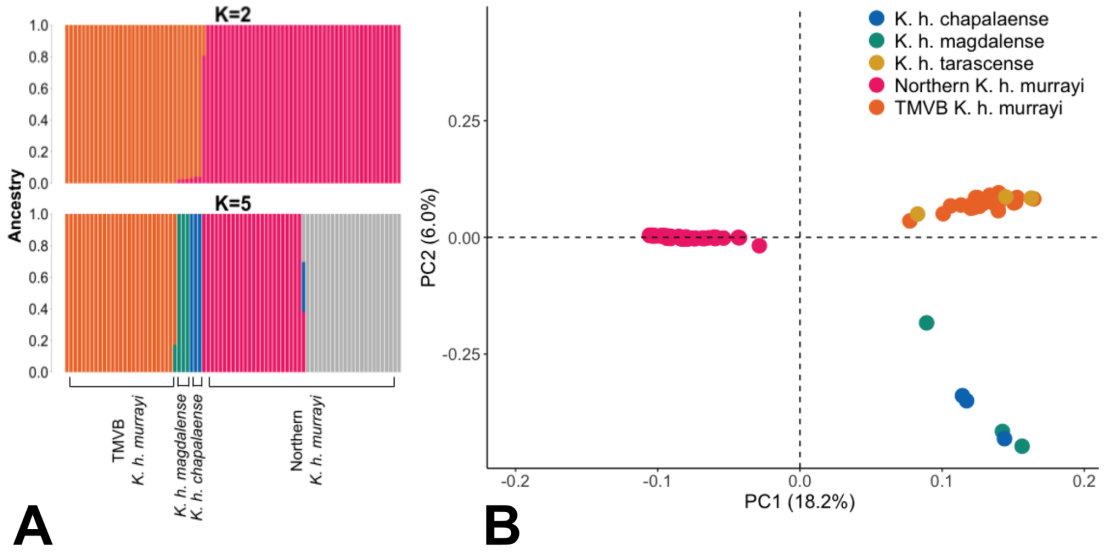

Figure 3.3) Population structure within *K. hirtipes* A) Admixture ancestry assignments for samples of *Kinosternon hirtipes* included in this study when assigned to either 2 (top) or 5 (bottom) populations. These two k values are shown because they have the lowest Cross-validation errors for a range of K values between 2 and 10. Population membership is represented by the color, and individuals with multiple colored bars represent individuals with ancestry from multiple populations. When K=5, the magenta and gray represent a split between populations of *K. h. murrayi* from north and south of the Rio Grande, respectively. **B)** Genomic PCA of all *Kinosternon hirtipes* subspecies included this study. The amount of variance explained by each principal component (PC) is displayed on the axis. PC1 clearly distinguishes Northern *K. h. murrayi* from the TMVB lineages. *K. h. tarascense* is fully contained within the TMVB *K. h. murrayi* cluster on each PC axis**.** PC2 separates a cluster containing *K. h. magdalense* and *K. h. chapalaense* from a cluster containing all other populations.

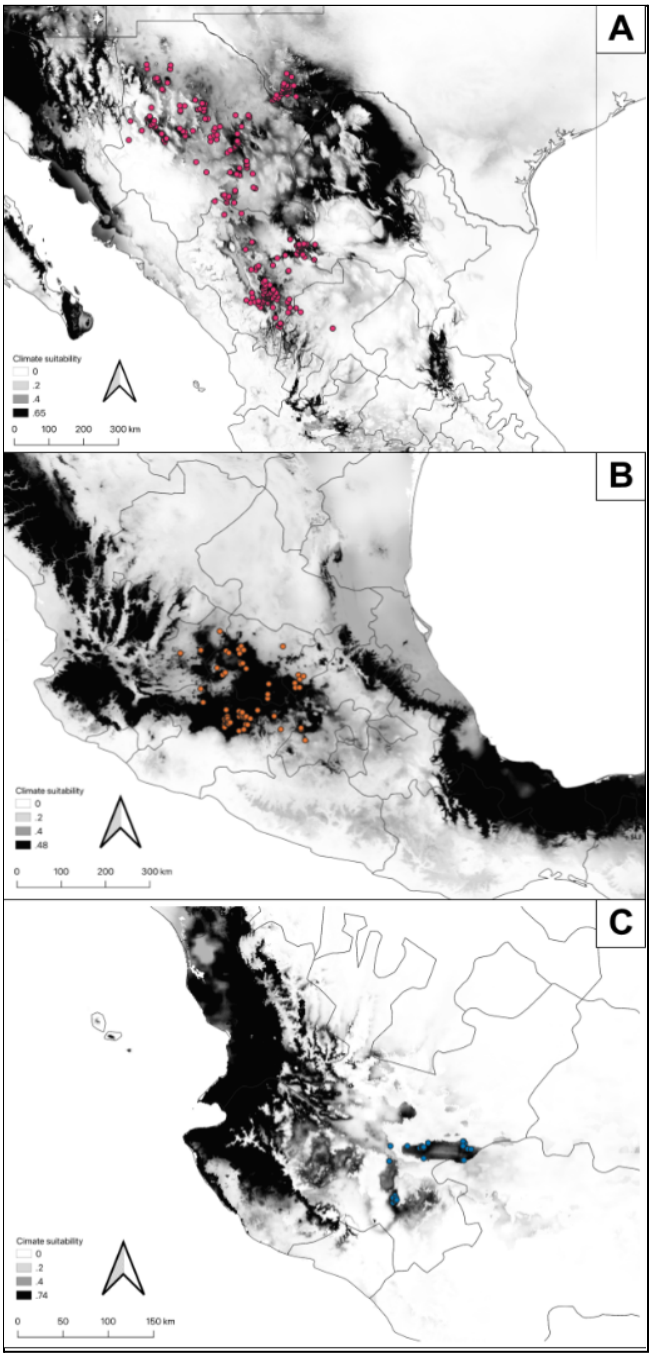

Figure 3.4) Distribution models for *K. hirtipes* lineages. Present-day distribution Models for **A)** Northern *Kinosternon hirtipes murrayi,* **B)** TMVB *K. h. murrayi,* and **C)** *K. h. chapalaense.* Habitat suitability scores are represented by varying shades of gray, with suitable habitat for each species shown in black. Colored dots represent the occurrence records used to construct the distribution models for each lineage.

Table 3.1) D_{xy} and π for all lineages. Inter and intra-population average pairwise nucleotide differences for all lineages and lineage pairs in this study (D_{xy} and π, respectively). Values in gray on the diagonal represent average pi for that population, and values below the diagonal are D_{xy} for the population pair. Values above the diagonal represent coarse estimates of the number of generations since population splits occurred.

	K. chimalhuaca	*K. integrum*	*K. oaxacae*	*K. sonoriense*	Northern *K. h. murrayi*	TMVB *K. h. murrayi*	*K. h. chapalaense*	*K. h. magdalense*
K. chimalhuaca	*0.008*	0.020	0.022	0.022	0.021	0.021	0.021	0.021
K. integrum		*0.008*	0.019	0.022	0.020	0.019	0.018	0.018
K. oaxacae			*0.009*	0.023	0.022	0.021	0.021	0.021
K. sonoriense				*0.005*	0.020	0.020	0.020	0.020
Northern *K. h. murrayi*					*0.004*	0.014	0.015	0.015
TMVB *K. h. murrayi*						*0.010*	0.013	0.013
K. h. chapalaense							*0.006*	0.013
K. h. magdalense								*0.006*

Table 3.2) Changes in climatically suitable habitat. The estimated amount of climatically suitable habitat (relative to 2020) for each subspecies under future emission scenarios within a 10km buffer around their current distribution.

Lineage	2050 (Low Emissions)	2050 (High Emissions)	2070 (Low Emissions)	2070 (High Emissions)
Northern *K. h. murrayi*	19.24%	3.87%	16.98%	0.44%
TMVB *K. h. murrayi*	135.30%	117.51%	114.35%	96.70%
K. h. chapalaense	321.41%	186.59%	83.72%	128.84%

Supplementary Figures

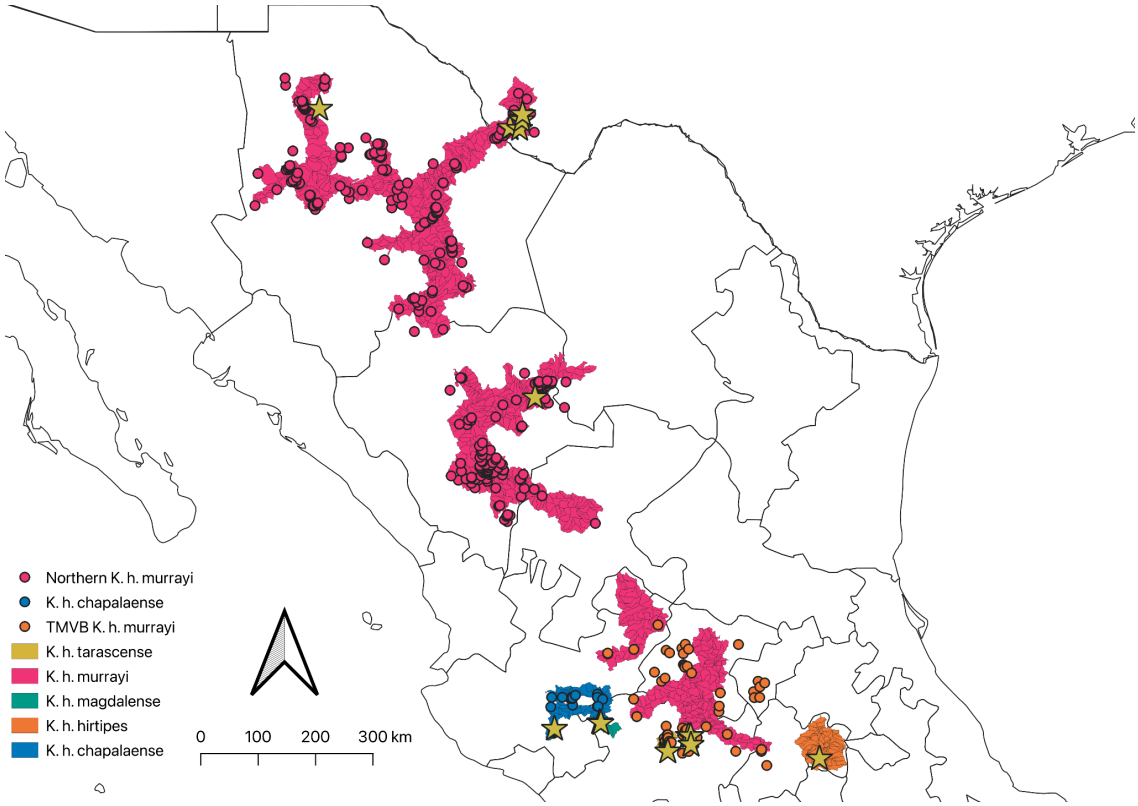

Figure S3.1: Sampling localities and subspecies ranges. Sampling localities of *Kinosternon hirtipes* subspecies used for genomic analyses in this study are represented by gold stars. Sampling localities of occurrences used for lineage climatic niche modeling are represented by colored dots. Ranges for each subspecies are indicated by shaded polygons which were obtained from shapefiles provided by Dr. Anders Rhodin.

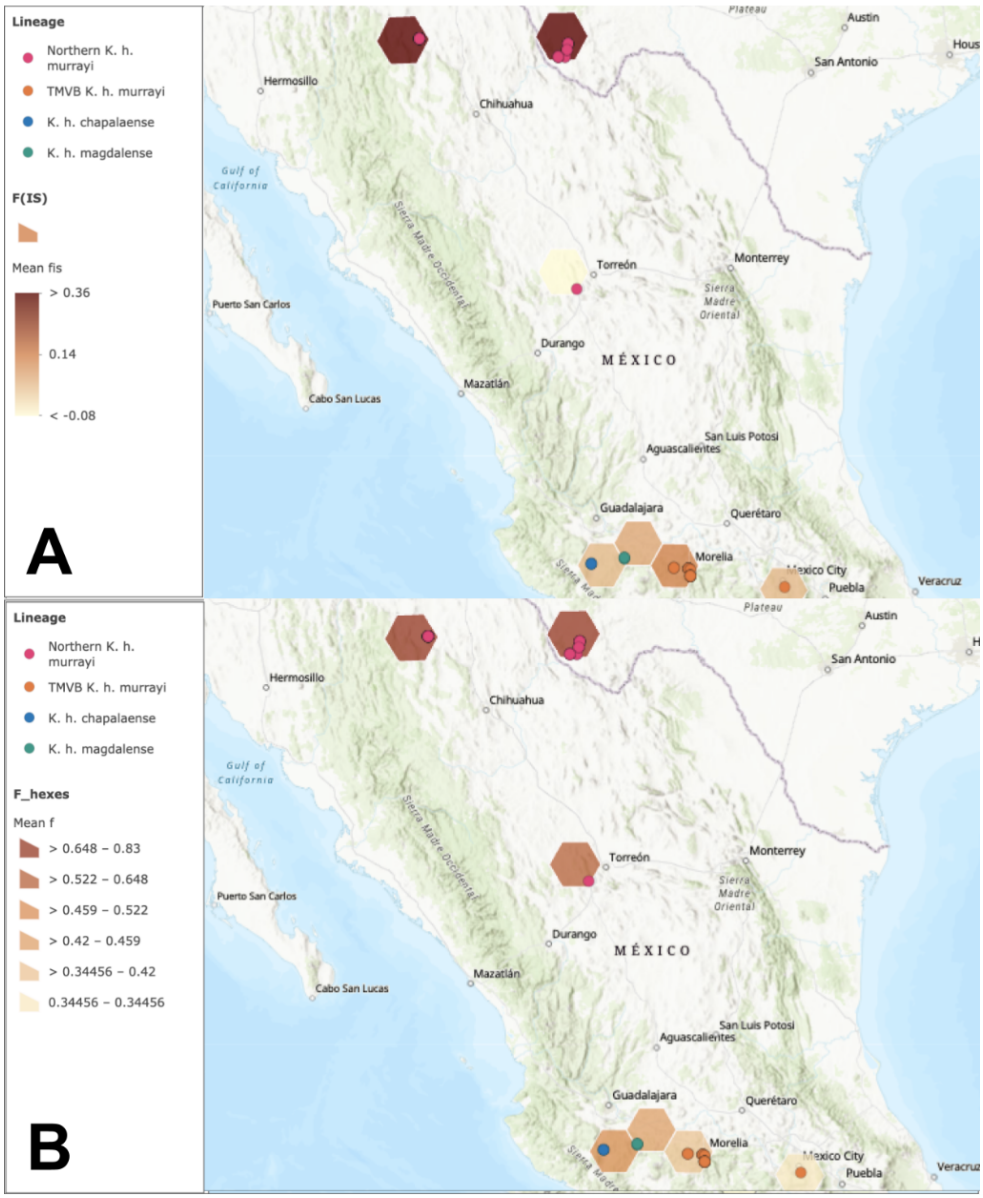

Figure S3.2) Geographic patterns of inbreeding. Mean Inbreeding coefficients for all individuals sampled in this study, binned into 100km hexagons. The inbreeding coefficient represented by each hexagon is the average of all individuals from the populations contained in the hexagon. **A)** Represents inbreeding coefficients with respect to the subpopulation (F_{IS}) and **B)** Represents inbreeding coefficients where all samples are treated as parts of one panmictic population.

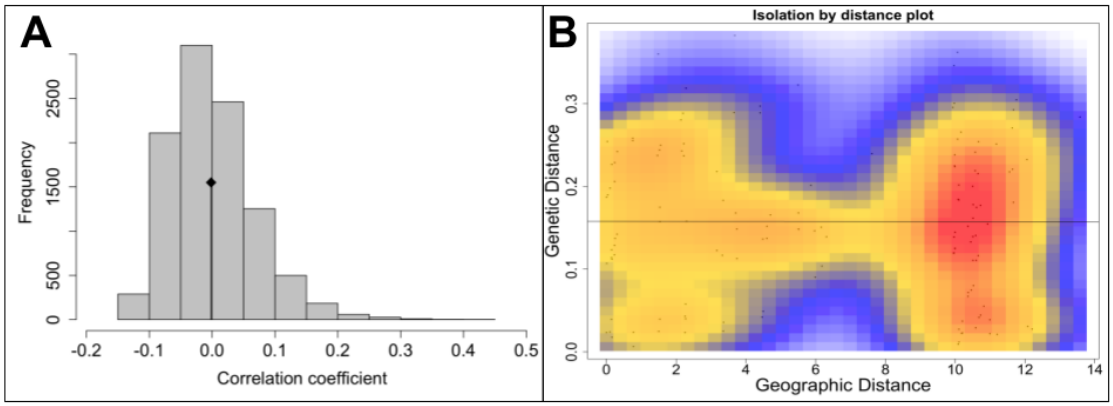

Figure S3.3) Isolation by distance. A) Histogram showing the distribution of correlation coefficients between geographic and genetic distance matrices under 10,000 random permutations. The correlation between the observed matrices is indicated by the black line and diamond. **B)** Correlation between genetic and geographic distances between all *Kinosternon hirtipes* samples. Under IBD alone, a continuous, positive correlation should exist between genetic and geographic distance, but no such trend is observed here. This suggests IBD alone cannot explain the patterns of population structure observed within *K. hirtipes* and that evolutionary independent units are likely contained within the species. Red shades indicate a higher density of observations for cells, and blue shades indicate a lower density of observations.

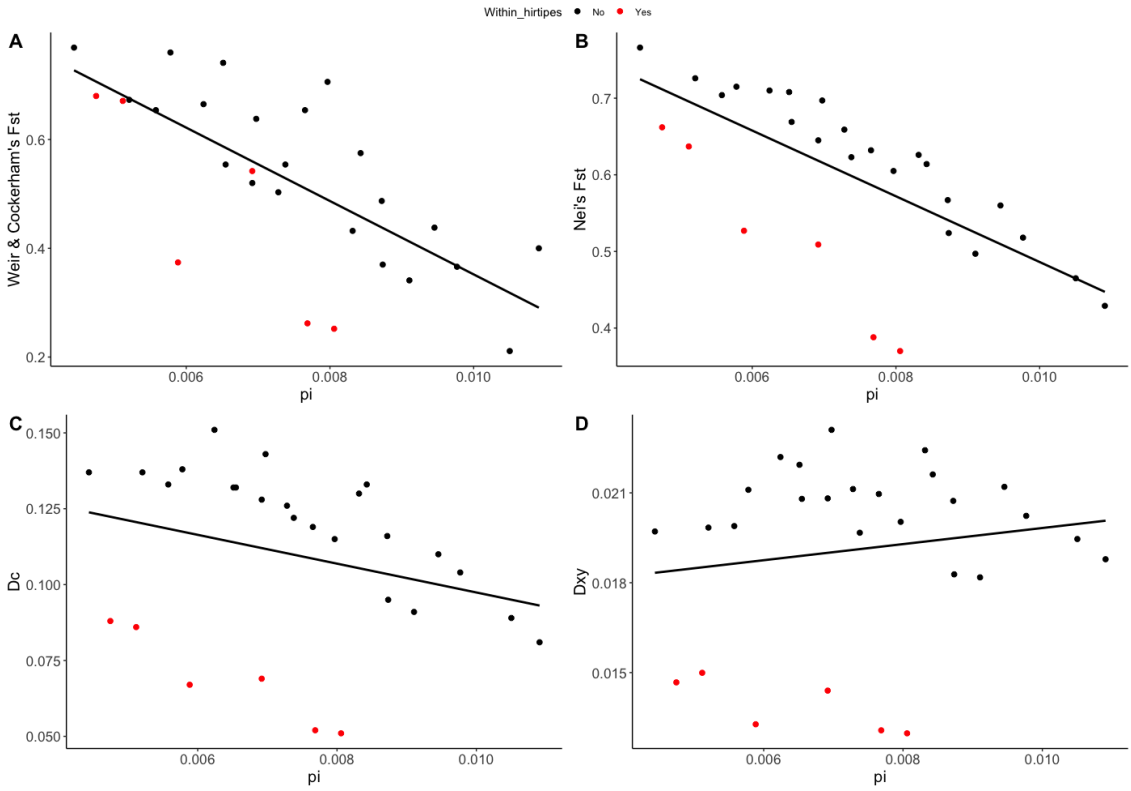

Figure S3.4) Association between genetic diversity and measures of differentiation. Correlation between intraspecific genetic diversity and various metrics of differentiation. Relative measures, shown in panels **A, B,** and **C,** show that, when comparisons are between two species with low diversity, estimates of F_{ST} increase as the mean genetic diversity of two species being compared decreases. This relationship is not observed when estimating D_{XY}, an absolute measure of diversity **(D)**. Red dots represent comparisons among the *K. hirtipes* subspecies.

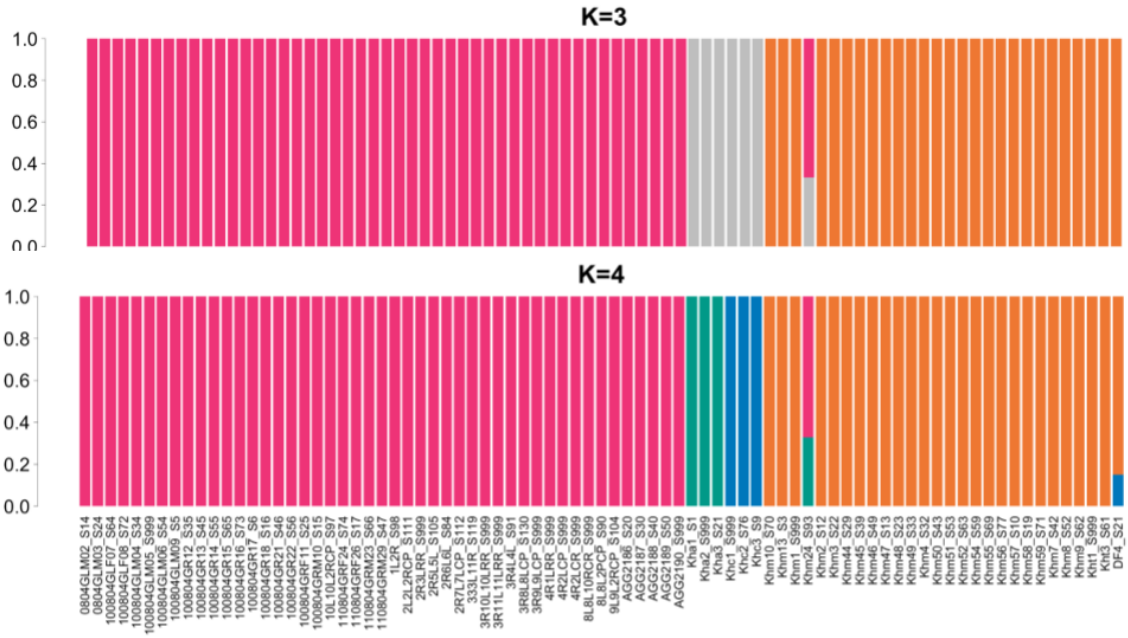

Figure S3.5) ADMIXTURE models for K=3 and K=4. Admixture ancestry assignments for samples of *Kinosternon hirtipes* included in this study when assigned to either 3 (top) or 4 (bottom) populations. Population membership is represented by the color, and individuals with multiple colored bars represent individuals with ancestry from multiple populations.

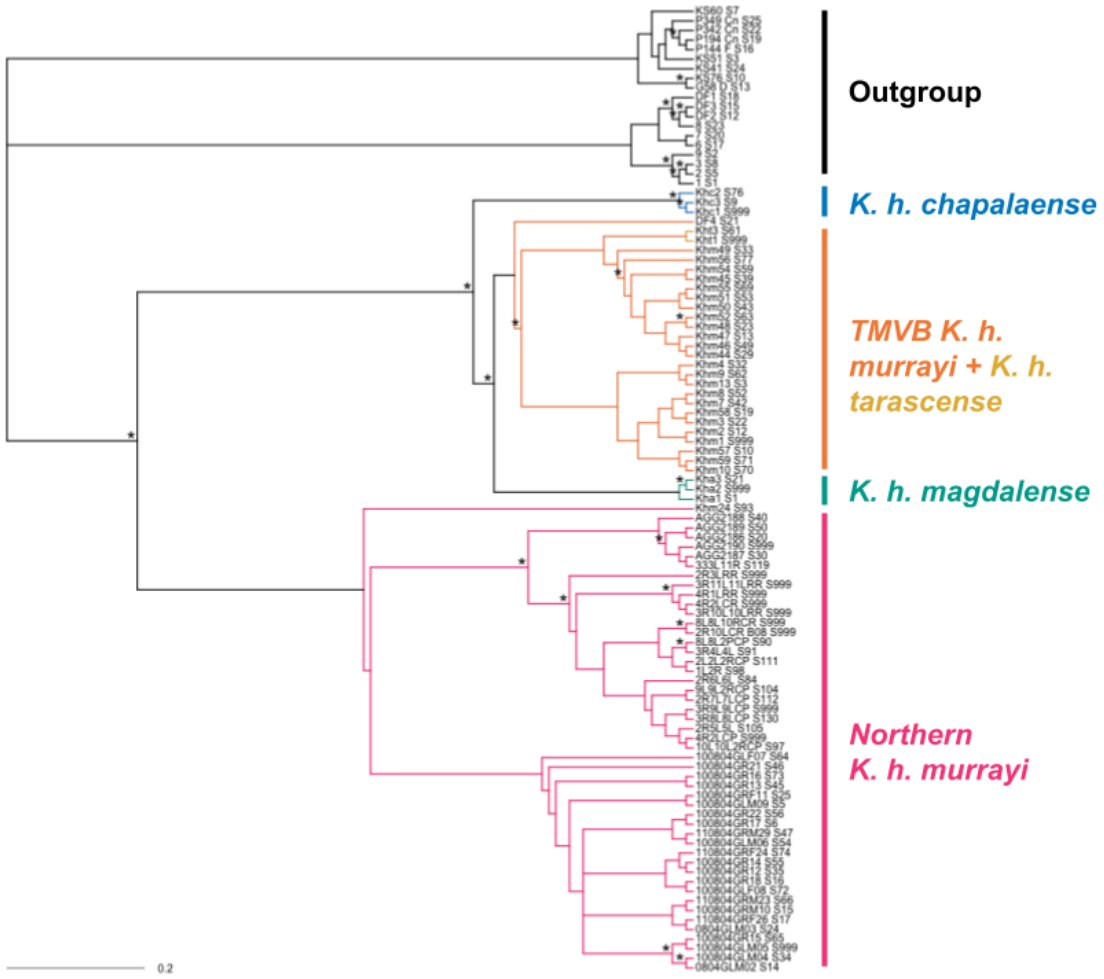

Figure S3.6) SVDQuartets phylogeny. Phylogeny generated using SVDQuartets. All individuals and clades are labeled, and stars indicate nodes with over 95% support. Branch lengths do not represent units of time or mutation, as SVDquartets does not estimate divergence times, only topology.

Table S3.1) Appendix. Information for all samples used in this study. Samples with gray backgrounds were excluded from genomic analyses due to high missingness. Morphological designations were based on subspecies descriptions from Iverson (1981).

Sample Name	Raw Reads	Batch	Morphological taxon designation	Genetic taxon designation	Basin/Locality	Locality	Tissue Type	SRA Accession #
1	1041929	3	*K. chimalhuaca*	*K. chimalhuaca*	Pacific	Chamela	Skin	SRR13101790
2	1104182	3	*K. chimalhuaca*	*K. chimalhuaca*	Pacific	Chamela	Skin	SRR13101789
3	1132241	3	*K. chimalhuaca*	*K. chimalhuaca*	Pacific	Chamela	Skin	SRR13101714
6	1154316	3	*K. oaxacae*	*K. oaxacae*	Pacific	Pochutla	Muscle	SRR13101681
7	1141121	3	*K. oaxacae*	*K. oaxacae*	Pacific	Pochutla	Muscle	SRR13101670
8	1430760	3	*K. integrum*	*K. integrum*	Chapala	Jamay	Blood	SRR13101659
9	838829	3	*K. integrum*	*K. integrum*	Chapala	Jamay	Blood	SRR13101648
0804GLM02	882992	2	*K. h. murrayi*	*Northern K. h. murrayi*	Casas Grandes	Galeana	Blood	SRR13101761
0804GLM03	542900	2	*K. h. murrayi*	*Northern K. h. murrayi*	Casas Grandes	Galeana	Blood	SRR13101782
100804GLF07	817370	2	*K. h. murrayi*	*Northern K. h. murrayi*	Casas Grandes	Galeana	Blood	SRR13101755
100804GLF08	917254	2	*K. h. murrayi*	*Northern K. h. murrayi*	Casas Grandes	Galeana	Blood	SRR13101744
100804GLM04	649935	2	*K. h. murrayi*	*Northern K. h. murrayi*	Casas Grandes	Galeana	Blood	SRR13101733
100804GLM05	4127171	1	*K. h. murrayi*	*Northern K. h. murrayi*	Casas Grandes	Galeana	Blood	SRR13101722
100804GLM05	931151	2	*K. h. murrayi*	*Northern K. h. murrayi*	Casas Grandes	Galeana	Blood	SRR13101717
100804GLM06	678331	2	*K. h. murrayi*	*Northern K. h. murrayi*	Casas Grandes	Galeana	Blood	SRR13101716
100804GLM09	816009	2	*K. h. murrayi*	*Northern K. h. murrayi*	Casas Grandes	Galeana	Blood	SRR13101715
100804GR12	593300	2	*K. h. murrayi*	*Northern K. h. murrayi*	Casas Grandes	Galeana	Blood	SRR13101713
100804GR13	816341	2	*K. h. murrayi*	*Northern K. h. murrayi*	Casas Grandes	Galeana	Blood	SRR13101712
100804GR14	574419	2	*K. h. murrayi*	*Northern K. h. murrayi*	Casas Grandes	Galeana	Blood	SRR13101711
100804GR15	691526	2	*K. h. murrayi*	*Northern K. h. murrayi*	Casas Grandes	Galeana	Blood	SRR13101710
100804GR16	910952	2	*K. h. murrayi*	*Northern K. h. murrayi*	Casas Grandes	Galeana	Blood	SRR13101709
100804GR17	722228	2	*K. h. murrayi*	*Northern K. h. murrayi*	Casas Grandes	Galeana	Blood	SRR13101708

100804GR18	1188258	2	*K. h. murrayi*	*Northern K. h. murrayi*	Casas Grandes	Galeana	Blood	SRR13101707
100804GR19	473561	2	*K. h. murrayi*	NA	Casas Grandes	Galeana	Blood	SRR13101706
100804GR20	487332	2	*K. h. murrayi*	NA	Casas Grandes	Galeana	Blood	SRR13101705
100804GR21	787453	2	*K. h. murrayi*	*Northern K. h. murrayi*	Casas Grandes	Galeana	Blood	SRR13101704
100804GR22	598714	2	*K. h. murrayi*	*Northern K. h. murrayi*	Casas Grandes	Galeana	Blood	SRR13101702
100804GRF11	803639	2	*K. h. murrayi*	*Northern K. h. murrayi*	Casas Grandes	Galeana	Blood	SRR13101701
100804GRM10	706828	2	*K. h. murrayi*	*Northern K. h. murrayi*	Casas Grandes	Galeana	Blood	SRR13101700
10L10L2RCP	977124	2	*K. h. murrayi*	*Northern K. h. murrayi*	Casas Grandes	Galeana	Claw, Carapace	SRR13101699
110804GRF24	761661	2	*K. h. murrayi*	*Northern K. h. murrayi*	Casas Grandes	Galeana	Blood	SRR13101698
110804GRF26	808790	2	*K. h. murrayi*	*Northern K. h. murrayi*	Casas Grandes	Galeana	Blood	SRR13101697
110804GRM23	783176	2	*K. h. murrayi*	*Northern K. h. murrayi*	Casas Grandes	Galeana	Blood	SRR13101696
110804GRM25	511531	2	*K. h. murrayi*	NA	Casas Grandes	Galeana	Blood	SRR13101695
110804GRM27	426164	2	*K. h. murrayi*	NA	Casas Grandes	Galeana	Blood	SRR13101694
110804GRM28	516371	2	*K. h. murrayi*	NA	Casas Grandes	Galeana	Blood	SRR13101693
110804GRM29	946097	2	*K. h. murrayi*	*Northern K. h. murrayi*	Casas Grandes	Galeana	Blood	SRR13101691
11L11L2RCP	523502	2	*K. h. murrayi*	NA	Bravo	Presidio	Claw, Carapace	SRR13101690
1L2R	939621	2	*K. h. murrayi*	*Northern K. h. murrayi*	Bravo	Presidio	Claw, Carapace	SRR13101689
2L2L2RCP	973811	2	*K. h. murrayi*	*Northern K. h. murrayi*	Bravo	Presidio	Claw, Carapace	SRR13101688
2R10LCR.B05	1147582	2	*K. h. murrayi*	NA	Bravo	Presidio	Claw, Carapace	SRR13101687
2R10LCR.B08	808088	2	*K. h. murrayi*	*Northern K. h. murrayi*	Bravo	Presidio	Claw, Carapace	SRR13101686
2R3LRR.G07	912413	2	*K. h. murrayi*	*Northern K. h. murrayi*	Bravo	Presidio	Claw, Carapace	SRR13101685
2R3LRR.H06	933416	2	*K. h. murrayi*	NA	Bravo	Presidio	Webbing, Blood	SRR13101684
2R5L5L	921456	2	*K. h. murrayi*	*Northern K. h. murrayi*	Bravo	Presidio	Claw, Carapace	SRR13101683
2R6L6L	811927	2	*K. h. murrayi*	*Northern K. h. murrayi*	Bravo	Presidio	Claw, Carapace	SRR13101682
2R7L7LCP	1021874	2	*K. h. murrayi*	*Northern K. h. murrayi*	Bravo	Presidio	Claw, Carapace	SRR13101680
333L11R	682894	2	*K. h. murrayi*	*Northern K. h. murrayi*	Bravo	Presidio	Claw, Webbing	SRR13101679

3R10L10LRR.A08	787011	2	*K. h. murrayi*	*Northern K. h. murrayi*	Bravo	Presidio	Claw, Carapace	SRR13101678
3R10L10LRR.H04	1103789	2	*K. h. murrayi*	NA	Bravo	Presidio	Webbing, Blood	SRR13101677
3R11L11LRR	4488125	1	*K. h. murrayi*	*Northern K. h. murrayi*	Bravo	Presidio	Claw, Carapace	SRR13101676
3R11L11LRR.G04	1042741	2	*K. h. murrayi*	NA	Bravo	Presidio	Webbing, Blood	SRR13101675
3R11L11LRR.H07	911338	2	*K. h. murrayi*	NA	Bravo	Presidio	Webbing, Blood	SRR13101674
3R4L4L	990283	2	*K. h. murrayi*	*Northern K. h. murrayi*	Bravo	Presidio	Claw, Carapace	SRR13101673
3R8L8LCP	938271	2	*K. h. murrayi*	*Northern K. h. murrayi*	Bravo	Presidio	Claw, Carapace	SRR13101672
3R9L9LCP.G05	942345	2	*K. h. murrayi*	*Northern K. h. murrayi*	Bravo	Presidio	Claw, Carapace	SRR13101671
3R9L9LCP.G08	862730	2	*K. h. murrayi*	NA	Bravo	Presidio	Webbing, Blood	SRR13101669
4R1LCR.D05	570066	2	*K. h. murrayi*	NA	Bravo	Presidio	Claw, Carapace	SRR13101668
4R1LCR.D08	707900	2	*K. h. murrayi*	NA	Bravo	Presidio	Webbing, Blood	SRR13101667
4R1LRR.F07	642668	2	*K. h. murrayi*	*Northern K. h. murrayi*	Bravo	Presidio	Claw, Carapace	SRR13101666
4R1LRR.G06	797009	2	*K. h. murrayi*	NA	Bravo	Presidio	Webbing, Blood	SRR13101665
4R2LCP	3599531	1	*K. h. murrayi*	*Northern K. h. murrayi*	Bravo	Presidio	Claw, Carapace	SRR13101664
4R2LCP.F05	671151	2	*K. h. murrayi*	NA	Bravo	Presidio	Webbing, Blood	SRR13101663
4R2LCP.F08	821814	2	*K. h. murrayi*	NA	Bravo	Presidio	Webbing, Blood	SRR13101662
4R2LCR.E05	1081270	2	*K. h. murrayi*	*Northern K. h. murrayi*	Bravo	Presidio	Claw, Carapace	SRR13101661
4R2LCR.E08	1127355	2	*K. h. murrayi*	NA	Bravo	Presidio	Webbing, Blood	SRR13101660
8L8L10RCR.A05	964096	2	*K. h. murrayi*	*Northern K. h. murrayi*	Bravo	Presidio	Claw, Carapace	SRR13101658
8L8L10RCR.F06	422244	2	*K. h. murrayi*	NA	Bravo	Presidio	Webbing, Blood	SRR13101657
8L8L2PCP	969259	2	*K. h. murrayi*	*Northern K. h. murrayi*	Bravo	Presidio	Claw, Carapace	SRR13101656
9L9L2RCP	796923	2	*K. h. murrayi*	NA	Bravo	Presidio	Claw, Carapace	SRR13101655
9R9R11LCR.C05	956750	2	*K. h. murrayi*	NA	Bravo	Presidio	Claw, Carapace	SRR13101654
9R9R11LCR.C08	979169	2	*K. h. murrayi*	NA	Bravo	Presidio	Webbing, Blood	SRR13101653
AGG2186	845042	2	*K. h. murrayi*	*Northern K. h. murrayi*	Bravo	Presidio	Webbing	SRR13101652
AGG2187	918375	2	*K. h. murrayi*	*Northern K. h. murrayi*	Bravo	Presidio	Webbing	SRR13101651

AGG2188	**754381**	**2**	***K. h. murrayi***	***Northern K. h. murrayi***	**Bravo**	**Presidio**	**Webbing**	**SRR13101650**
AGG2189	**871017**	**2**	***K. h. murrayi***	***Northern K. h. murrayi***	**Bravo**	**Presidio**	**Webbing**	**SRR13101649**
AGG2190	**4375705**	**1**	***K. h. murrayi***	***Northern K. h. murrayi***	**Bravo**	**Presidio**	**Webbing**	**SRR13101647**
AGG2190	**603277**	**2**	***K. h. murrayi***	**NA**	**Bravo**	**Presidio**	**Webbing**	**SRR13101646**
DF1	**1368256**	**3**	***K. integrum***	***K. integrum***	**Valley Of Mexico**	**Mexico City**	**Blood**	**SRR13101645**
DF2	**1060506**	**3**	***K. integrum***	***K. integrum***	**Valley Of Mexico**	**Mexico City**	**Blood**	**SRR13101644**
DF3	**1585131**	**3**	***K. integrum***	***K. integrum***	**Valley Of Mexico**	**Mexico City**	**Blood**	**SRR13101643**
DF4	**909252**	**3**	***K. h. murrayi***	***TMVB K. h. murrayi***	**Valley Of Mexico**	**Mexico City**	**Blood**	**SRR13101642**
G58.D	**1454765**	**3**	***K. s. sonoriense***	***K. sonoriense***	**Madrean Sky Islands**	**Peloncillo Mountains**	**Blood**	**SRR13101641**
Kha1	**689664**	**2**	***K. h. magdalense***	***K. h. magdalense***	**Magdalena**	**Cotija**	**Blood**	**SRR13101640**
Kha2	**3963329**	**1**	***K. h. magdalense***	***K. h. magdalense***	**Magdalena**	**Cotija**	**Blood**	**SRR13101639**
Kha2	**984160**	**2**	***K. h. magdalense***	***K. h. magdalense***	**Magdalena**	**Cotija**	**Blood**	**SRR13101638**
Kha3	**1158179**	**2**	***K. h. magdalense***	***K. h. magdalense***	**Magdalena**	**Cotija**	**Blood**	**SRR13101636**
Khc1	**4243775**	**1**	***K. h. chapalaense***	***K. h. chapalaense***	**Chapala**	**Zapotlán**	**Blood**	**SRR13101635**
Khc1	**998275**	**2**	***K. h. chapalaense***	***K. h. chapalaense***	**Chapala**	**Zapotlán**	**Muscle**	**SRR13101634**
Khc2	**894868**	**2**	***K. h. chapalaense***	***K. h. chapalaense***	**Chapala**	**Zapotlán**	**Muscle**	**SRR13101633**
Khc3	**770276**	**2**	***K. h. chapalaense***	***K. h. chapalaense***	**Chapala**	**Zapotlán**	**Muscle**	**SRR13101632**
Khm1	**4256889**	**1**	***K. h. murrayi***	***TMVB K. h. murrayi***	**Cuitzeo**	**Morelia**	**Blood**	**SRR13101631**
Khm1	**808694**	**2**	***K. h. murrayi***	***TMVB K. h. murrayi***	**Cuitzeo**	**Morelia**	**Blood**	**SRR13101630**
Khm10	**1064487**	**2**	***K. h. murrayi***	***TMVB K. h. murrayi***	**Cuitzeo**	**Morelia**	**Blood**	**SRR13101629**
Khm13	**613859**	**2**	***K. h. murrayi***	***TMVB K. h. murrayi***	**Cuitzeo**	**Morelia**	**Blood**	**SRR13101628**
Khm14	**719049**	**2**	***K. h. murrayi***	**NA**	**Presidio-San Pedro**	**Durango**	**Blood**	**SRR13101627**
Khm15	**517141**	**2**	***K. h. murrayi***	**NA**	**Lerma**	**Villa Victoria**	**Blood**	**SRR13101771**
Khm16	**753704**	**2**	***K. h. murrayi***	**NA**	**Presidio-San Pedro**	**Durango**	**Blood**	**SRR13101770**
Khm17	**192195**	**2**	***K. h. murrayi***	**NA**	**Presidio-San Pedro**	**Durango**	**Blood**	**SRR13101769**
Khm18	**229186**	**2**	***K. h. murrayi***	**NA**	**Lerma**	**Villa Victoria**	**Blood**	**SRR13101768**
Khm19	**498571**	**2**	***K. h. murrayi***	**NA**	**Camecuaro**	**Zamora**	**Blood**	**SRR13101767**
Khm2	**993447**	**2**	***K. h. murrayi***	***TMVB K. h. murrayi***	**Cuitezo**	**Morelia**	**Blood**	**SRR13101766**

Khm20	**330420**	**2**	***K. h. murrayi***	**NA**	**Nazas**	**Durango**	**Blood**	**SRR13101765**
Khm21	**499061**	**2**	***K. h. murrayi***	**NA**	**Lerma**	**Valle de Guadalupe**	**Blood**	**SRR13101764**
Khm22	**385987**	**2**	***K. h. murrayi***	**NA**	**Lerma**	**Valle de Guadalupe**	**Bone**	**SRR13101763**
Khm23	**285840**	**2**	***K. h. murrayi***	**NA**	**Conchos**	**Durango**	**Bone**	**SRR13101762**
Khm24	**910356**	**2**	***K. h. murrayi***	***TMVB K. h. murrayi***	**Nazas**	**Durango**	**Bone**	**SRR13101760**
Khm25	**244125**	**2**	***K. h. murrayi***	**NA**	**Nazas**	**Durango**	**Bone**	**SRR13101759**
Khm26	**867305**	**2**	***K. h. murrayi***	**NA**	**Santiago**	**Valle de Guadalupe**	**Bone**	**SRR13101758**
Khm27	**407972**	**2**	***K. h. murrayi***	**NA**	**Santiago**	**Valle de Guadalupe**	**Bone**	**SRR13101757**
Khm28	**442247**	**2**	***K. h. murrayi***	**NA**	**Santiago**	**Valle de Guadalupe**	**Bone**	**SRR13101788**
Khm29	**430179**	**2**	***K. h. murrayi***	**NA**	**Lerma**	**Villa Victoria**	**Bone**	**SRR13101787**
Khm3	**717087**	**2**	***K. h. murrayi***	***TMVB K. h. murrayi***	**Cuitezo**	**Morelia**	**Bone**	**SRR13101786**
Khm30	**269662**	**2**	***K. h. murrayi***	**NA**	**Santiago**	**Jalisco**	**Bone**	**SRR13101785**
Khm31	**506690**	**2**	***K. h. murrayi***	**NA**	**Santiago**	**Jalisco**	**Bone**	**SRR13101784**
Khm32	**818128**	**2**	***K. h. murrayi***	**NA**	**Nazas**	**Durango**	**Bone**	**SRR13101783**
Khm33	**462333**	**2**	***K. h. murrayi***	**NA**	**Nazas**	**Durango**	**Bone**	**SRR13101781**
Khm34	**633745**	**2**	***K. h. murrayi***	**NA**	**Camecuaro**	**Zamora**	**Bone**	**SRR13101780**
Khm35	**289681**	**2**	***K. h. murrayi***	**NA**	**Camecuaro**	**Zamora**	**Bone**	**SRR13101779**
Khm36	**271825**	**2**	***K. h. murrayi***	**NA**	**Nazas**	**Durango**	**Bone**	**SRR13101778**
Khm37	**388546**	**2**	***K. h. murrayi***	**NA**	**Nazas**	**Durango**	**Bone**	**SRR13101777**
Khm38	**239548**	**2**	***K. h. murrayi***	**NA**	**Camecuaro**	**Zamora**	**Bone**	**SRR13101776**
Khm39	**209373**	**2**	***K. h. murrayi***	**NA**	**Nazas**	**Durango**	**Bone**	**SRR13101775**
Khm4	**907044**	**2**	***K. h. murrayi***	***TMVB K. h. murrayi***	**Cuitzeo**	**Morelia**	**Bone**	**SRR13101774**
Khm40	**467125**	**2**	***K. h. murrayi***	**NA**	**San Pedro Mezquital**	**Durango**	**Bone**	**SRR13101773**
Khm41	**401349**	**2**	***K. h. murrayi***	**NA**	**Camecuaro**	**Zamora**	**Bone**	**SRR13101756**
Khm42	**108898**	**2**	***K. h. murrayi***	**NA**	**San Pedro Mezquital**	**Durango**	**Bone**	**SRR13101754**
Khm43	**361814**	**2**	***K. h. murrayi***	**NA**	**Santiago**	**Jalisco**	**Bone**	**SRR13101753**
Khm44	**745855**	**2**	***K. h. murrayi***	***TMVB K. h. murrayi***	**Cuitzeo**	**Morelia Highlands**	**Bone**	**SRR13101752**
Khm45	**744621**	**2**	***K. h. murrayi***	***TMVB K. h. murrayi***	**Cuitzeo**	**Morelia Highlands**	**Bone**	**SRR13101751**
Khm46	**901210**	**2**	***K. h. murrayi***	***TMVB K. h. murrayi***	**Cuitzeo**	**Morelia Highlands**	**Bone**	**SRR13101750**

Khm47	**904417**	**2**	***K. h. murrayi***	***TMVB K. h. murrayi***	**Cuitzeo**	**Morelia Highlands**	**Bone**	**SRR13101749**
Khm48	**854297**	**2**	***K. h. murrayi***	***TMVB K. h. murrayi***	**Cuitzeo**	**Morelia Highlands**	**Bone**	**SRR13101748**
Khm49	**779826**	**2**	***K. h. murrayi***	***TMVB K. h. murrayi***	**Cuitzeo**	**Morelia Highlands**	**Bone**	**SRR13101747**
Khm50	**945053**	**2**	***K. h. murrayi***	***TMVB K. h. murrayi***	**Cuitzeo**	**Morelia Highlands**	**Bone**	**SRR13101746**
Khm51	**694151**	**2**	***K. h. murrayi***	***TMVB K. h. murrayi***	**Cuitzeo**	**Morelia Highlands**	**Bone**	**SRR13101745**
Khm52	**869349**	**2**	***K. h. murrayi***	***TMVB K. h. murrayi***	**Cuitzeo**	**Morelia Highlands**	**Bone**	**SRR13101743**
Khm54	**621778**	**2**	***K. h. murrayi***	***TMVB K. h. murrayi***	**Cuitzeo**	**Morelia Highlands**	**Bone**	**SRR13101742**
Khm55	**777336**	**2**	***K. h. murrayi***	***TMVB K. h. murrayi***	**Cuitzeo**	**Morelia Highlands**	**Bone**	**SRR13101741**
Khm56	**863863**	**2**	***K. h. murrayi***	***TMVB K. h. murrayi***	**Cuitzeo**	**Morelia Highlands**	**Bone**	**SRR13101740**
Khm57	**742894**	**2**	***K. h. murrayi***	***TMVB K. h. murrayi***	**Cuitzeo**	**Morelia**	**Bone**	**SRR13101739**
Khm58	**869447**	**2**	***K. h. murrayi***	***TMVB K. h. murrayi***	**Cuitzeo**	**Morelia**	**Bone**	**SRR13101738**
Khm59	**873146**	**2**	***K. h. murrayi***	***TMVB K. h. murrayi***	**Cuitzeo**	**Morelia**	**Bone**	**SRR13101737**
Khm60	**589366**	**2**	***K. h. murrayi***	***TMVB K. h. murrayi***	**Cuitzeo**	**Morelia**	**Bone**	**SRR13101736**
Khm7	**1029685**	**2**	***K. h. murrayi***	***TMVB K. h. murrayi***	**Cuitzeo**	**Morelia**	**Blood**	**SRR13101735**
Khm8	**786512**	**2**	***K. h. murrayi***	***TMVB K. h. murrayi***	**Cuitzeo**	**Morelia**	**Blood**	**SRR13101734**
Khm9	**1090241**	**2**	***K. h. murrayi***	***TMVB K. h. murrayi***	**Cuitzeo**	**Morelia**	**Blood**	**SRR13101732**
Kht1	**4312499**	**1**	***K. h. tarascense***	***TMVB K. h. murrayi***	**Patzcuaro**	**Patzcuaro Lake**	**Blood**	**SRR13101731**
Kht1	**741938**	**2**	***K. h. tarascense***	**NA**	**Patzcuaro**	**Patzcuaro Lake**	**Blood**	**SRR13101730**
Kht2	**526389**	**2**	***K. h. tarascense***	***TMVB K. h. murrayi***	**Patzcuaro**	**Patzcuaro Lake**	**Blood**	**SRR13101729**
Kht3	**1080599**	**2**	***K. h. tarascense***	***TMVB K. h. murrayi***	**Patzcuaro**	**Patzcuaro Lake**	**Blood**	**SRR13101728**
KS41	**1231798**	**3**	***K. s. sonoriense***	***K. s. sonoriense***	**Rio Sonora**	**Sonora Highlands**	**Blood**	**SRR13101727**
KS51	**1038635**	**3**	***K. s. sonoriense***	***K. s. sonoriense***	**Casas Grandes**	**Nuevo Casas Grandes**	**Blood**	**SRR13101726**
KS60	**1041906**	**3**	***K. s. sonoriense***	***K. s. sonoriense***	**Yaqui**	**Sonora**	**Blood**	**SRR13101725**
KS76	**1153585**	**3**	***K. s. longifemorale***	***K. s. sonoriense***	**Sonoyta**	**Xochimilco stream**	**Blood**	**SRR13101724**

P144.F	1427443	3	*K. s. sonoriense*	*K. s. sonoriense*	Madrean Sky Islands	Peloncillo Mountains	Blood	SRR13101723
P194.Cn	1378581	3	*K. s. sonoriense*	*K. s. sonoriense*	Madrean Sky Islands	Peloncillo Mountains	Blood	SRR13101721
P2247.F	627526	3	*K. s. sonoriense*	*K. s. sonoriense*	Madrean Sky Islands	Peloncillo Mountains	Blood	SRR13101720
P342.Cn	1085452	3	*K. s. sonoriense*	*K. s. sonoriense*	Madrean Sky Islands	Peloncillo Mountains	Blood	SRR13101719
P349.Cn	1672430	3	*K. s. sonoriense*	*K. s. sonoriense*	Madrean Sky Islands	Peloncillo Mountains	Blood	SRR13101718

Table S3.2) Climatic variables for niche modeling. Climate variables used in this study and their descriptions.

Bioclim Variable	Description	Retained
Bio1	Annual Mean Temperature	Yes
Bio2	Mean Diurnal Range (Mean of monthly (max temp - min temp))	No
Bio3	Isothermality (BIO2/BIO7) (×100)	No
Bio4	Temperature Seasonality (standard deviation ×100)	Yes
Bio5	Max Temperature of Warmest Month	No
Bio6	Min Temperature of Coldest Month	No
Bio7	Temperature Annual Range (BIO5-BIO6)	No
Bio8	Mean Temperature of Wettest Quarter	No
Bio9	Mean Temperature of Driest Quarter	No
Bio10	Mean Temperature of Warmest Quarter	No
Bio11	Mean Temperature of Coldest Quarter	No
Bio12	Annual Precipitation	Yes
Bio13	Precipitation of Wettest Month	No
Bio14	Precipitation of Driest Month	No
Bio15	Precipitation Seasonality (Coefficient of Variation)	No
Bio16	Precipitation of Wettest Quarter	Yes
Bio17	Precipitation of Driest Quarter	Yes
Bio18	Precipitation of Warmest Quarter	Yes
Bio19	Precipitation of Coldest Quarter	No
Elevation	Elevation	Yes

Table S3.3) Population differentiation. Measures of differentiation between all species pairwise comparisons in this study.

Taxon 1	Taxon 2	Weir & Cockerham's Fst	Nei's Fst	Cavalli-Sforza chord distance	Dxy
K. h. chapalaense	*K. h. magdalense*	0.374	0.527	0.067	0.013
K. chimalhuaca	*K. h. chapalaense*	0.554	0.669	0.132	0.021
K. chimalhuaca	TMVB *K. h. murrayi*	0.487	0.567	0.116	0.021
K. chimalhuaca	*K. integrum*	0.366	0.518	0.104	0.020
K. chimalhuaca	*K. h. magdalense*	0.52	0.645	0.128	0.021
K. chimalhuaca	Northern *K. h. murrayi*	0.76	0.715	0.138	0.021
K. chimalhuaca	*K. oaxacae*	0.432	0.626	0.13	0.022
K. chimalhuaca	*K. sonoriense*	0.665	0.71	0.151	0.022
TMVB *K. h. murrayi*	*K. h. chapalaense*	0.262	0.388	0.052	0.013
TMVB *K. h. murrayi*	*K. h. magdalense*	0.252	0.37	0.051	0.013
K. integrum	*K. h. chapalaense*	0.37	0.524	0.095	0.018
K. integrum	TMVB *K. h. murrayi*	0.4	0.429	0.081	0.019
K. integrum	*K. h. magdalense*	0.341	0.497	0.091	0.018
K. integrum	Northern *K. h. murrayi*	0.706	0.605	0.115	0.020
K. integrum	*K. oaxacae*	0.211	0.465	0.089	0.019
K. integrum	*K. sonoriense*	0.575	0.614	0.133	0.022
Northern *K. h. murrayi*	*K. h. chapalaense*	0.68	0.662	0.088	0.015
Northern *K. h. murrayi*	TMVB *K. h. murrayi*	0.542	0.509	0.069	0.014

Northern *K. h. murrayi*	*K. h. magdalense*	0.671	0.637	0.086	0.015
K. oaxacae	*K. h. chapalaense*	0.503	0.659	0.126	0.021
K. oaxacae	TMVB *K. h. murrayi*	0.438	0.56	0.11	0.021
K. oaxacae	*K. h. magdalense*	0.654	0.632	0.119	0.021
K. oaxacae	Northern *K. h. murrayi*	0.741	0.708	0.132	0.022
K. oaxacae	*K. sonoriense*	0.638	0.697	0.143	0.023
K. sonoriense	*K. h. chapalaense*	0.673	0.726	0.137	0.020
K. sonoriense	TMVB *K. h. murrayi*	0.554	0.623	0.122	0.020
K. sonoriense	*K. h. magdalense*	0.654	0.704	0.133	0.020
K. sonoriense	Northern *K. h. murrayi*	0.769	0.766	0.137	0.020

Table S3.4) Inbreeding coefficients. Mean inbreeding coefficients for each population when all *K. hirtipes* samples are considered as one panmictic population (F) and within their genetic subpopulation (F_{IS}).

Lineage	F	F(IS)
Northern *K. h. murrayi*	0.817	0.426
TMVB *K. h. murrayi*	0.418	0.137
K. h. magdalense	0.46	0.073
K. h. chapalaense	0.523	0.037

Table S3.5) Variance explained by migration events. Proportion of variance explained by different numbers of migration events using Treemix.

Migration events	Variance Explained
0	0.785
1	0.828
2	0.829
3	0.828
4	0.825
5	0.828
6	0.824
7	0.823
8	0.823
9	0.824
10	0.824

Table S3.6) ADMIXTURE model parameters. Cross-validation errors and Log Likelihood estimates for runs of ADMIXTURE ranging from K=2 to K=16. The two models with the lowest CV error rates (K=2 and K=5) were considered the best-supported models.

K	CV Error	Log Likelihood
2	0.13112	-117951.5311
3	0.13957	-108542.1403
4	0.15306	-104292.4047
5	0.13953	-90533.32028
6	0.14927	-88740.68336
7	0.14231	-87198.12702
8	0.14905	-82504.09774
9	0.16566	-81040.66288
10	0.17433	-79327.95202
11	0.18984	-76060.80466
12	0.22762	-74753.80172
13	0.20325	-74820.84398
14	0.19453	-75494.32992
15	0.20327	-73788.63348
16	0.25774	-70420.58693

Table S3.7) Climatic variable permutation importance. Permutation importance of each ecological variable in determining habitat suitability for Northern *K. h. murrayi*, TMVB *K. h. murrayi*, and *K. h. chapalaense*. Higher values indicate greater importance.

Variable	Northern *K. h. murrayi*	TMVB *K. h. murrayi*	*K. h. chapalaense*
Annual Precipitation	4.9253	20.5368	1.1441
Annual Mean Temperature	17.9393	14.2234	29.3892
Elevation	27.018	13.5548	6.9324
Precipitation Driest Quarter	10.5181	7.6223	1.588
Precipitation Warmest Quarter	18.3045	0	25.719
Precipitation Wettest Quarter	11.7511	24.6887	0
Temperature Seasonality	9.5437	19.374	35.2273

Table S3.8) Niche overlap metrics. Estimates of pairwise niche overlap between *K. hirtipes* subspecies, and p-values for background comparison tests (Warren et al. 2008). Significant p-values indicate lower overlap values of the realized climatic niche of each species than given their environmental backgrounds.

Species 1	Species 2	Observed D	Observed I	Median background D	Median background I	P-value (D)	P-value (I)
Northern *K. h. murrayi*	TMVB *K. h. murrayi*	0.084	0.215	0.101	0.246	0.020	0.030
Northern *K. h. murrayi*	*K. h. chapalaense*	0.041	0.139	0.096	0.216	0.010	0.010
TMVB *K. h. murrayi*	*K. h. chapalaense*	0.175	0.414	0.471	0.747	0.059	0.059

BIBLIOGRAPHY

Abbott, R. J., and A. C. Brennan. 2014. Altitudinal gradients, plant hybrid zones and evolutionary novelty. Philosophical Transactions of the Royal Society B: Biological Sciences 369:20130346. Royal Society.

Ackerly, D. D., D. W. Schwilk, and C. O. Webb. 2006. Niche Evolution and Adaptive Radiation: Testing the Order of Trait Divergence. Ecology 87:S50–S61.

Adams, D. C. 2014. Quantifying and Comparing Phylogenetic Evolutionary Rates for Shape and Other High-Dimensional Phenotypic Data. Systematic Biology 63:166–177.

Adams, D. C., and E. Otárola-Castillo. 2013. geomorph: an r package for the collection and analysis of geometric morphometric shape data. Methods in Ecology and Evolution 4:393–399.

Alex Sotola, V., D. S. Ruppel, T. H. Bonner, C. C. Nice, and N. H. Martin. 2019. Asymmetric introgression between fishes in the Red River basin of Texas is associated with variation in water quality. Ecology and Evolution 9:2083–2095.

Alexander, D. H., J. Novembre, and K. Lange. 2009. Fast model-based estimation of ancestry in unrelated individuals. Genome Res. 19:1655–1664.

Allendorf, F. W., P. A. Hohenlohe, and G. Luikart. 2010. Genomics and the future of conservation genetics. Nature Reviews Genetics 11:697–709. Nature Publishing Group.

Allendorf, F. W., R. F. Leary, P. Spruell, and J. K. Wenburg. 2001. The problems with hybrids: setting conservation guidelines. Trends in Ecology & Evolution 16:613–622.

Ålund, M., S. Immler, A. M. Rice, and A. Qvarnström. 2013. Low fertility of wild hybrid male flycatchers despite recent divergence. Biology Letters 9:20130169. Royal Society.

Alvarado-Sizzo, H., A. Casas, F. Parra, H. J. Arreola-Nava, T. Terrazas, and C. Sánchez. 2018. Species delimitation in the Stenocereus griseus (Cactaceae) species complex reveals a new species, S. huastecorum. PLOS ONE 13:e0190385. Public Library of Science.

Amadon, D. 1949. The seventy-five per cent rule for subspecies. The Condor 51:250–258. JSTOR.

Andersen, E. J., S. Ali, E. Byamukama, Y. Yen, and M. P. Nepal. 2018. Disease Resistance Mechanisms in Plants. Genes 9:339. Multidisciplinary Digital Publishing Institute.

Anderson, E. 1948. Hybridization of the Habitat. Evolution 2:1–9. [Society for the Study of Evolution, Wiley].

Anderson, E., and G. L. Stebbins. 1954. Hybridization as an Evolutionary Stimulus. Evolution 8:378–388. [Society for the Study of Evolution, Wiley].

Antunes, B., G. Velo-Antón, D. Buckley, R. J. Pereira, and I. Martínez-Solano. 2021. Physical and ecological isolation contribute to maintain genetic differentiation between fire salamander subspecies. Heredity 126:776–789.

Aparicio, Á., I. E. Mercado, A. M. Ugalde, E. Gaona-Murillo, T. Butterfield, and R. Macip-Ríos. 2018. Ecological Observations of the Mexican Mud Turtle (Kinosternon integrum) in the Pátzcuaro Basin, Michoacán, México. Chelonian Conservation and Biology 17:284–290. Allen Press.

Archer, F. I., K. K. Martien, and B. L. Taylor. 2017. Diagnosability of mt DNA with Random Forests: Using sequence data to delimit subspecies. Marine Mammal Science 33:101–131. Wiley Online Library.

Arida, B. L., G. Scopece, R. M. Machado, A. P. Moraes, E. Forni-Martins, and F. Pinheiro. 2021. Reproductive barriers and fertility of two neotropical orchid species and their natural hybrid. Evol Ecol 35:41–64.

Armbruster, P., W. E. Bradshaw, and C. M. Holzapfel. 1997. Evolution of the Genetic Architecture Underlying Fitness in the Pitcher-Plant Mosquito, Wyeomyia Smithii. Evolution 51:451–458.

Arriaga-Jiménez, A., B. Kohlmann, L. Vázquez-Selem, Y. Umaña, and M. Rös. 2020. Past and future sky-island dynamics of tropical mountains: A model for two Geotrupes (Coleoptera: Geotrupidae) species in Oaxaca, Mexico. The Holocene 30:1462–1470. SAGE Publications Ltd.

AubinI, GarbeC.M, ColomboS, DreverC.R, McKenneyD.W, MessierC, PedlarJ, SanerM.A, VenierL, WellsteadA.M, WinderR, WittenE, and Ste-MarieC. 2011. Why we disagree about assisted migration1: Ethical implications of a key debate regarding the future of Canada's forests. The Forestry Chronicle, doi: 10.5558/tfc2011-092. NRC Research Press.

Baiz, M. D., P. K. Tucker, and L. Cortés-Ortiz. 2019. Multiple forms of selection shape reproductive isolation in a primate hybrid zone. Molecular Ecology 28:1056–1069.

Baker, R. J., and R. D. Bradley. 2006. Speciation in mammals and the genetic species concept. Journal of mammalogy 87:643–662. American Society of Mammalogists.

Barrientos-Villalobos, J., J. J. Schmitter-Soto, and A. J. E. de los Monteros. 2018. Several subspecies or phenotypic plasticity? A geometric morphometric and molecular analysis of variability of the Mayan cichlid Mayaheros urophthalmus in the Yucatan. Copeia 106:268–278. The American Society of Ichthyologists and Herpetologists.

Barton, N. H. 1979. The dynamics of hybrid zones. Heredity 43:341–359.

Barton, N. H. 1980. The fitness of hybrids between two chromosomal races of the grasshopper Podisma pedestris. Heredity 45:47–59.

Barton, N. H., and G. M. Hewitt. 1989. Adaptation, speciation and hybrid zones. Nature 341:497–503.

Barton, N. H., and G. M. Hewitt. 1985. Analysis of Hybrid Zones. Annual Review of Ecology and Systematics 16:113–148.

Barton, N. H., and G. M. Hewitt. 1981. The genetic basis of hybrid inviability in the grasshopper Podisma pedestris. Heredity 47:367–383.

Baselga, A., E. Recuero, G. Parra-Olea, and M. García-París. 2011. Phylogenetic patterns in zopherine beetles are related to ecological niche width and dispersal limitation. Molecular Ecology 20:5060–5073.

Beamer, D. A., and T. Lamb. 2008. Dusky salamanders (Desmognathus, Plethodontidae) from the Coastal Plain: Multiple independent lineages and their bearing on the molecular phylogeny of the genus. Molecular Phylogenetics and Evolution 47:143–153.

Beamer, D. A., and T. Lamb. 2020. Towards rectifying limitations on species delineation in dusky salamanders (Desmognathus: Plethodontidae): An ecoregion-drainage sampling grid reveals additional cryptic clades. Zootaxa 4734.

Becker, M., N. Gruenheit, M. Steel, C. Voelckel, O. Deusch, P. B. Heenan, P. A. McLenachan, O. Kardailsky, J. W. Leigh, and P. J. Lockhart. 2013. Hybridization may facilitate in situ survival of endemic species through periods of climate change. Nature Climate Change 3:1039–1043. Nature Publishing Group.

Behm, J. E., A. R. Ives, and J. W. Boughman. 2010. Breakdown in Postmating Isolation and the Collapse of a Species Pair through Hybridization. The American Naturalist 175:11–26. The University of Chicago Press.

Bell, D. A., Z. L. Robinson, W. C. Funk, S. W. Fitzpatrick, F. W. Allendorf, D. A. Tallmon, and A. R. Whiteley. 2019. The Exciting Potential and Remaining Uncertainties of Genetic Rescue. Trends in Ecology & Evolution 34:1070–1079.

Bernardo, J., R. J. Ossola, J. Spotila, and K. A. Crandall. 2007. Interspecies physiological variation as a tool for cross-species assessments of global warming-induced endangerment: validation of an intrinsic determinant of macroecological and phylogeographic structure. Biology Letters 3:695–699. Royal Society.

Berriozabal-Islas, C., A. Ramírez-Bautista, F. Torres-Ángeles, J. F. Mota Rodrigues, R. Macip-Ríos, and P. Octavio-Aguilar. 2020a. Climate change effects on turtles of the genus Kinosternon (Testudines: Kinosternidae): an assessment of habitat suitability and climate niche conservatism. Hydrobiologia 847:4091–4110.

Berriozabal-Islas, C., A. Ramírez-Bautista, F. Torres-Ángeles, J. F. Mota Rodrigues, R. Macip-Ríos, and P. Octavio-Aguilar. 2020b. Climate change effects on turtles of the genus Kinosternon (Testudines: Kinosternidae): an assessment of habitat suitability and climate niche conservatism. Hydrobiologia 847:4091–4110.

Billerman, S. M., M. A. Murphy, and M. D. Carling. 2016. Changing climate mediates sapsucker (Aves: Sphyrapicus) hybrid zone movement. Ecology and Evolution 6:7976–7990.

Birand, A., A. Vose, and S. Gavrilets. 2012. Patterns of Species Ranges, Speciation, and Extinction. The American Naturalist 179:1–21. The University of Chicago Press.

Blanckaert, A., and B. A. Payseur. 2021. Finding Hybrid Incompatibilities Using Genome Sequences from Hybrid Populations. Molecular Biology and Evolution, doi: 10.1093/molbev/msab168.

Blechschmidt, J., M. J. Wittmann, and C. Blüml. 2020. Climate Change and Green Sea Turtle Sex Ratio—Preventing Possible Extinction. Genes 11:588. Multidisciplinary Digital Publishing Institute.

Bog, M., C. Bässler, and C. Oberprieler. 2017a. Lost in the hybridisation vortex: high-elevation Senecio hercynicus (Compositae, Senecioneae) is genetically swamped by its congener S. ovatus in the Bavarian Forest National Park (SE Germany). Evol Ecol 31:401–420.

Bog, M., C. Bässler, and C. Oberprieler. 2017b. Lost in the hybridisation vortex: high-elevation Senecio hercynicus (Compositae, Senecioneae) is genetically swamped by its congener S. ovatus in the Bavarian Forest National Park (SE Germany). Evol Ecol 31:401–420.

Bolger, A. M., M. Lohse, and B. Usadel. 2014. Trimmomatic: a flexible trimmer for Illumina sequence data. Bioinformatics 30:2114–2120. Oxford Academic.

Bouckaert, R., J. Heled, D. Kühnert, T. Vaughan, C.-H. Wu, D. Xie, M. A. Suchard, A. Rambaut, and A. J. Drummond. 2014. BEAST 2: A Software Platform for Bayesian Evolutionary Analysis. PLOS Computational Biology 10:e1003537. Public Library of Science.

Brennan, A. C., G. Woodward, O. Seehausen, V. Muñoz-Fuentes, C. Moritz, A. Guelmami, R. J. Abbott, and P. Edelaar. 2014. Hybridization due to changing species distributions: adding problems or solutions to conservation of biodiversity during global change? Evolutionary Ecology Research 16:475–491. Evolutionary Ecology Ltd.

Bruce, R. C. 1996. Life-History Perspective of Adaptive Radiation in Desmognathine Salamanders. Copeia 1996:783–790. [American Society of Ichthyologists and Herpetologists (ASIH), Allen Press].

Brunet, J., J. E. Zalapa, F. Pecori, and A. Santini. 2013. Hybridization and introgression between the exotic Siberian elm, Ulmus pumila, and the native Field elm, U. minor, in Italy. Biol Invasions 15:2717–2730.

Bryant, D., R. Bouckaert, J. Felsenstein, N. A. Rosenberg, and A. RoyChoudhury. 2012. Inferring Species Trees Directly from Biallelic Genetic Markers: Bypassing Gene Trees in a Full Coalescent Analysis. Molecular Biology and Evolution 29:1917–1932.

Bryson, R. W., U. O. García‐Vázquez, and B. R. Riddle. 2011. Phylogeography of Middle American gophersnakes: mixed responses to biogeographical barriers across the Mexican Transition Zone. Journal of Biogeography 38:1570–1584.

Butler, C. J., B. D. Stanila, J. B. Iverson, P. A. Stone, and M. Bryson. 2016. Projected changes in climatic suitability for Kinosternon turtles by 2050 and 2070. Ecology and Evolution 6:7690–7705.

Calfee, E., M. N. Agra, M. A. Palacio, S. R. Ramírez, and G. Coop. 2020. Selection and hybridization shaped the rapid spread of African honey bee ancestry in the Americas. PLOS Genetics 16:e1009038. Public Library of Science.

Camp, C. D., J. L. Marshall, and R. M. Austin, Jr. 2000. The evolution of adult body size in black-bellied salamanders (Desmognathus quadramaculatus complex). Can. J. Zool. 78:1712–1722. NRC Research Press.

Carlson, S. M., C. J. Cunningham, and P. A. H. Westley. 2014. Evolutionary rescue in a changing world. Trends in Ecology & Evolution 29:521–530.

Carneiro, M., J. A. Blanco-Aguiar, R. Villafuerte, N. Ferrand, and M. W. Nachman. 2010. Speciation in the European Rabbit (oryctolagus Cuniculus): Islands of Differentiation on the X Chromosome and Autosomes. Evolution 64:3443–3460.

Castro-Insua, A., C. Gómez-Rodríguez, J. J. Wiens, and A. Baselga. 2018. Climatic niche divergence drives patterns of diversification and richness among mammal families. Sci Rep 8:8781. Nature Publishing Group.

Catchen, J. M., A. Amores, P. Hohenlohe, W. Cresko, and J. H. Postlethwait. 2011. Stacks: Building and Genotyping Loci De Novo From Short-Read Sequences. G3: Genes, Genomes, Genetics 1:171–182. G3: Genes, Genomes, Genetics.

Cavalli-Sforza, L. L., and A. W. F. Edwards. 1967. Phylogenetic analysis. Models and estimation procedures. Am J Hum Genet 19:233–257.

Chang, C. C., C. C. Chow, L. C. Tellier, S. Vattikuti, S. M. Purcell, and J. J. Lee. 2015. Second-generation PLINK: rising to the challenge of larger and richer datasets. Gigascience 4. Oxford Academic.

Chase, M. A., H. Ellegren, and C. F. Mugal. 2021. Positive selection plays a major role in shaping signatures of differentiation across the genomic landscape of two independent Ficedula flycatcher species pairs. Evolution n/a.

Chatfield, M. W. H., K. H. Kozak, B. M. Fitzpatrick, and P. K. Tucker. 2010. Patterns of differential introgression in a salamander hybrid zone: inferences from genetic data and ecological niche modelling. Molecular Ecology 19:4265–4282.

Chen, I.-C., J. K. Hill, R. Ohlemüller, D. B. Roy, and C. D. Thomas. 2011. Rapid Range Shifts of Species Associated with High Levels of Climate Warming. Science. American Association for the Advancement of Science.

Chen, I.-C., H.-J. Shiu, S. Benedick, J. D. Holloway, V. K. Chey, H. S. Barlow, J. K. Hill, and C. D. Thomas. 2009. Elevation increases in moth assemblages over 42 years on a tropical mountain. PNAS 106:1479–1483. National Academy of Sciences.

Cherepanov, G. O. 2016. Nature of the turtle shell: Morphogenetic causes of bone variability and its evolutionary implication. Paleontol. J. 50:1641–1648.

Chifman, J., and L. Kubatko. 2014. Quartet Inference from SNP Data Under the Coalescent Model. Bioinformatics 30:3317–3324.

Chippindale, P. T., R. M. Bonett, A. S. Baldwin, and J. J. Wiens. 2004. Phylogenetic Evidence for a Major Reversal of Life-History Evolution in Plethodontid Salamanders. Evolution 58:2809–2822.

Chunco, A. J. 2014. Hybridization in a warmer world. Ecology and Evolution 4:2019–2031.

Coleman, R. R., M. R. Gaither, B. Kimokeo, F. G. Stanton, B. W. Bowen, and R. J. Toonen. 2014. Large-scale introduction of the Indo-Pacific damselfish Abudefduf vaigiensis into Hawai'i promotes genetic swamping of the endemic congener A. abdominalis. Molecular Ecology 23:5552–5565.

Cooper, N., R. P. Freckleton, and W. Jetz. 2011. Phylogenetic conservatism of environmental niches in mammals. Proceedings of the Royal Society B: Biological Sciences 278:2384–2391. Royal Society.

Cordier, J. M., J. N. Lescano, N. E. Ríos, G. C. Leynaud, and J. Nori. 2020. Climate change threatens micro-endemic amphibians of an important South American high-altitude center of endemism. Amphibia-Reptilia 41:233–243. Brill.

Cortés, A. J., L. N. Garzón, J. B. Valencia, and S. Madriñán. 2018. On the Causes of Rapid Diversification in the Páramos: Isolation by Ecology and Genomic Divergence in Espeletia. Frontiers in Plant Science 9:1700.

Coughlan, J. M., and D. R. Matute. 2020a. The importance of intrinsic postzygotic barriers throughout the speciation process. Philosophical Transactions of the Royal Society B: Biological Sciences 375:20190533. Royal Society.

Coughlan, J. M., and D. R. Matute. 2020b. The importance of intrinsic postzygotic barriers throughout the speciation process. Philosophical Transactions of the Royal Society B: Biological Sciences 375:20190533. Royal Society.

Coyne, J. A., and H. A. Orr. 2004. Speciation. Sinauer.

Cracraft, J. 1983. Species concepts and speciation analysis. Pp. 159–187 *in* Current ornithology. Springer.

Crawford, D. J., and T. F. Stuessy. 2016. Cryptic variation, molecular data, and the challenge of conserving plant diversity in oceanic archipelagos: the critical role of plant systematics. Korean J. Pl. Taxon 46:129–148. Korean Society of Plant Taxonomists.

Cruickshank, T. E., and M. W. Hahn. 2014. Reanalysis suggests that genomic islands of speciation are due to reduced diversity, not reduced gene flow. Molecular Ecology 23:3133–3157.

Csapó, H., P. Krzywoźniak, M. Grabowski, R. Wattier, K. Bącela-Spychalska, T. Mamos, M. Jelić, and T. Rewicz. 2020. Successful post-glacial colonization of Europe by single lineage of freshwater amphipod from its Pannonian Plio-Pleistocene diversification hotspot. Sci Rep 10:18695.

Curry, C. M. 2015. An Integrated Framework for Hybrid Zone Models. Evol Biol 42:359–365.

Danecek, P., A. Auton, G. Abecasis, C. A. Albers, E. Banks, M. A. DePristo, R. E. Handsaker, G. Lunter, G. T. Marth, S. T. Sherry, G. McVean, R. Durbin, and 1000 Genomes Project Analysis Group. 2011a. The variant call format and VCFtools. Bioinformatics 27:2156–2158.

Danecek, P., A. Auton, G. Abecasis, C. A. Albers, E. Banks, M. A. DePristo, R. E. Handsaker, G. Lunter, G. T. Marth, S. T. Sherry, G. McVean, R. Durbin, and 1000 Genomes Project Analysis Group. 2011b. The variant call format and VCFtools. Bioinformatics 27:2156–2158.

Dawson, T. P., S. T. Jackson, J. I. House, I. C. Prentice, and G. M. Mace. 2011. Beyond Predictions: Biodiversity Conservation in a Changing Climate. Science 332:53–58. American Association for the Advancement of Science.

De Queiroz, K. 2005. A unified concept of species and its consequences for the future of taxonomy. Proceedings of the California Academy of Sciences 56:196–215.
De Queiroz, K. 2007. Species Concepts and Species Delimitation. Systematic Biology 56:879–886.
Delić, T., P. Trontelj, M. Rendoš, and C. Fišer. 2017. The importance of naming cryptic species and the conservation of endemic subterranean amphipods. Sci Rep 7:3391.
Dmitriev, D. A., and R. A. Rakitov. 2008. Decoding of Superimposed Traces Produced by Direct Sequencing of Heterozygous Indels. PLOS Computational Biology 4:e1000113. Public Library of Science.
Drummond, A. J., and R. R. Bouckaert. 2015. Bayesian Evolutionary Analysis with BEAST. Cambridge University Press.
Drummond, A. J., and A. Rambaut. 2007. BEAST: Bayesian evolutionary analysis by sampling trees. BMC Evol Biol 7:214.
Drummond, J. P. n.d. Aggression affects distributions and hybrid zone expansion in montane Plethodon salamanders. Western Carolina University, United States -- North Carolina.
DuBay, S. G., and C. C. Witt. 2014. Differential high-altitude adaptation and restricted gene flow across a mid-elevation hybrid zone in Andean tit-tyrant flycatchers. Molecular Ecology 23:3551–3565.
Dufresnes, C., A. Brelsford, D. L. Jeffries, G. Mazepa, T. Suchan, D. Canestrelli, A. Nicieza, L. Fumagalli, S. Dubey, I. Martínez-Solano, S. N. Litvinchuk, M. Vences, N. Perrin, and P.-A. Crochet. 2021. Mass of genes rather than master genes underlie the genomic architecture of amphibian speciation. PNAS 118. National Academy of Sciences.
Ebersbach, J., A. Posso-Terranova, S. Bogdanowicz, M. Gómez-Díaz, Ma. X. García-González, W. Bolívar-García, and J. Andrés. 2020. Complex patterns of differentiation and gene flow underly the divergence of aposematic phenotypes in Oophaga poison frogs. Molecular Ecology 29:1944–1956.
Edgar, R. C. 2004. MUSCLE: multiple sequence alignment with high accuracy and high throughput. Nucleic Acids Research 32:1792–1797.
Ekblom, R., B. Brechlin, J. Persson, L. Smeds, M. Johansson, J. Magnusson, Ø. Flagstad, and H. Ellegren. 2018. Genome sequencing and conservation genomics in the Scandinavian wolverine population. Conservation Biology 32:1301–1312.
Ennen, J. R., M. E. Kalis, A. L. Patterson, B. R. Kreiser, J. E. Lovich, J. Godwin, and C. P. Qualls. 2014. Clinal variation or validation of a subspecies? A case study of the Graptemys nigrinoda complex (Testudines: Emydidae). Biological Journal of the Linnean Society 111:810–822. Oxford University Press.
Everson, K. M., L. N. Gray, A. G. Jones, N. M. Lawrence, M. E. Foley, K. L. Sovacool, J. D. Kratovil, S. Hotaling, P. M. Hime, A. Storfer, G. Parra-Olea, R. Percino-Daniel, X. Aguilar-Miguel, E. M. O'Neill, L. Zambrano, H. B. Shaffer, and D. W. Weisrock. 2021a. Geography is more important than life history in

the recent diversification of the tiger salamander complex. PNAS 118. National Academy of Sciences.
Everson, K. M., L. N. Gray, A. G. Jones, N. M. Lawrence, M. E. Foley, K. L. Sovacool, J. D. Kratovil, S. Hotaling, P. M. Hime, A. Storfer, G. Parra-Olea, R. Percino-Daniel, X. Aguilar-Miguel, E. M. O'Neill, L. Zambrano, H. B. Shaffer, and D. W. Weisrock. 2021b. Geography is more important than life history in the recent diversification of the tiger salamander complex. PNAS 118. National Academy of Sciences.
Ewert, M., C. R. Etchberger, and C. Nelson. 2004. Turtle Sex-Determining Modes and TSD Patterns, and Some TSD Pattern Correlates. Pp. 21–32 *in* Temperature-dependent Sex Determination in Vertebrates.
Ferris, K. G., J. P. Sexton, and J. H. Willis. 2014. Speciation on a local geographic scale: the evolution of a rare rock outcrop specialist in Mimulus. Philosophical Transactions of the Royal Society B: Biological Sciences 369:20140001. Royal Society.
Fick, S. E., and R. J. Hijmans. 2017. WorldClim 2: new 1-km spatial resolution climate surfaces for global land areas. International Journal of Climatology 37:4302–4315.
Filatov, D. A., O. G. Osborne, and A. S. T. Papadopulos. 2016. Demographic history of speciation in a Senecio altitudinal hybrid zone on Mt. Etna. Molecular Ecology 25:2467–2481.
Fisher-Reid, M. C., K. H. Kozak, and J. J. Wiens. 2012. How Is the Rate of Climatic-Niche Evolution Related to Climatic-Niche Breadth? Evolution 66:3836–3851.
Foltz, D. W. 1997. Hybridization Frequency is Negatively Correlated with Divergence Time of Mitochondrial DNA Haplotypes in a Sea Star (Leptasterias SPP.) Species Complex. Evolution 51:283–288. [Society for the Study of Evolution, Wiley].
Freeman, B. G., M. N. Scholer, V. Ruiz-Gutierrez, and J. W. Fitzpatrick. 2018. Climate change causes upslope shifts and mountaintop extirpations in a tropical bird community. PNAS 115:11982–11987. National Academy of Sciences.
Frost, D. R., and D. M. Hillis. 1990. Species in concept and practice: herpetological applications. Herpetologica 86–104. JSTOR.
Funk, D. J., P. Nosil, and W. J. Etges. 2006. Ecological divergence exhibits consistently positive associations with reproductive isolation across disparate taxa. PNAS 103:3209–3213. National Academy of Sciences.
Futuyma, D. J., and G. Moreno. 1988. The Evolution of Ecological Specialization. Annual Review of Ecology and Systematics 19:207–233.
Gallego-García, N., S. Caballero, and H. B. Shaffer. 2021. Are Genomic Updates of Well-Studied Species Worth the Investment for Conservation? A Case Study of the Critically Endangered Magdalena River Turtle. Journal of Heredity 112:575–589.

Garcia, G., S. Pereyra, V. Gutierrez, S. Oviedo, P. Miller, and A. Domingo. 2015. Population structure of Squatina guggenheim (Squatiniformes, Squatinidae) from the south-western Atlantic Ocean. Journal of Fish Biology 86:186–202.

Garroway, C. J., J. Bowman, T. J. Cascaden, G. L. Holloway, C. G. Mahan, J. R. Malcolm, M. A. Steele, G. Turner, and P. J. Wilson. 2010. Climate change induced hybridization in flying squirrels. Global Change Biology 16:113–121.

Gaston, K. J., and T. M. Blackburn. 1996. Global Scale Macroecology: Interactions between Population Size, Geographic Range Size and Body Size in the Anseriformes. Journal of Animal Ecology 65:701–714. [Wiley, British Ecological Society].

Gibson, G., and I. Dworkin. 2004. Uncovering cryptic genetic variation. Nature Reviews Genetics 5:681–690. Nature Publishing Group.

Gibson, J. D., O. Niehuis, B. R. E. Peirson, E. I. Cash, and J. Gadau. 2013. Genetic and Developmental Basis of F2 Hybrid Breakdown in Nasonia Parasitoid Wasps. Evolution 67:2124–2132.

Gidden, M., K. Riahi, S. Smith, S. Fujimori, G. Luderer, E. Kriegler, D. P. van Vuuren, M. van den Berg, L. Feng, D. Klein, K. Calvin, J. Doelman, S. Frank, O. Fricko, M. Harmsen, T. Hasegawa, P. Havlik, J. Hilaire, R. Hoesly, J. Horing, A. Popp, E. Stehfest, and K. Takahashi. 2019. Global emissions pathways under different socioeconomic scenarios for use in CMIP6: a dataset of harmonized emissions trajectories through the end of the century. Geoscientific Model Development Discussions 12:1443–1475. European Geosciences Union.

Gifford, M. E., and K. H. Kozak. 2012. Islands in the sky or squeezed at the top? Ecological causes of elevational range limits in montane salamanders. Ecography 35:193–203.

Glass, B., and N. Hartweg. 1951. Kinosternon murrayi, a New Muskturtle of the hirtipes Group from Texas. Copeia 1951:50–52. [American Society of Ichthyologists and Herpetologists (ASIH), Allen Press].

Goldberg, E. E., J. R. Kohn, R. Lande, K. A. Robertson, S. A. Smith, and B. Igić. 2010. Species Selection Maintains Self-Incompatibility. Science 330:493–495. American Association for the Advancement of Science.

Gómez, J. M., A. González-Megías, J. Lorite, M. Abdelaziz, and F. Perfectti. 2015. The silent extinction: climate change and the potential hybridization-mediated extinction of endemic high-mountain plants. Biodivers Conserv 24:1843–1857.

Gómez-Rodríguez, C., A. Baselga, and J. J. Wiens. 2015. Is diversification rate related to climatic niche width? Global Ecology and Biogeography 24:383–395.

Gompert, Z., and C. A. Buerkle. 2011. Bayesian estimation of genomic clines. Molecular Ecology 20:2111–2127.

Gompert, Z., and C. A. Buerkle. 2012. bgc: Software for Bayesian estimation of genomic clines. Molecular Ecology Resources 12:1168–1176.

Gompert, Z., L. K. Lucas, C. C. Nice, and C. A. Buerkle. 2013. Genome Divergence and the Genetic Architecture of Barriers to Gene Flow Between Lycaeides Idas and L. Melissa. Evolution 67:2498–2514.

Gompert, Z., L. K. Lucas, C. C. Nice, J. A. Fordyce, M. L. Forister, and C. A. Buerkle. 2012a. Genomic Regions with a History of Divergent Selection Affect Fitness of Hybrids Between Two Butterfly Species. Evolution 66:2167–2181.

Gompert, Z., T. L. Parchman, and C. A. Buerkle. 2012b. Genomics of isolation in hybrids. Philosophical Transactions of the Royal Society B: Biological Sciences 367:439–450. Royal Society.

Grabenstein, K. C., and S. A. Taylor. 2018. Breaking Barriers: Causes, Consequences, and Experimental Utility of Human-Mediated Hybridization. Trends in Ecology & Evolution 33:198–212.

Green, R. E., E. L. Braun, J. Armstrong, D. Earl, N. Nguyen, G. Hickey, M. W. Vandewege, J. A. S. John, S. Capella-Gutiérrez, T. A. Castoe, C. Kern, M. K. Fujita, J. C. Opazo, J. Jurka, K. K. Kojima, J. Caballero, R. M. Hubley, A. F. Smit, R. N. Platt, C. A. Lavoie, M. P. Ramakodi, J. W. Finger, A. Suh, S. R. Isberg, L. Miles, A. Y. Chong, W. Jaratlerdsiri, J. Gongora, C. Moran, A. Iriarte, J. McCormack, S. C. Burgess, S. V. Edwards, E. Lyons, C. Williams, M. Breen, J. T. Howard, C. R. Gresham, D. G. Peterson, J. Schmitz, D. D. Pollock, D. Haussler, E. W. Triplett, G. Zhang, N. Irie, E. D. Jarvis, C. A. Brochu, C. J. Schmidt, F. M. McCarthy, B. C. Faircloth, F. G. Hoffmann, T. C. Glenn, T. Gabaldón, B. Paten, and D. A. Ray. 2014. Three crocodilian genomes reveal ancestral patterns of evolution among archosaurs. Science 346. American Association for the Advancement of Science.

Grinnell, J. 1917. The Niche-Relationships of the California Thrasher. The Auk 34:427–433. American Ornithological Society.

Gruber, K., C. Schöning, M. Otte, W. Kinuthia, and M. Hasselmann. 2013. Distinct subspecies or phenotypic plasticity? Genetic and morphological differentiation of mountain honey bees in East Africa. Ecology and evolution 3:3204–3218. Wiley Online Library.

Guindon, S., and O. Gascuel. 2003. A Simple, Fast, and Accurate Algorithm to Estimate Large Phylogenies by Maximum Likelihood. Systematic Biology 52:696–704.

Hairston, N. G. 1949. The Local Distribution and Ecology of the Plethodontid Salamanders of the Southern Appalachians. Ecological Monographs 19:47–73.

Hairston Sr., N. G., R. H. Wiley, C. K. Smith, and K. A. Kneidel. 1992. The Dynamics of Two Hybrid Zones in Appalachian Salamanders of the Genus Plethodon. Evolution 46:930–938.

Hall, D. H., and R. J. Steidl. 2007. Movements, Activity, and Spacing of Sonoran Mud Turtles (Kinosternon Sonoriense) in Interrupted Mountain Streams. Copeia 2007:403–412.

Hall, M. C., and J. H. Willis. 2005. Transmission Ratio Distortion in Intraspecific Hybrids of Mimulus guttatus: Implications for Genomic Divergence. Genetics 170:375–386.

Hällfors, M. H., S. Aikio, and L. E. Schulman. 2017. Quantifying the need and potential of assisted migration. Biological Conservation 205:34–41.

Hanson, J. O., A. Marques, A. Veríssimo, M. Camacho-Sanchez, G. Velo-Antón, Í. Martínez-Solano, and S. B. Carvalho. 2020. Conservation planning for adaptive and neutral evolutionary processes. Journal of Applied Ecology 57:2159–2169.

Harmon, L. J., J. B. Losos, T. Jonathan Davies, R. G. Gillespie, J. L. Gittleman, W. Bryan Jennings, K. H. Kozak, M. A. McPeek, F. Moreno-Roark, T. J. Near, A. Purvis, R. E. Ricklefs, D. Schluter, J. A. Schulte II, O. Seehausen, B. L. Sidlauskas, O. Torres-Carvajal, J. T. Weir, and A. Ø. Mooers. 2010. Early Bursts of Body Size and Shape Evolution Are Rare in Comparative Data. Evolution 64:2385–2396.

Hatfield, T., and D. Schluter. 1999. Ecological Speciation in Sticklebacks: Environment-Dependent Hybrid Fitness. Evolution 53:866–873.

Hedrick, P. W., J. A. Robinson, R. O. Peterson, and J. A. Vucetich. 2019. Genetics and extinction and the example of Isle Royale wolves. Animal Conservation 22:302–309.

Heinrichs, J. A., D. T. McKinnon, C. L. Aldridge, and A. Moehrenschlager. 2019. Optimizing the use of endangered species in multi-population collection, captive breeding and release programs. Global Ecology and Conservation 17:e00558.

Heled, J., and A. J. Drummond. 2010. Bayesian Inference of Species Trees from Multilocus Data. Molecular Biology and Evolution 27:570–580.

Helmuth, B., J. G. Kingsolver, and E. Carrington. 2005. BIOPHYSICS, PHYSIOLOGICAL ECOLOGY, AND CLIMATE CHANGE: Does Mechanism Matter? Annual Review of Physiology 67:177–201.

Herman, A., Y. Brandvain, J. Weagley, W. R. Jeffery, A. C. Keene, T. J. Y. Kono, H. Bilandžija, R. Borowsky, L. Espinasa, K. O'Quin, C. P. Ornelas‐García, M. Yoshizawa, B. Carlson, E. Maldonado, J. B. Gross, R. A. Cartwright, N. Rohner, W. C. Warren, and S. E. McGaugh. 2018. The role of gene flow in rapid and repeated evolution of cave-related traits in Mexican tetra, Astyanax mexicanus. Molecular Ecology 27:4397–4416.

Herman, J. S., A. D. McDevitt, A. Kawałko, M. Jaarola, J. M. Wójcik, and J. B. Searle. 2014. Land-Bridge Calibration of Molecular Clocks and the Post-Glacial Colonization of Scandinavia by the Eurasian Field Vole Microtus agrestis. PLOS ONE 9:e103949. Public Library of Science.

Highton, R., and R. B. Peabody. 2000a. Geographic Protein Variation and Speciation in Salamanders of the Plethodon Jordani and Plethodon Glutinosus Complexes in the Southern Appalachian Mountains with the Description of Four New Species. Pp. 31–93 *in* R. C. Bruce, R. G. Jaeger, and L. D. Houck, eds. The Biology of Plethodontid Salamanders. Springer US, Boston, MA.

Highton, R., and R. B. Peabody. 2000b. Geographic protein variation and speciation in salamanders of the Plethodon jordani and Plethodon glutinosus complexes in the southern Appalachian Mountains with the descriptions of four new species. Pp. 31–94 *in* The biology of Plethodontid Salamanders. Kluwer Academic / Mlenum Publishers.

Hijmans, R. J., S. E. Cameron, J. L. Parra, P. G. Jones, and A. Jarvis. 2005. Very high resolution interpolated climate surfaces for global land areas. International Journal of Climatology 25:1965–1978.

Hillis, D. M. 2019. Species delimitation in herpetology. Journal of Herpetology 53:3–12. the Society for the Study of Amphibians and Reptiles.

Hillis, D. M. 2020. The detection and naming of geographic variation within species. Herpetological Review 51:52–56.

Hogg, J. T., S. H. Forbes, B. M. Steele, and G. Luikart. 2006. Genetic rescue of an insular population of large mammals. Proceedings of the Royal Society B: Biological Sciences 273:1491–1499. Royal Society.

Holt, R. D. 1990. The microevolutionary consequences of climate change. Trends in Ecology & Evolution 5:311–315.

Huang, J.-P., and L. L. Knowles. 2016. The species versus subspecies conundrum: quantitative delimitation from integrating multiple data types within a single Bayesian approach in Hercules beetles. Systematic Biology 65:685–699. Oxford University Press.

Hudson, R. R., M. Kreitman, and M. Aguadé. 1987. A Test of Neutral Molecular Evolution Based on Nucleotide Data. Genetics 116:153–159. Genetics.

Hughes, W. O. H., and J. J. Boomsma. 2007. Genetic polymorphism in leaf-cutting ants is phenotypically plastic. Proceedings of the Royal Society B: Biological Sciences 274:1625–1630. Royal Society.

Humeau, L., M. Le Corre, S. J. Reynolds, C. Wearn, J. C. Hennicke, J. C. Russell, Y. Gomard, H. Magalon, P. Pinet, P. Gélin, F.-X. Couzi, E. Bemanaja, V. Tatayah, B. Ousseni, G. Rocamora, P. Talbot, N. Shah, L. Bugoni, D. Da Silva, and A. Jaeger. 2020. Genetic structuring among colonies of a pantropical seabird: Implication for subspecies validation and conservation. Ecology and Evolution 10:11886–11905.

Iverson, J. 1981. Biosystematics of the Kinosternon hirtipes Species Group (Testudines: Kinosternidae). Tulane Studies in Zoology and Botany 23.

Iverson, J. B., M. Le, and C. Ingram. 2013. Molecular phylogenetics of the mud and musk turtle family Kinosternidae. Molecular Phylogenetics and Evolution 69:929–939.

Janjua, S., J. L. Peters, B. Weckworth, F. I. Abbas, V. Bahn, O. Johansson, and T. P. Rooney. 2020. Improving our conservation genetic toolkit: ddRAD-seq for SNPs in snow leopards. Conservation Genet Resour 12:257–261.

Jansson, R., and M. Dynesius. 2002. The Fate of Clades in a World of Recurrent Climatic Change: Milankovitch Oscillations and Evolution. Annual Review of Ecology and Systematics 33:741–777.

Jezkova, T., and J. J. Wiens. 2016. Rates of change in climatic niches in plant and animal populations are much slower than projected climate change. Proceedings of the Royal Society B: Biological Sciences 283:20162104. Royal Society.

Jiggins, C. D., and J. Mallet. 2000. Bimodal hybrid zones and speciation. Trends in Ecology & Evolution 15:250–255.

Jombart, T. 2008. adegenet: a R package for the multivariate analysis of genetic markers. Bioinformatics 24:1403–1405. Oxford Academic.

Jombart, T., and I. Ahmed. 2011. adegenet 1.3-1: new tools for the analysis of genome-wide SNP data. Bioinformatics 27:3070–3071. Oxford Academic.

Jones, C. C., S. A. Acker, and C. B. Halpern. 2010. Combining local- and large-scale models to predict the distributions of invasive plant species. Ecological Applications 20:311–326.

Kearney, M., and W. Porter. 2009. Mechanistic niche modelling: combining physiological and spatial data to predict species' ranges. Ecology Letters 12:334–350.

Kearse, M., R. Moir, A. Wilson, S. Stones-Havas, M. Cheung, S. Sturrock, S. Buxton, A. Cooper, S. Markowitz, C. Duran, T. Thierer, B. Ashton, P. Meintjes, and A. Drummond. 2012. Geneious Basic: An integrated and extendable desktop software platform for the organization and analysis of sequence data. Bioinformatics 28:1647–1649.

Keller, I., C. E. Wagner, L. Greuter, S. Mwaiko, O. M. Selz, A. Sivasundar, S. Wittwer, and O. Seehausen. 2013. Population genomic signatures of divergent adaptation, gene flow and hybrid speciation in the rapid radiation of Lake Victoria cichlid fishes. Molecular Ecology 22:2848–2863.

Kisel, Y., and T. G. Barraclough. 2010. Speciation Has a Spatial Scale That Depends on Levels of Gene Flow. The American Naturalist 175:316–334. The University of Chicago Press.

Kling, M. M., B. D. Mishler, A. H. Thornhill, B. G. Baldwin, and D. D. Ackerly. 2019. Facets of phylodiversity: evolutionary diversification, divergence and survival as conservation targets. Philosophical Transactions of the Royal Society B: Biological Sciences 374:20170397. Royal Society.

Kosch, T. A., C. N. S. Silva, L. A. Brannelly, A. A. Roberts, Q. Lau, G. Marantelli, L. Berger, and L. F. Skerratt. 2019. Genetic potential for disease resistance in critically endangered amphibians decimated by chytridiomycosis. Animal Conservation 22:238–250.

Kozak, K. H., A. Larson, R. M. Bonett, and L. J. Harmon. 2005. Phylogenetic Analysis of Ecomorphological Divergence, Community Structure, and Diversification Rates in Dusky Salamanders (plethodontidae: Desmognathus). Evolution 59:2000–2016.

Kozak, K. H., R. W. Mendyk, and J. J. Wiens. 2009. Can Parallel Diversification Occur in Sympatry? Repeated Patterns of Body-Size Evolution in Coexisting Clades of North American Salamanders. Evolution 63:1769–1784.

Kozak, K. H., and J. J. Wiens. 2010a. Accelerated rates of climatic-niche evolution underlie rapid species diversification. Ecology Letters 13:1378–1389.

Kozak, K. H., and J. J. Wiens. 2010b. Accelerated rates of climatic-niche evolution underlie rapid species diversification. Ecology Letters 13:1378–1389.

Kozak, K. H., and J. J. Wiens. 2007. Climatic zonation drives latitudinal variation in speciation mechanisms. Proceedings of the Royal Society B: Biological Sciences 274:2995–3003. Royal Society.

Kozak, K. H., and J. J. Wiens. 2016. What explains patterns of species richness? The relative importance of climatic-niche evolution, morphological evolution, and ecological limits in salamanders. Ecology and Evolution 6:5940–5949.

Kozlov, A. M., D. Darriba, T. Flouri, B. Morel, and A. Stamatakis. 2019. RAxML-NG: a fast, scalable and user-friendly tool for maximum likelihood phylogenetic inference. Bioinformatics 35:4453–4455. Oxford Academic.

Kruckeberg, A. R., and D. Rabinowitz. 1985. Biological Aspects of Endemism in Higher Plants. Annu. Rev. Ecol. Syst. 16:447–479. Annual Reviews.

Kyriazis, C. C., R. K. Wayne, and K. E. Lohmueller. 2021. Strongly deleterious mutations are a primary determinant of extinction risk due to inbreeding depression. Evolution Letters 5:33–47.

Lafon-Placette, C., and C. Köhler. 2015. Epigenetic mechanisms of postzygotic reproductive isolation in plants. Current Opinion in Plant Biology 23:39–44.

Laspiur, A., J. C. Santos, S. M. Medina, J. E. Pizarro, E. A. Sanabria, B. Sinervo, and N. R. Ibargüengoytía. 2021. Vulnerability to climate change of a microendemic lizard species from the central Andes. Sci Rep 11:11653.

Lavinia, P. D., A. S. Barreira, L. Campagna, P. L. Tubaro, and D. A. Lijtmaer. 2019. Contrasting evolutionary histories in Neotropical birds: Divergence across an environmental barrier in South America. Molecular Ecology 28:1730–1747.

Lawson, A. M., and J. T. Weir. 2014a. Latitudinal gradients in climatic-niche evolution accelerate trait evolution at high latitudes. Ecology Letters 17:1427–1436.

Lawson, A. M., and J. T. Weir. 2014b. Latitudinal gradients in climatic-niche evolution accelerate trait evolution at high latitudes. Ecology Letters 17:1427–1436.

Leaché, A. D., B. L. Banbury, J. Felsenstein, A. nieto-Montes de Oca, and A. Stamatakis. 2015. Short Tree, Long Tree, Right Tree, Wrong Tree: New Acquisition Bias Corrections for Inferring SNP Phylogenies. Systematic Biology 64:1032–1047.

Levins, R. 2020. Evolution in Changing Environments: Some Theoretical Explorations. (MPB-2). Princeton University Press.

Li, M.-R., H.-Y. Wang, N. Ding, T. Lu, Y.-C. Huang, H.-X. Xiao, B. Liu, and L.-F. Li. 2019. Rapid Divergence Followed by Adaptation to Contrasting Ecological Niches of Two Closely Related Columbine Species Aquilegia japonica and A. oxysepala. Genome Biology and Evolution 11:919–930.

Liang, Z.-Q., W.-T. Chen, D.-Q. Wang, S.-H. Zhang, C.-R. Wang, S.-P. He, Y.-A. Wu, P. He, J. Xie, C.-W. Li, J. Merilä, and Q.-W. Wei. 2019. Phylogeographic patterns and conservation implications of the endangered Chinese giant salamander. Ecology and Evolution 9:3879–3890.

Lindtke, D., and C. A. Buerkle. 2015. The genetic architecture of hybrid incompatibilities and their effect on barriers to introgression in secondary contact. Evolution 69:1987–2004.

Litsios, G., L. Pellissier, F. Forest, C. Lexer, P. B. Pearman, N. E. Zimmermann, and N. Salamin. 2012. Trophic specialization influences the rate of environmental

niche evolution in damselfishes (Pomacentridae). Proceedings of the Royal Society B: Biological Sciences 279:3662–3669. Royal Society.
Liu, C., P. M. Berry, T. P. Dawson, and R. G. Pearson. 2005. Selecting thresholds of occurrence in the prediction of species distributions. Ecography 28:385–393.
Loc-Barragán, J. A., J. Reyes-Velasco, G. A. Woolrich-Piña, C. I. Grünwald, M. V. D. Anaya, J. A. Rangel-Mendoza, and M. A. López-Luna. 2020a. A New Species of Mud Turtle of Genus Kinosternon (Testudines: Kinosternidae) from the Pacific Coastal Plain of Northwestern Mexico . Zootaxa 4885:509-529-509–529.
Loc-Barragán, J. A., J. Reyes-Velasco, G. A. Woolrich-Piña, C. I. Grünwald, M. V. D. Anaya, J. A. Rangel-Mendoza, and M. A. López-Luna. 2020b. New Species of Mud Turtle of Genus Kinosternon (Testudines: Kinosternidae) from the Pacific Coastal Plain of Northwestern Mexico. Zootaxa 4885:509–529.
Love Stowell, S. M., C. A. Pinzone, and A. P. Martin. 2017. Overcoming barriers to active interventions for genetic diversity. Biodiversity & Conservation; Dordrecht 26:1753–1765. Springer Nature B.V., Dordrecht, Netherlands, Dordrecht.
Lowe, B. 2016. How Salamander Species Can Hybridize Extensively Yet Remain Distinct: Insights from Habitat Data, Molecules, and Behavior.
Lozada, T., G. H. J. de Koning, M. Kessler, A.-M. Klein, and T. Tscharntke. 2008. Geographical range size of tropical plants influences their response to anthropogenic activities. Diversity and Distributions 14:59–68.
Lynch, M., J. Conery, and R. Burger. 1995. Mutation Accumulation and the Extinction of Small Populations. The American Naturalist 146:489–518. The University of Chicago Press.
Lyons, M. P., and K. H. Kozak. 2020. Vanishing islands in the sky? A comparison of correlation- and mechanism-based forecasts of range dynamics for montane salamanders under climate change. Ecography 43:481–493.
Macip-Ríos, R., C. A. Merchant, E. G. Murillo, A. M. Ugalde, and M. de La Cruz-Merlo. 2021. Population Viability Analysis of Kinosternon hirtipes murrayi in Central México, with Notes on the Conservation Status of the Other Three Subspecies of the Lineage. Chelonian Conservation and Biology 20:50–59.
Macip-Ríos, R., R. Ontiveros, S. López-Alcaide, and G. Casas-Andreu. 2015. The conservation status of the freshwater and terrestrial turtles of Mexico: a critical review of biodiversity conservation strategies. Revista Mexicana de Biodiversidad 86:1048–1057.
MacLean, S. A., and S. R. Beissinger. 2017. Species' traits as predictors of range shifts under contemporary climate change: A review and meta-analysis. Global Change Biology 23:4094–4105.
Malinsky, M., M. Matschiner, and H. Svardal. 2021. Dsuite - Fast D-statistics and related admixture evidence from VCF files. Molecular Ecology Resources 21:584–595.
Mallet, J. 2007. Hybrid speciation. Nature 446:279–283.

Mallet, J. 2005. Hybridization as an invasion of the genome. Trends in Ecology & Evolution 20:229–237.
Manthey, J. D., J. Klicka, and G. M. Spellman. 2021. The Genomic Signature of Allopatric Speciation in a Songbird Is Shaped by Genome Architecture (Aves: Certhia americana). Genome Biology and Evolution 13:evab120.
Mao, X., G. He, P. Hua, G. Jones, S. Zhang, and S. J. Rossiter. 2013. Historical introgression and the persistence of ghost alleles in the intermediate horseshoe bat (Rhinolophus affinis). Molecular Ecology 22:1035–1050.
Markle, T. M. n.d. Ecology and Evolution of Geographic Range Size Variation in North American Plethodontid Salamanders: Perspectives from Thermal Physiology. University of Minnesota, United States -- Minnesota.
Markle, T. M., and K. H. Kozak. 2018. Low acclimation capacity of narrow-ranging thermal specialists exposes susceptibility to global climate change. Ecology and Evolution 8:4644–4656.
Mayr, E. 1963. Animal Species and Evolution. Harvard University Press.
Mayr, E. 1947. Ecological Factors in Speciation. Evolution 1:263–288. [Society for the Study of Evolution, Wiley].
McElroy, K., K. Beattie, M. R. E. Symonds, and L. Joseph. 2018. Mitogenomic and nuclear diversity in the Mulga Parrot of the Australian arid zone: cryptic subspecies and tests for selection. Emu - Austral Ornithology 118:22–35. Taylor & Francis.
McLachlan, J. S., J. J. Hellmann, and M. W. Schwartz. 2007. A Framework for Debate of Assisted Migration in an Era of Climate Change. Conservation Biology 21:297–302.
Mead, L. S., S. G. Tilley, and L. A. Katz. 2001. Genetic Structure of the Blue Ridge Dusky Salamander (desmognathus Orestes): Inferences from Allozymes, Mitochondrial Dna, and Behavior. Evolution 55:2287–2302.
Means, D., J. Lamb, and J. Bernardo. 2017. A new species of dusky salamander (Amphibia: Plethodontidae: Desmognathus) from the Eastern Gulf Coastal Plain of the United States and a redescription of D. auriculatus. Zootaxa 4263:467–506.
Meik, J. M., J. W. Streicher, A. M. Lawing, O. Flores-Villela, and M. K. Fujita. 2015. Limitations of Climatic Data for Inferring Species Boundaries: Insights from Speckled Rattlesnakes. PLOS ONE 10:e0131435. Public Library of Science.
Melander, S. L., and R. L. Mueller. 2020. Comprehensive Analysis of Salamander Hybridization Suggests a Consistent Relationship between Genetic Distance and Reproductive Isolation across Tetrapods. Copeia 108:987–1003.
Montwé, D., M. Isaac-Renton, A. Hamann, and H. Spiecker. 2018. Cold adaptation recorded in tree rings highlights risks associated with climate change and assisted migration. Nature Communications 9:1574. Nature Publishing Group.
Moore, W. S. 1977. An Evaluation of Narrow Hybrid Zones in Vertebrates. The Quarterly Review of Biology 52:263–277. The University of Chicago Press.

Mueller, R. L., J. R. Macey, M. Jaekel, D. B. Wake, and J. L. Boore. 2004. Morphological homoplasy, life history evolution, and historical biogeography of plethodontid salamanders inferred from complete mitochondrial genomes. PNAS 101:13820–13825. National Academy of Sciences.

Muhlfeld, C. C., S. T. Kalinowski, T. E. McMahon, M. L. Taper, S. Painter, R. F. Leary, and F. W. Allendorf. 2009. Hybridization rapidly reduces fitness of a native trout in the wild. Biology Letters 5:328–331. Royal Society.

Muscarella, R., P. J. Galante, M. Soley-Guardia, R. A. Boria, J. M. Kass, M. Uriarte, and R. P. Anderson. 2014a. ENM eval: An R package for conducting spatially independent evaluations and estimating optimal model complexity for Maxent ecological niche models. Methods in ecology and evolution 5:1198–1205. Wiley Online Library.

Muscarella, R., P. J. Galante, M. Soley‐Guardia, R. A. Boria, J. M. Kass, M. Uriarte, and R. P. Anderson. 2014b. ENMeval: An R package for conducting spatially independent evaluations and estimating optimal model complexity for Maxent ecological niche models. Methods in Ecology and Evolution 5:1198–1205.

Nei, M. 1987. Molecular Evolutionary Genetics. Columbia University Press.

Nice, C. C., J. A. Fordyce, V. A. Sotola, J. Crow, and P. H. Diaz. 2021. Geographic patterns of genomic variation in the threatened Salado salamander, Eurycea chisholmensis. Conserv Genet 22:811–821.

Ornelas-García, C. P., O. Domínguez-Domínguez, and I. Doadrio. 2008. Evolutionary history of the fish genus Astyanax Baird & Girard (1854) (Actinopterygii, Characidae) in Mesoamerica reveals multiple morphological homoplasies. BMC Evolutionary Biology 8:340.

Osborne, M. J., S. J. Cordova, A. C. Cameron, and T. F. Turner. 2019. Isolation by elevation: mitochondrial divergence among sky island populations of Sacramento Mountain salamander (Aneides hardii). Conserv Genet 20:545–556.

Owens, I. P. F., and P. M. Bennett. 1995. Ancient ecological diversification explains life-history variation among living birds. Proceedings of the Royal Society of London. Series B: Biological Sciences 261:227–232. Royal Society.

Papadopulos, A. S. T., J. Igea, L. T. Dunning, O. G. Osborne, X. Quan, J. Pellicer, C. Turnbull, I. Hutton, W. J. Baker, R. K. Butlin, and V. Savolainen. 2019. Ecological speciation in sympatric palms: 3. Genetic map reveals genomic islands underlying species divergence in Howea. Evolution 73:1986–1995.

Parmesan, C. 2006. Ecological and Evolutionary Responses to Recent Climate Change. Annual Review of Ecology, Evolution, and Systematics 37:637–669.

Parmesan, C., and G. Yohe. 2003. A globally coherent fingerprint of climate change impacts across natural systems. Nature 421:37–42.

Parra‐Olea, G., J. C. Windfield, G. Velo‐Antón, and K. R. Zamudio. 2012. Isolation in habitat refugia promotes rapid diversification in a montane tropical salamander. Journal of Biogeography 39:353–370.

Pato, J., J. C. Illera, J. R. Obeso, and P. Laiolo. 2019. The roles of geography, climate and sexual selection in driving divergence among insect populations on mountaintops. Journal of Biogeography 46:784–795.

Patterson, N., P. Moorjani, Y. Luo, S. Mallick, N. Rohland, Y. Zhan, T. Genschoreck, T. Webster, and D. Reich. 2012a. Ancient Admixture in Human History. Genetics 192:1065–1093.

Patterson, N., P. Moorjani, Y. Luo, S. Mallick, N. Rohland, Y. Zhan, T. Genschoreck, T. Webster, and D. Reich. 2012b. Ancient Admixture in Human History. Genetics 192:1065–1093.

Pauls, S. U., C. Nowak, M. Bálint, and M. Pfenninger. 2013. The impact of global climate change on genetic diversity within populations and species. Molecular Ecology 22:925–946.

Phillimore, A. B., and I. P. Owens. 2006. Are subspecies useful in evolutionary and conservation biology? Proceedings of the Royal Society B: Biological Sciences 273:1049–1053. The Royal Society London.

Phillips, N. M., J. A. Chaplin, D. L. Morgan, and S. C. Peverell. 2011. Population genetic structure and genetic diversity of three critically endangered Pristis sawfishes in Australian waters. Mar Biol 158:903–915.

Phillips, S. J., R. P. Anderson, and R. E. Schapire. 2006. Maximum entropy modeling of species geographic distributions. Ecological Modelling 190:231–259.

Phillips, S. J., and M. Dudík. 2008. Modeling of species distributions with Maxent: new extensions and a comprehensive evaluation. Ecography 31:161–175.

Pickrell, J., and J. Pritchard. 2012. Inference of population splits and mixtures from genome-wide allele frequency data. Nature Precedings 1–1. Nature Publishing Group.

Pie, M. R., L. L. F. Campos, A. L. S. Meyer, and A. Duran. 2017. The evolution of climatic niches in squamate reptiles. Proceedings of the Royal Society B: Biological Sciences 284:20170268. Royal Society.

Portik, D. M., A. D. Leaché, D. Rivera, M. F. Barej, M. Burger, M. Hirschfeld, M.-O. Rödel, D. C. Blackburn, and M. K. Fujita. 2017. Evaluating mechanisms of diversification in a Guineo-Congolian tropical forest frog using demographic model selection. Molecular Ecology 26:5245–5263.

Posada, D. 2008. jModelTest: Phylogenetic Model Averaging. Molecular Biology and Evolution 25:1253–1256.

Pöyry, J., M. Luoto, R. K. Heikkinen, M. Kuussaari, and K. Saarinen. 2009. Species traits explain recent range shifts of Finnish butterflies. Global Change Biology 15:732–743.

Prentice, I. C., P. J. Bartlein, and T. Webb III. 1991. Vegetation and Climate Change in Eastern North America Since the Last Glacial Maximum. Ecology 72:2038–2056.

Pyron, M. 1999. Relationships between geographical range size, body size, local abundance, and habitat breadth in North American suckers and sunfishes. Journal of Biogeography 26:549–558.

Pyron, R. A., K. A. O'Connell, E. M. Lemmon, A. R. Lemmon, and D. A. Beamer. 2020. Phylogenomic data reveal reticulation and incongruence among

mitochondrial candidate species in Dusky Salamanders (Desmognathus). Molecular Phylogenetics and Evolution 146:106751.
Quintero, I., and J. J. Wiens. 2013. Rates of projected climate change dramatically exceed past rates of climatic niche evolution among vertebrate species. Ecology Letters 16:1095–1103.
Rafferty, A. R., and R. D. Reina. 2012. Arrested embryonic development: a review of strategies to delay hatching in egg-laying reptiles. Proceedings of the Royal Society B: Biological Sciences 279:2299–2308. Royal Society.
Rambaut, A., M. A. Suchard, D. Xie, and A. J. Drummond. 2014. Tracer v 1.6. University of Edinburgh, Edinburgh, UK.
Rand, D. M., and R. G. Harrison. 1989. Ecological Genetics of a Mosaic Hybrid Zone: Mitochondrial, Nuclear, and Reproductive Differentiation of Crickets by Soil Type. Evolution 43:432–449.
Rasmussen, J. B., M. D. Robinson, A. Hontela, and D. D. Heath. 2012. Metabolic traits of westslope cutthroat trout, introduced rainbow trout and their hybrids in an ecotonal hybrid zone along an elevation gradient. Biological Journal of the Linnean Society 105:56–72.
Raxworthy, C. J., C. M. Ingram, N. Rabibisoa, and R. G. Pearson. 2007. Applications of ecological niche modeling for species delimitation: a review and empirical evaluation using day geckos (Phelsuma) from Madagascar. Syst Biol 56:907–923.
Ray, C. 1958. Vital Limits and Rates of Desiccation in Salamanders. Ecology 39:75–83. Ecological Society of America.
Razgour, O., B. Forester, J. B. Taggart, M. Bekaert, J. Juste, C. Ibáñez, S. J. Puechmaille, R. Novella-Fernandez, A. Alberdi, and S. Manel. 2019. Considering adaptive genetic variation in climate change vulnerability assessment reduces species range loss projections. PNAS 116:10418–10423. National Academy of Sciences.
Reis, J., C. J. Bidau, R. Maestri, and P. A. Martinez. 2018. Diversification of the climatic niche drove the recent processes of speciation in Sigmodontinae (Rodentia, Cricetidae). Mammal Review 48:328–332.
Revell, L. J. 2012. phytools: an R package for phylogenetic comparative biology (and other things): *phytools: R package*. Methods in Ecology and Evolution 3:217–223.
Reyes-Velasco, J., J. B. Iverson, and O. Flores-Villela. 2013. The Conservation Status of Several Endemic Mexican Kinosternid Turtles. Chelonian Conservation and Biology 12:203–208. Allen Press.
Rhymer, J. M., and D. Simberloff. 1996. Extinction by Hybridization and Introgression. Annual Review of Ecology and Systematics 27:83–109.
Ricciardi, A., and D. Simberloff. 2009. Assisted colonization is not a viable conservation strategy. Trends in Ecology & Evolution 24:248–253.
Rice, W. R., and E. E. Hostert. 1993. Laboratory Experiments on Speciation: What Have We Learned in 40 Years? Evolution 47:1637–1653.

Richards, E. J., and C. H. Martin. 2017. Adaptive introgression from distant Caribbean islands contributed to the diversification of a microendemic adaptive radiation of trophic specialist pupfishes. PLOS Genetics 13:e1006919. Public Library of Science.

Ricklefs, R. E., and M. Wikelski. 2002. The physiology/life-history nexus. Trends in Ecology & Evolution 17:462–468.

Rissler, L. J., and J. J. Apodaca. 2007. Adding more ecology into species delimitation: ecological niche models and phylogeography help define cryptic species in the black salamander (Aneides flavipunctatus). Syst Biol 56:924–942.

Rissler, L. J., and D. R. Taylor. 2003. The phylogenetics of Desmognathine salamander populations across the southern Appalachians. Molecular Phylogenetics and Evolution 27:197–211.

Rochette, N. C., A. G. Rivera‐Colón, and J. M. Catchen. 2019. Stacks 2: Analytical methods for paired-end sequencing improve RADseq-based population genomics. Molecular Ecology 28:4737–4754.

Rodríguez, A., B. Rodríguez, T. Montelongo, J. Garcia-Porta, T. Pipa, M. Carty, J. Danielsen, J. Nunes, C. Silva, P. Geraldes, F. M. Medina, and J. C. Illera. 2020. Cryptic differentiation in the Manx shearwater hinders the identification of a new endemic subspecies. Journal of Avian Biology 51.

Rodríguez‐Gómez, F., and J. F. Ornelas. 2015. At the passing gate: past introgression in the process of species formation between Amazilia violiceps and A. viridifrons hummingbirds along the Mexican Transition Zone. Journal of Biogeography 42:1305–1318.

Root, T. L., J. T. Price, K. R. Hall, S. H. Schneider, C. Rosenzweig, and J. A. Pounds. 2003. Fingerprints of global warming on wild animals and plants. Nature 421:57–60.

Rosauer, D. F., L. J. Pollock, S. Linke, and W. Jetz. 2017. Phylogenetically informed spatial planning is required to conserve the mammalian tree of life. Proc. R. Soc. B. 284:20170627.

Roux, C., C. Fraisse, J. Romiguier, Y. Anciaux, N. Galtier, and N. Bierne. 2016. Shedding light on the grey zone of speciation along a continuum of genomic divergence. PLoS biology 14:e2000234. Public Library of Science San Francisco, CA USA.

Russell, J., M. van Zonneveld, I. K. Dawson, A. Booth, R. Waugh, and B. Steffenson. 2014. Genetic Diversity and Ecological Niche Modelling of Wild Barley: Refugia, Large-Scale Post-LGM Range Expansion and Limited Mid-Future Climate Threats? PLOS ONE 9:e86021. Public Library of Science.

Ryan, S. F., J. M. Deines, J. M. Scriber, M. E. Pfrender, S. E. Jones, S. J. Emrich, and J. J. Hellmann. 2018. Climate-mediated hybrid zone movement revealed with genomics, museum collection, and simulation modeling. PNAS 115:E2284–E2291. National Academy of Sciences.

Salemi, M., and A.-M. Vandamme. 2003. The Phylogenetic Handbook: A Practical Approach to DNA and Protein Phylogeny. Cambridge University Press.

Saremi, N. F., M. A. Supple, A. Byrne, J. A. Cahill, L. L. Coutinho, L. Dalén, H. V. Figueiró, W. E. Johnson, H. J. Milne, S. J. O'Brien, B. O'Connell, D. P. Onorato, S. P. D. Riley, J. A. Sikich, D. R. Stahler, P. M. S. Villela, C. Vollmers, R. K. Wayne, E. Eizirik, R. B. Corbett-Detig, R. E. Green, C. C. Wilmers, and B. Shapiro. 2019. Puma genomes from North and South America provide insights into the genomic consequences of inbreeding. Nature Communications 10:4769. Nature Publishing Group.

Schluter, D. 2000a. The Ecology of Adaptive Radiation. OUP Oxford.

Schluter, D. 2000b. The Ecology of Adaptive Radiation. OUP Oxford.

Schoener, T. W., and G. C. Gorman. 1968. Some Niche Differences in Three Lesser Antillean Lizards of the Genus Anolis. Ecology 49:819–830.

Scott, P. A., T. C. Glenn, and L. J. Rissler. 2018. Resolving taxonomic turbulence and uncovering cryptic diversity in the musk turtles (Sternotherus) using robust demographic modeling. Molecular Phylogenetics and Evolution 120:1–15.

Seeholzer, G. F., S. Claramunt, and R. T. Brumfield. 2017. Niche evolution and diversification in a Neotropical radiation of birds (Aves: Furnariidae). Evolution 71:702–715.

Serb, J. M., C. A. Phillips, and J. B. Iverson. 2001. Molecular phylogeny and biogeography of Kinosternon flavescens based on complete mitochondrial control region sequences. Molecular Phylogenetics and Evolution 18:149–162. Elsevier.

Seutin, G., B. N. White, and P. T. Boag. 1991. Preservation of avian blood and tissue samples for DNA analyses. Can. J. Zool. 69:82–90. NRC Research Press.

Shaffer, B. H., P. Minx, D. E. Warren, A. M. Shedlock, R. C. Thomson, N. Valenzuela, J. Abramyan, C. T. Amemiya, D. Badenhorst, K. K. Biggar, G. M. Borchert, C. W. Botka, R. M. Bowden, E. L. Braun, A. M. Bronikowski, B. G. Bruneau, L. T. Buck, B. Capel, T. A. Castoe, M. Czerwinski, K. D. Delehaunty, S. V. Edwards, C. C. Fronick, M. K. Fujita, L. Fulton, T. A. Graves, R. E. Green, W. Haerty, R. Hariharan, O. Hernandez, L. W. Hillier, A. K. Holloway, D. Janes, F. J. Janzen, C. Kandoth, L. Kong, A. J. de Koning, Y. Li, R. Literman, S. E. McGaugh, L. Mork, M. O'Laughlin, R. T. Paitz, D. D. Pollock, C. P. Ponting, S. Radhakrishnan, B. J. Raney, J. M. Richman, J. St John, T. Schwartz, A. Sethuraman, P. Q. Spinks, K. B. Storey, N. Thane, T. Vinar, L. M. Zimmerman, W. C. Warren, E. R. Mardis, and R. K. Wilson. 2013. The western painted turtle genome, a model for the evolution of extreme physiological adaptations in a slowly evolving lineage. Genome Biology 14:R28.

Shaner, P.-J. L., T.-H. Tsao, R.-C. Lin, W. Liang, C.-F. Yeh, X.-J. Yang, F.-M. Lei, F. Zhou, C.-C. Yang, L. M. Hung, Y.-C. Hsu, and S.-H. Li. 2015. Climate niche differentiation between two passerines despite ongoing gene flow. Journal of Animal Ecology 84:829–839.

Shcheglovitova, M., and R. P. Anderson. 2013. Estimating optimal complexity for ecological niche models: A jackknife approach for species with small sample sizes. Ecological Modelling 269:9–17.

Shen, X.-X., D. Liang, M.-Y. Chen, R.-L. Mao, D. B. Wake, and P. Zhang. 2016. Enlarged Multilocus Data set Provides Surprisingly Younger Time of Origin for the Plethodontidae, the Largest Family of Salamanders. Systematic Biology 65:66–81.

Simler, A. B., M. A. Williamson, M. W. Schwartz, and D. M. Rizzo. 2019. Amplifying plant disease risk through assisted migration. Conservation Letters 12:e12605.

Simpson, G. G. 1984. Tempo and Mode in Evolution. Columbia University Press.

Slatyer, R. A., M. Hirst, and J. P. Sexton. 2013. Niche breadth predicts geographical range size: a general ecological pattern. Ecology Letters 16:1104–1114.

Smith, H. J., H. Fischer, M. Wahlen, D. Mastroianni, and B. Deck. 1999. Dual modes of the carbon cycle since the Last Glacial Maximum. Nature 400:248–250.

Smith, S. A., and J. M. Beaulieu. 2009. Life history influences rates of climatic niche evolution in flowering plants. Proceedings of the Royal Society B: Biological Sciences 276:4345–4352. Royal Society.

Sobel, J. M., G. F. Chen, L. R. Watt, and D. W. Schemske. 2010. The Biology of Speciation. Evolution 64:295–315.

Soberón, J. 2007. Grinnellian and Eltonian niches and geographic distributions of species. Ecology Letters 10:1115–1123.

Spielman, D., B. W. Brook, D. A. Briscoe, and R. Frankham. 2004. Does Inbreeding and Loss of Genetic Diversity Decrease Disease Resistance? Conservation Genetics 5:439–448.

Spinks, P. Q., and H. B. Shaffer. 2005. Range-wide molecular analysis of the western pond turtle (Emys marmorata): cryptic variation, isolation by distance, and their conservation implications. Molecular Ecology 14:2047–2064. Wiley Online Library.

Spinks, P. Q., R. C. Thomson, M. Gidiş, and H. Bradley Shaffer. 2014. Multilocus phylogeny of the New-World mud turtles (Kinosternidae) supports the traditional classification of the group. Molecular Phylogenetics and Evolution 76:254–260.

Stelkens, R. B., C. Schmid, and O. Seehausen. 2015. Hybrid Breakdown in Cichlid Fish. PLOS ONE 10:e0127207. Public Library of Science.

Stephens, M., N. J. Smith, and P. Donnelly. 2001. A New Statistical Method for Haplotype Reconstruction from Population Data. The American Journal of Human Genetics 68:978–989.

Streicher, J. W., T. J. Devitt, C. S. Goldberg, J. H. Malone, H. Blackmon, and M. K. Fujita. 2014. Diversification and asymmetrical gene flow across time and space: lineage sorting and hybridization in polytypic barking frogs. Molecular Ecology 23:3273–3291.

Sun, Y., Y. Surget‐Groba, and S. Gao. 2016. Divergence maintained by climatic selection despite recurrent gene flow: a case study of Castanopsis carlesii (Fagaceae). Molecular Ecology 25:4580–4592.

Sunny, A., L. Duarte-deJesus, A. Aguilera-Hernández, F. Ramírez-Corona, M. Suárez-Atilano, R. Percino-Daniel, J. Manjarrez, O. Monroy-Vilchis, and A.

González-Fernández. 2019. Genetic diversity and demography of the critically endangered Roberts' false brook salamander (Pseudoeurycea robertsi) in Central Mexico. Genetica 147:149–164.
Swafford, D. 2003. PAUP*. Phylogenetic Analysis Using Parsimony (*and Other Methods). Pp. 160–206 *in* The Phylogenetic Handbook: A Practical Approach to DNA and Protein Phylogeny. Cambridge University Press.
Sweigart, A. L., and J. H. Willis. 2003a. Patterns of Nucleotide Diversity in Two Species of Mimulus Are Affected by Mating System and Asymmetric Introgression. Evolution 57:2490–2506.
Sweigart, A. L., and J. H. Willis. 2003b. Patterns of Nucleotide Diversity in Two Species of Mimulus Are Affected by Mating System and Asymmetric Introgression. Evolution 57:2490–2506.
Swenson, N. G. 2006. Gis-based niche models reveal unifying climatic mechanisms that maintain the location of avian hybrid zones in a North American suture zone. Journal of Evolutionary Biology 19:717–725.
Talla, V., A. Johansson, V. Dincă, R. Vila, M. Friberg, C. Wiklund, and N. Backström. 2019. Lack of gene flow: Narrow and dispersed differentiation islands in a triplet of Leptidea butterfly species. Molecular Ecology 28:3756–3770.
Tallmon, D. A., G. Luikart, and R. S. Waples. 2004. The alluring simplicity and complex reality of genetic rescue. Trends in Ecology & Evolution 19:489–496.
Taylor, B. L., W. F. Perrin, R. R. Reeves, P. E. Rosel, J. Y. Wang, F. Cipriano, C. Scott Baker, and R. L. Brownell Jr. 2017. Why we should develop guidelines and quantitative standards for using genetic data to delimit subspecies for data-poor organisms like cetaceans. Marine Mammal Science 33:12–26. Wiley Online Library.
Taylor, S. A., R. L. Curry, T. A. White, V. Ferretti, and I. Lovette. 2014a. Spatiotemporally consistent genomic signatures of reproductive isolation in a moving hybrid zone. Evolution 68:3066–3081.
Taylor, S. A., T. A. White, W. M. Hochachka, V. Ferretti, R. L. Curry, and I. Lovette. 2014b. Climate-Mediated Movement of an Avian Hybrid Zone. Current Biology 24:671–676.
Thakur, M., E. W. Schättin, and W. J. McShea. 2018. Globally common, locally rare: revisiting disregarded genetic diversity for conservation planning of widespread species. Biodivers Conserv 27:3031–3035.
Thomson, R. C., P. Q. Spinks, and H. B. Shaffer. 2021. A global phylogeny of turtles reveals a burst of climate-associated diversification on continental margins. PNAS 118. National Academy of Sciences.
Tilley, S. G., and J. Bernardo. 1993. Life History Evolution in Plethodontid Salamanders. Herpetologica 49:154–163. [Herpetologists' League, Allen Press].
Tilley, S. G., J. Bernardo, L. A. Katz, L. López, J. Devon Roll, R. L. Eriksen, J. Kratovil, N. K. J. Bittner, and K. A. Crandall. 2013. Failed species, innominate forms, and the vain search for species limits: cryptic diversity in dusky

salamanders (Desmognathus) of eastern Tennessee. Ecology and Evolution 3:2547–2567.
TILLEY, S. G., R. L. ERIKSEN, and L. A. KATZ. 2008. Systematics of dusky salamanders, Desmognathus (Caudata: Plethodontidae), in the mountain and Piedmont regions of Virginia and North Carolina, USA. Zoological Journal of the Linnean Society 152:115–130.
Tíscar, P. A., M. E. Lucas-Borja, and D. Candel-Pérez. 2018. Lack of local adaptation to the establishment conditions limits assisted migration to adapt drought-prone Pinus nigra populations to climate change. Forest Ecology and Management 409:719–728.
Title, P. O., and K. J. Burns. 2015a. Rates of climatic niche evolution are correlated with species richness in a large and ecologically diverse radiation of songbirds. Ecology Letters 18:433–440.
Title, P. O., and K. J. Burns. 2015b. Rates of climatic niche evolution are correlated with species richness in a large and ecologically diverse radiation of songbirds. Ecology Letters 18:433–440.
Titus, T. A., and A. Larson. 1996. Molecular Phylogenetics of Desmognathine Salamanders (Caudata: Plethodontidae): A Reevaluation of Evolution in Ecology, Life History, and Morphology. Systematic Biology 45:451–472.
Todesco, M., M. A. Pascual, G. L. Owens, K. L. Ostevik, B. T. Moyers, S. Hübner, S. M. Heredia, M. A. Hahn, C. Caseys, D. G. Bock, and L. H. Rieseberg. 2016. Hybridization and extinction. Evolutionary Applications 9:892–908.
Toews, D. P., and D. E. Irwin. 2008. Cryptic speciation in a Holarctic passerine revealed by genetic and bioacoustic analyses. Molecular Ecology 17:2691–2705. Wiley Online Library.
Torre, A. R. D. L., D. R. Roberts, and S. N. Aitken. 2014. Genome-wide admixture and ecological niche modelling reveal the maintenance of species boundaries despite long history of interspecific gene flow. Molecular Ecology 23:2046–2059.
Tracy, C. R., K. A. Christian, and C. R. Tracy. 2010. Not just small, wet, and cold: effects of body size and skin resistance on thermoregulation and arboreality of frogs. Ecology 91:1477–1484.
Turner, L. M., D. J. Schwahn, and B. Harr. 2012. Reduced Male Fertility Is Common but Highly Variable in Form and Severity in a Natural House Mouse Hybrid Zone. Evolution 66:443–458.
Urban, M. C. 2018. Escalator to extinction. PNAS 115:11871–11873. National Academy of Sciences.
Vargas-Ramírez, M., H. Stuckas, O. V. Castaño-Mora, and U. Fritz. 2012a. Extremely low genetic diversity and weak population differentiation in the endangered Colombian river turtle Podocnemis lewyana (Testudines: Podocnemididae). Conservation Genetics 1:65–77.
Vargas-Ramírez, M., H. Stuckas, O. V. Castaño-Mora, and U. Fritz. 2012b. Extremely low genetic diversity and weak population differentiation in the

endangered Colombian river turtle Podocnemis lewyana (Testudines: Podocnemididae). Conserv Genet 13:65–77.
Voldoire, A., E. Sanchez-Gomez, D. S. y Mélia, B. Decharme, C. Cassou, S. Sénési, S. Valcke, I. Beau, A. Alias, M. Chevallier, M. Déqué, J. Deshayes, H. Douville, E. Fernandez, G. Madec, E. Maisonnave, M.-P. Moine, S. Planton, D. Saint-Martin, S. Szopa, S. Tyteca, R. Alkama, S. Belamari, A. Braun, L. Coquart, and F. Chauvin. 2013. The CNRM-CM5.1 global climate model: description and basic evaluation. Clim Dyn 40:2091–2121.
Wagler, J. G. 1830. Natürliches System der Amphibien: mit vorangehender Classification der Säugethiere und Vögel : ein Beitrag zur vergleichenden Zoologie. J.G. Cotta.
Walls, S. C. 2009. The role of climate in the dynamics of a hybrid zone in Appalachian salamanders. Global Change Biology 15:1903–1910.
Wang, F., D. Wang, G. Guo, Y. Hu, J. Wei, and J. Liu. 2019. Species delimitation of the Dermacentor ticks based on phylogenetic clustering and niche modeling. PeerJ 7:e6911. PeerJ Inc.
Wang, G.-D., B.-L. Zhang, W.-W. Zhou, Y.-X. Li, J.-Q. Jin, Y. Shao, H. Yang, Y.-H. Liu, F. Yan, H.-M. Chen, L. Jin, F. Gao, Y. Zhang, H. Li, B. Mao, R. W. Murphy, D. B. Wake, Y.-P. Zhang, and J. Che. 2018. Selection and environmental adaptation along a path to speciation in the Tibetan frog Nanorana parkeri. PNAS 115:E5056–E5065. National Academy of Sciences.
Warren, D. L., R. E. Glor, and M. Turelli. 2010a. ENMTools: a toolbox for comparative studies of environmental niche models. Ecography 33:607–611.
Warren, D. L., R. E. Glor, and M. Turelli. 2010b. ENMTools: a toolbox for comparative studies of environmental niche models. Ecography 33:607–611.
Warren, D. L., R. E. Glor, and M. Turelli. 2008. Environmental Niche Equivalency Versus Conservatism: Quantitative Approaches to Niche Evolution. Evolution 62:2868–2883.
Weaver, S., D. B. Shepard, and K. H. Kozak. 2020. Developmental life history is associated with variation in rates of climatic niche evolution in a salamander adaptive radiation*. Evolution 74:1804–1814.
Weeks, A. R., D. Heinze, L. Perrin, J. Stoklosa, A. A. Hoffmann, A. van Rooyen, T. Kelly, and I. Mansergh. 2017. Genetic rescue increases fitness and aids rapid recovery of an endangered marsupial population. Nature Communications 8:1071. Nature Publishing Group.
Weir, B. S., and C. C. Cockerham. 1984. Estimating F-Statistics for the Analysis of Population Structure. Evolution 38:1358–1370. [Society for the Study of Evolution, Wiley].
Weir, J. T., and D. Schluter. 2004. Ice sheets promote speciation in boreal birds. Proceedings of the Royal Society of London. Series B: Biological Sciences 271:1881–1887. Royal Society.
Weisrock, D. W., K. H. Kozak, and A. Larson. 2005. Phylogeographic analysis of mitochondrial gene flow and introgression in the salamander, Plethodon shermani. Molecular Ecology 14:1457–1472.

Wenner, T. J., M. A. Russello, and T. F. Wright. 2012. Cryptic species in a Neotropical parrot: genetic variation within the Amazona farinosa species complex and its conservation implications. Conservation Genetics 13:1427–1432. Springer.

Wernberg, T., M. A. Coleman, S. Bennett, M. S. Thomsen, F. Tuya, and B. P. Kelaher. 2018. Genetic diversity and kelp forest vulnerability to climatic stress. Sci Rep 8:1851.

Whitlock, M. C., and K. E. Lotterhos. 2015. Reliable Detection of Loci Responsible for Local Adaptation: Inference of a Null Model through Trimming the Distribution of FST. The American Naturalist 186:S24–S36. The University of Chicago Press.

Wielstra, B. 2019. Historical hybrid zone movement: More pervasive than appreciated. Journal of Biogeography 46:1300–1305.

Wiens, J. J. 2007. Species delimitation: new approaches for discovering diversity. Systematic Biology 56:875–878. Society of Systematic Zoology.

Wiley, E. O. 1978. The evolutionary species concept reconsidered. Systematic zoology 27:17–26. Society of Systematic Zoology.

Wilson, E. O., and W. L. Brown Jr. 1953. The subspecies concept and its taxonomic application. Systematic zoology 2:97–111. Society of Systematic Zoology.

Winemiller, K. O., and K. A. Rose. 1992. Patterns of Life-History Diversification in North American Fishes: implications for Population Regulation. Can. J. Fish. Aquat. Sci. 49:2196–2218. NRC Research Press.

Wolf, D. E., N. Takebayashi, and L. H. Rieseberg. 2001. Predicting the Risk of Extinction through Hybridization. Conservation Biology 15:1039–1053.

Yang, W., N. Feiner, C. Pinho, G. M. While, A. Kaliontzopoulou, D. J. Harris, D. Salvi, and T. Uller. 2021. Extensive introgression and mosaic genomes of Mediterranean endemic lizards. Nat Commun 12:2762.

Yoder, J. B., E. Clancey, S. Des Roches, J. M. Eastman, L. Gentry, W. Godsoe, T. J. Hagey, D. Jochimsen, B. P. Oswald, J. Robertson, B. a. J. Sarver, J. J. Schenk, S. F. Spear, and L. J. Harmon. 2010. Ecological opportunity and the origin of adaptive radiations. Journal of Evolutionary Biology 23:1581–1596.

Zalapa, J. E., J. Brunet, and R. P. Guries. 2010a. ORIGINAL ARTICLE: The extent of hybridization and its impact on the genetic diversity and population structure of an invasive tree, Ulmus pumila (Ulmaceae). Evolutionary Applications 3:157–168.

Zalapa, J. E., J. Brunet, and R. P. Guries. 2010b. ORIGINAL ARTICLE: The extent of hybridization and its impact on the genetic diversity and population structure of an invasive tree, Ulmus pumila (Ulmaceae). Evolutionary Applications 3:157–168.

Zhang, D., L. Tang, Y. Cheng, Y. Hao, Y. Xiong, G. Song, Y. Qu, F. E. Rheindt, P. Alström, C. Jia, and F. Lei. 2019. “Ghost Introgression” As a Cause of Deep Mitochondrial Divergence in a Bird Species Complex. Molecular Biology and Evolution 36:2375–2386.

Zheng, H., L. Fan, R. I. Milne, L. Zhang, Y. Wang, and K. Mao. 2017. Species Delimitation and Lineage Separation History of a Species Complex of Aspens in China. Front. Plant Sci. 8. Frontiers.

Zheng, X., D. Levine, J. Shen, S. M. Gogarten, C. Laurie, and B. S. Weir. 2012. A high-performance computing toolset for relatedness and principal component analysis of SNP data. Bioinformatics 28:3326–3328. Oxford Academic.

Zink, R. M. 2004. The role of subspecies in obscuring avian biological diversity and misleading conservation policy. Proceedings of the Royal Society of London. Series B: Biological Sciences 271:561–564. The Royal Society.

N.d. Texas Conservation Action Plan 2012 - 2016: Overview. Texas Parks and Wildlife Department, Austin, TX.